

LBL-7448

c.2

RECEIVED
LAWRENCE
BERKELEY LABORATORY

OCT 19 1978

LIBRARY AND
DOCUMENTS SECTION

annual
report
1977

TWO-WEEK LOAN COPY

*This is a Library Circulating Copy
which may be borrowed for two weeks.
For a personal retention copy, call
Tech. Info. Division, Ext. 6782*

**Biology &
Medicine
Division**

**Lawrence Berkeley Laboratory
University of California, Berkeley**

PREPARED FOR THE U.S. DEPARTMENT OF ENERGY UNDER CONTRACT W-7405-ENG-48

LBL-7448
c.2

DISCLAIMER

This document was prepared as an account of work sponsored by the United States Government. While this document is believed to contain correct information, neither the United States Government nor any agency thereof, nor the Regents of the University of California, nor any of their employees, makes any warranty, express or implied, or assumes any legal responsibility for the accuracy, completeness, or usefulness of any information, apparatus, product, or process disclosed, or represents that its use would not infringe privately owned rights. Reference herein to any specific commercial product, process, or service by its trade name, trademark, manufacturer, or otherwise, does not necessarily constitute or imply its endorsement, recommendation, or favoring by the United States Government or any agency thereof, or the Regents of the University of California. The views and opinions of authors expressed herein do not necessarily state or reflect those of the United States Government or any agency thereof or the Regents of the University of California.

LBL-7448
UC-48

**BIOLOGY AND MEDICINE DIVISION
ANNUAL REPORT 1977**

Lawrence Berkeley Laboratory
University of California
Berkeley, California

CONTENTS

1. INTRODUCTION	1
Edward L. Alpen	
2. RESEARCH MEDICINE	3
ALGORITHMS FOR COMPUTERIZED TRANSAXIAL RADIONUCLIDE RECONSTRUCTION	3
R. H. Huesman, G. T. Gullberg, W. L. Greenberg, and T. F. Budinger	
INSTRUMENT DEVELOPMENT FOR MEDICAL STUDIES	4
H. O. Anger	
INSTRUMENTATION FOR THREE-DIMENSIONAL TOMOGRAPHY	7
S. E. Derenzo	
METABOLISM OF BRAIN DISORDERS	8
T. W. Sargent	
DEVELOPMENT OF RADIONUCLIDES AND RADIOPHARMACEUTICALS FOR EXPERIMENTAL MEDICINE	10
Y. Yano	
EPIDEMIOLOGY OF THE EFFECTS OF MAGNETIC FIELDS ON HUMAN BEINGS	11
T. F. Budinger	
KINETICS OF MEGAKARYOCYTE AND PLATELET TURNOVER	12
S. N. Ebbe	
Donner Clinic	
DONNER CLINIC OUTPATIENT FACILITY	13
S. N. Ebbe	
3. DONNER PAVILION	15
TREATMENT OF PITUITARY TUMORS WITH ALPHA PARTICLE IRRADIATION	15
J. A. Linfoot and E. Wiedemann	
EFFECT OF HEAVY PARTICLE PITUITARY IRRADIATION ON VASCULAR COMPLICATIONS OF DIABETES MELLITUS	17
J. A. Linfoot and J. S. Nakagawa	
INVESTIGATIONS OF SOMATOMEDIN IN PITUITARY TUMOR PATIENTS	18
E. Wiedemann and J. A. Linfoot	

DEVELOPMENT AND APPLICATIONS OF BETA-LIPOTROPIN ASSAY FOR PITUITARY TUMOR PATIENTS E. Wiedemann and J. A. Linfoot	19
4. PERALTA CANCER RESEARCH INSTITUTE	21
HUMAN MAMMARY TUMOR VIROLOGY A. J. Hackett, H. S. Smith, and E. L. Springer	21
5. ENVIRONMENTAL PHYSIOLOGY	23
EFFECTS OF ENVIRONMENTAL POLLUTANTS ON HEMATOPOIETIC SYSTEM J. C. Schooley and M. E. Barker	23
EFFECTS OF ENVIRONMENTAL POLLUTANTS ON PROTEIN AND POLYPEPTIDE HORMONES J. F. Garcia and G. K. Clemons	26
EFFECTS OF ENVIRONMENTAL POLLUTANTS ON STEROID HORMONE MECHANISMS G. M. Connell	27
EFFECTS OF ENVIRONMENTAL POLLUTANTS ON PROTEIN METABOLISM IN SMALL ANIMALS J. S. Dixon and J. C. Schooley	29
STUDIES OF GROWTH AND DIFFERENTIATION OF LUNG IN FETAL MICE, ADULT MICE, AND REGENERATING LUNG TISSUE J. C. Schooley, W. J. Vaughan, and D. A. Pointer	30
EFFECTS OF TOXIC AIR POLLUTANTS ON TUMOR INCIDENCE IN MICE M. R. White	32
METABOLISM OF TRANSURANIC ELEMENTS IN NONHUMAN PRIMATES P. W. Durbin	34
6. RADIATION BIOPHYSICS	37
Bevalac Studies	
RADIOLOGICAL PHYSICS AND CHEMISTRY OF HEAVY PARTICLES A. Chatterjee and J. L. Magee	38
TRACER STUDIES WITH RADIOACTIVE BEAMS A. Chatterjee, C. A. Tobias, and J. Llacer	39
PHYSICAL CHARACTERIZATION OF ENERGETIC HEAVY-ION BEAMS W. Schimmerling	41

RESPONSE OF A RAT RHABDOMYOSARCOMA TO HEAVY-ION BEAMS	43
S. B. Curtis, T. S. Tenforde, W. Schilling, S. Daniels, and K. Crabtree	
CELL SURVIVAL STUDIES WITH HEAVY-ION BEAMS	48
C. A. Tobias, E. A. Blakely, and F. Q. Ngo	
HEAVY-ION RADIOGRAPHY	50
C. A. Tobias and E. V. Benton	
TREATMENT OF CANCER WITH HELIUM AND HEAVY IONS	52
J. R. Castro	
Magnetic Field Studies	
BIOLOGICAL EFFECTS OF HIGH MAGNETIC FIELDS	54
T. S. Tenforde	
Biophysical Studies	
CELL-MEMBRANE BIOPHYSICS AND ENVIRONMENTAL AGENTS	57
H. C. Mel	
7. STRUCTURAL BIOPHYSICS	61
Microscopic Studies	
BIOLOGICAL STRUCTURE ANALYSIS BY ELECTRON MICROSCOPY	62
R. M. Glaeser	
SCANNING ELECTRON MICROSCOPE STUDIES OF FLY ASH IN CELLS	63
T. L. Hayes and J. B. Pawley	
MEMBRANE RECYCLING HYPOTHESIS FOR GASTRIC HCl SECRETION	67
T. M. Forte, T. E. Machen, and J. G. Forte	
Lipoprotein Studies	
LIPOPROTEIN METHODOLOGY AND BIOMEDICAL APPLICATIONS INCLUDING EVALUATIONS OF POLLUTANT DAMAGE	69
F. T. Lindgren and R. M. Krauss	
SERUM HIGH-DENSITY LIPOPROTEINS IN HEALTH AND DISEASE	72
A. V. Nichols	
LIPOPROTEIN SYNTHESIS BY RAT HEPATOCYTE MONOLAYER CULTURES	72
T. M. Forte, J. B. Quint, and R. W. Nordhausen	

Genetic Studies

MAMMALIAN CELL MUTAGENESIS H. J. Burki	74
DNA REPAIR MECHANISM J. Hosoda	75
GENETIC STUDY OF YEAST R. K. Mortimer	77
EFFECTS OF POLLUTANTS ON SOMATIC MAMMALIAN CELLS D. A. Glaser	78

Biophysical Studies

RESONANCE STUDIES IN PHOTOSYNTHESIS A. J. Bearden	80
--	----

APPENDICES

A. 1977 PUBLICATIONS	81
B. BIOLOGY AND MEDICINE DIVISION STAFF	88

1. INTRODUCTION

E. L. Alpen

Some time has passed since the last regular issuance of an annual report for Lawrence Berkeley Laboratory's Biology and Medicine Division. During this interval much has happened. It has been a time of reorganization, revitalization, and moderate growth. It speaks well for the quality of the laboratory's senior staff that they have maintained high levels of creative productivity during this period and have continued to distinguish themselves in their special fields of research.

At the end of 1975 the division population included 30 principal investigators; 44 post-doctoral and other scientific staff; and technical, administrative and clerical support staff, for a total division staff of 131. By the end of 1977 these numbers were 36, 56, and 191 respectively. During this period the division's annual operating budget has grown from approximately \$7.1 million to its present level of \$12.2 million.

This significant growth occurred at a time when our principal sponsors, the Department of Energy and its predecessor agencies, were asking for very significant redirection of research efforts to respond to their new needs and new priorities.

Such pressures of growth, redirection, and internal reevaluation have certainly been sources of strain to laboratory staff. In particular, we have been under great constraints in the matter of space and facilities. However, in spite of these exigencies, the laboratory has functioned well and the staff has been uniformly supportive and understanding.

A number of new programs have been started during the last two years. Among them, the following are especially worthy of note.

Magnetic Fields. We have been given the assignment to launch a major new biological effects program to examine the action of intense and moderate magnetic fields on biological systems. New large-field magnet systems have been built and are now operating.

Human Epidemiology. Our medical staff, in cooperation with California State Health Department investigators, are examining the effects of employment in the petroleum refining and transporting industry on health. In addition,

we have launched a retrospective study of the health effects of long-term exposure to low-level magnetic fields by examining the health status of workers in national laboratories who have had long occupational exposures from accelerators and other magnetic devices.

Space Radiation Health Effects. The prospective development of the Space Power Satellite has renewed interest in the effects of extraterrestrial radiation environments. At the earth's surface, these environments can only be modeled by using the high-energy radiation beams of the LBL Bevalac. We have started a number of programs on the late effects of these heavy ions with the joint support of DOE and NASA.

Bevalac Radiotherapy. One program that the laboratory has been pursuing for some years, the applications of accelerated heavy ions in radiotherapy, is continuing to grow in new and interesting directions. Helium ion therapy has now been used on over 40 patients with tumors of various regions of the body. The program on treatment of pituitary tumors by helium ion radiation also continues to yield positive results. The newer developments include the use of the carbon ion beam of the Bevalac for the treatment of human tumors. These later studies started in the last half of 1977 and are expected to continue.

During 1977 the scientific staff has participated in numerous meetings and conferences. At the meeting of the Electron Microscope Society of America in Boston, Massachusetts, in August 1977, the first prize in the Physical Sciences Division was awarded to Drs. J. B. Pawley, T. W. Hayes, W. S. Tyler, and G. L. Fisher of LBL for their exhibit, "Multi-Element Mapping of Fly-Ash Particles in Lung."

Several workshops and conferences were held at LBL under the sponsorship of senior staff from the division.

Workshop on Carcinogenesis and Other Later Effects of Heavy Ions, October 20-21, 1977. Chaired by E. J. Ainsworth.

Conference on Carbonaceous Particles in

the Atmosphere, March 1978. This was sponsored by several divisions, and included T. W. Hayes from this division.

Miniconference on Microdosimetry, January 31, 1978. Chaired by S. B. Curtis.

Workshop on Research Needs in Actinide

Biology, held at the Battelle Seattle Research Center, April 5-7, 1977. Arranged and chaired by P. W. Durbin.

This report summarizes some of the highlights of the Division's scientific effort during 1977.

2. RESEARCH MEDICINE

The Research Medicine Group under the leadership of Dr. Thomas F. Budinger seeks new knowledge about human biochemistry in disease and in health. Its achievements contribute to our understanding of environmental effects on humans, for in addition to providing new methods for nuclear medicine, it gives us a method for assessing the biological impact of increased use of fossil fuels and other sources of energy production, including the effects of magnetic fields.

A major effort of this program is in the field of quantitative radionuclide imaging. Four approaches to noninvasive evaluation of human biochemical and physiological states are used: positron tomography for three-dimensional quantitative imaging; computerized whole-body scanning of isotope distribution; expired air analysis of $^{14}\text{CO}_2$ from the metabolism of injected pharmaceuticals; and whole-body counting.

This program is closely associated with the development of instrumentation and radiopharmaceuticals for radionuclide studies,

and the investigative studies using them. Its major emphasis is to apply the efforts of new instrumentation and radiopharmaceuticals to medical problems such as brain and heart blood flow and metabolism resulting from various disease and environmental conditions. Kinetic analyses are made based on the conservation-of-mass equation and precise information of the sequential tissue concentrations by three-dimensional imaging. The technology being developed embodies the concept of *in vivo* biochemistry of amino acids, fatty acids, and glucose.

This group continues its research effort in the hematology area. Currently studies of the megakaryocytic cell system are being carried out in an effort to understand platelet turnover and how the blood platelet count is regulated. This is important not only in a broad spectrum of blood disorders, but also in the evaluation of toxic environmental pollutants.

The highlights of the research effort during the past year are summarized in the following reports.

ALGORITHMS FOR COMPUTERIZED TRANSAXIAL RADIONUCLIDE RECONSTRUCTION

R. H. Huesman, G. T. Gullberg, W. L. Greenberg, and T. F. Budinger

A fully documented *Users Manual* was completed in 1977 for subscribers to the RECLBL Library. This library contains a package of computational subroutines that apply to the reconstruction of transverse sections from projection data. It has FORTRAN programs of reconstruction methods for emission and transmission tomography, which apply to data that represent the projection of density along parallel or diverging sets of straight-line paths (rays) through an object. The algorithms transform one-dimensional projections from multiple angles around the object to a corresponding transverse section through the object. Three-dimensional information is obtained by stacking successive transverse sections.

The *Users Manual* has examples of each

reconstructive methodology, and is distributed along with magnetic tapes of library source material.

Figure 1 shows an overview of the RECLBL Library with the names of the essential library subroutines. The library package applies to three-dimensional reconstruction problems that arise in medical and physical sciences. It includes programs for medical applications that can be used both for the determination of tissue attenuation coefficients using x-ray transmission data and for the determination of radionuclide concentration using data from nuclear medicine detectors. Work continues on library revisions and additions, and as these are tested and implemented they are made available to subscribers.

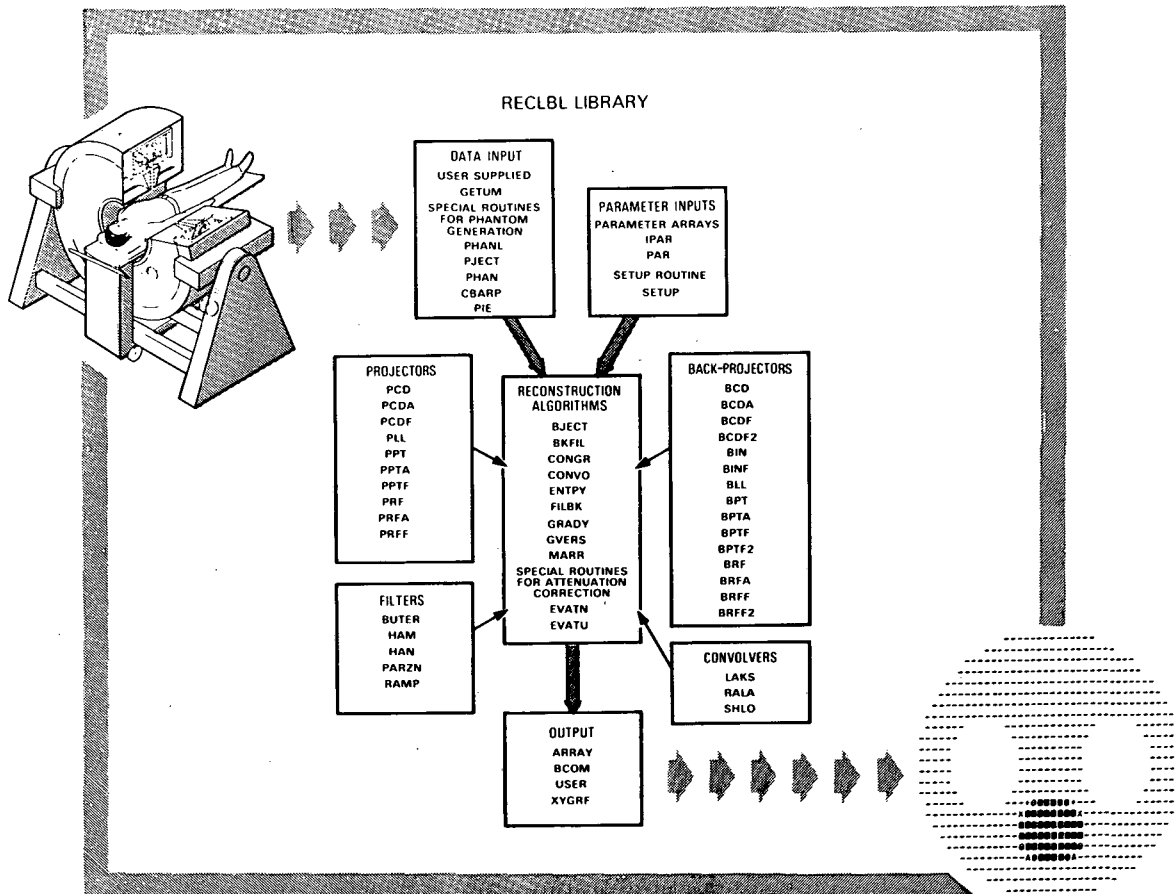


Figure 1. An overview of the RECLBL Library. There are nine user called reconstruction subroutines. PROJECTORS, BACK-PROJECTORS, CONVOLVERS, and FILTERS are passed to the RECONSTRUCTION ALGORITHMS as external subroutines. The data are input using the subroutine GETUM, and the parameter arrays IPAR and PAR are input using the subroutine SETUP. The reconstructions may be displayed using special output subroutines.

INSTRUMENT DEVELOPMENT FOR MEDICAL STUDIES

H. O. Anger

INTRODUCTION

In this program instruments are developed which utilize radioisotopes for biomedical studies. A major portion of this effort is involved with instruments used for imaging the distribution of gamma-ray and positron-emitting isotopes in animals and the human body. These instruments are used for the diagnosis of disease and play an important role in the study of biological effects of radiation and environmental toxic agents and the study of bodily distribution of any material that can be tagged with a radioactive tracer, including pollutants of all kinds.

TOMOGRAPHIC EMISSION SCANNER

The multiplane tomographic emission scanner, pictured in Figure 1, was developed under this program and a method has now been implemented for obtaining multiple oblique images from the instrument without turning the patient or the collimator at an oblique angle. Figure 2 shows typical multiangle views obtained from a bone scan patient. These images were obtained by manipulation of the same counting data that produce the multiplane tomographic images. Both kinds of images are obtained simultaneously during a single scan with no increase in the scanning time.

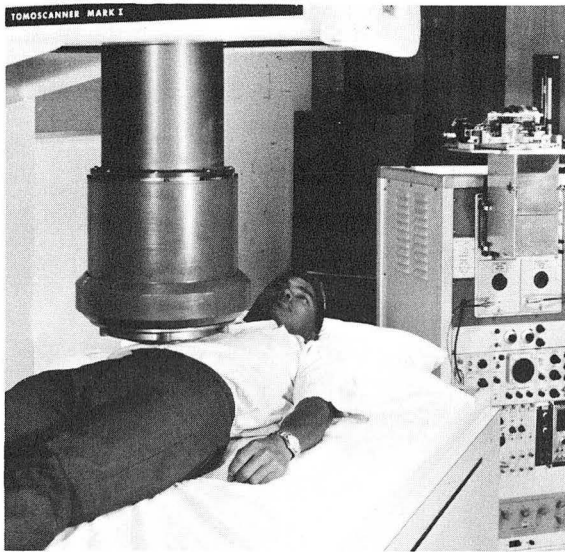


Figure 1. Multiplane tomographic emission scanner.

A preliminary clinical evaluation of the multiangle readouts from the tomographic scanner was conducted this past year at the University of California Medical Center in San Francisco, in collaboration with Dr. P. Hoffer (DOE Contract Con. #904-3-34; Radiology: Nuclear Medicine). The result from a limited number of patient studies is that the multiplane tomographic readouts were superior to the multiangle readouts in nearly all cases. They were also superior to conventional (nontomographic) bone scans, which were obtained by means of scintillation camera with parallel-hole collimator and moving patient table. The multiplane tomographic readouts have better overall resolution than the multiangle readouts, which have fewer dots per image and are therefore nearly always statistics-limited. Furthermore, the depth of a lesion (the distance from the collimator) is clearly shown in

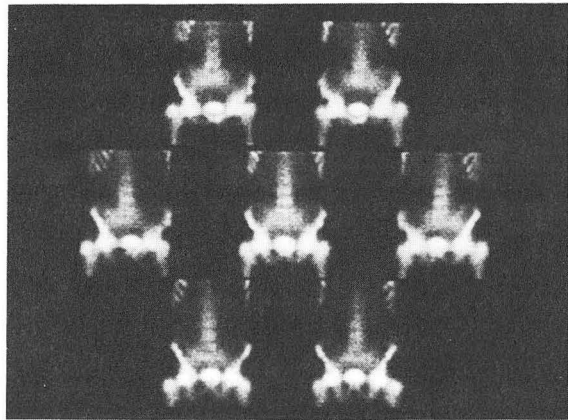
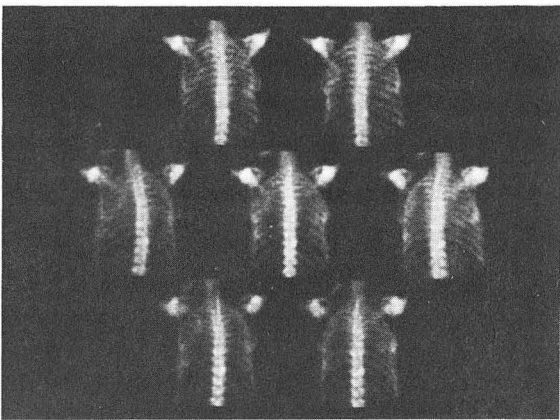
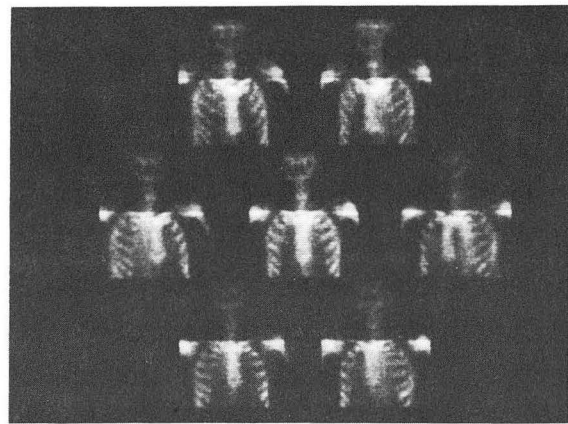
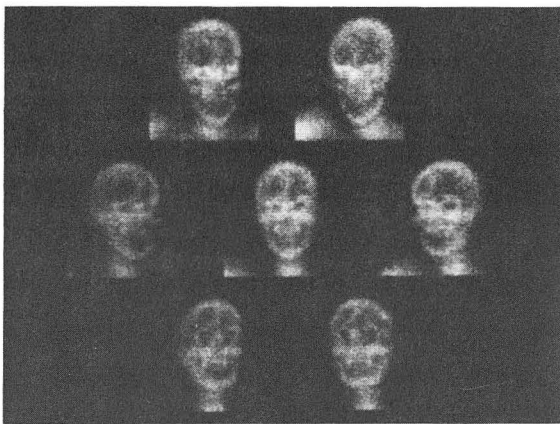


Figure 2. Typical multiple views of bone scan patient taken with multiplane tomographic scanner. This was the first bone patient scanned using oblique readout method.

the multiplane tomographic readouts, but is not shown in the multiangle readouts because they are essentially nontomographic. It was originally thought that the multiangle readouts would be useful for seeing around interfering overlying bone, but interference of this kind is usually not a problem in clinical bone scanning.

This instrument has been brought back to Donner Laboratory where new phototubes with higher quantum efficiency have been installed and circuit changes were made to improve the inherent resolution of the upper (8-in.) and lower (11-in.) detectors. Studies with phantoms will be performed to determine if improvements can be made in the multiangle readouts. Additional clinical trials will be conducted at Donner Laboratory. Scanners modeled after this instrument are now available commercially and dozens of these units are currently in use in research hospitals.

DUAL-AREA CARDIAC PROBE

The dual-area cardiac probe provides a portable, relatively inexpensive instrument to obtain cardiac ejection fraction. This essentially noninvasive, risk-free outpatient procedure, which can be repeated at frequent intervals, shows promise of being a significant supplement to conventional x-ray angiocardiography. The dual-area cardiac probe, constructed at Donner Laboratory, is shown in Figure 3. The counts are displayed in graphic form and provide quantitative information on the amount of radioactivity present under the probe as a function of time. For example, a stroke-by-stroke reading of the left ventricular ejection fraction could be obtained. This instrument has been moved to the Veterans Administration Hospital in San Francisco for clinical trial. The probe is being

tested in the cardiac operating room for evaluating the function of the left myocardium immediately before and after coronary bypass surgery. It is also being used as a portable instrument in the wards to evaluate cardiopulmonary problems and to help select satisfactory candidates for valve replacement and other kinds of heart surgery. The evaluation program is being conducted by Dr. Donald C. Van Dyke, a previous member of the Donner Laboratory staff.

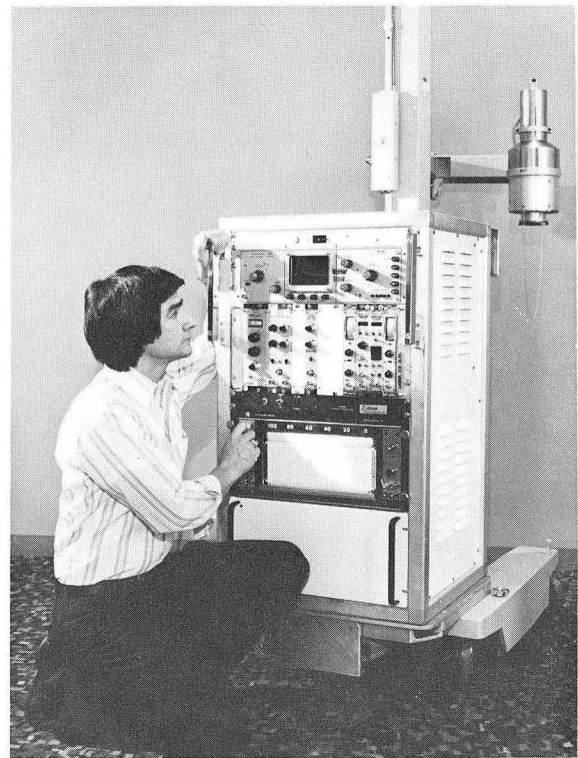


Figure 3. Dual-area cardiac probe.

INSTRUMENTATION FOR THREE-DIMENSIONAL TOMOGRAPHY

S. E. Derenzo

A major effort in the Research Medicine Group has been the construction of an unique "new" instrument for the three-dimensional imaging of positron-labeled compounds in the human body. The system consists of a continuous ring of 280 rectangular (8 mm × 30 mm × 50 mm) NaI(Tl) detector crystals that completely encircle the patient (Figs. 1 and 2). The instrument provides a transverse section image of any part of the human body.

When a positron is emitted by the labeled compound, it travels only a few millimeters and annihilates with an electron to produce two 511-keV gamma rays that are emitted in very nearly opposite directions. When two crystals detect gamma rays within 15×10^{-9} sec, the line of position between the crystals is stored in high-speed semiconductor

memory. Each of the 280 crystals can be in time coincidence with 105 opposing crystals, resulting in 14,700 lines of position that criss-cross throughout the 50-cm patient port. Several million events can be collected in a few minutes and a mathematical procedure called "computed tomographic reconstruction" then produces a clear (7.5-mm FWHM resolution), high-contrast image of the isotope distribution in the transverse section (Fig. 3). The patient bed is moved to image other transverse sections.

This instrument was designed to perform one of the most difficult goals in medicine—imaging blood flow in the muscle of the beating heart with high resolution. In addition, it will be used in the study of flow and metabolism in the brain, lungs, kidneys, and bone marrow. Specific medical projects include a study of the brain biochemistry in schizophrenia, a study of the glucose and fatty acid metabolism of heart muscle, and an investigation of methods for treating heart attacks by measuring the size of the affected muscle in response to various treatment schemes.

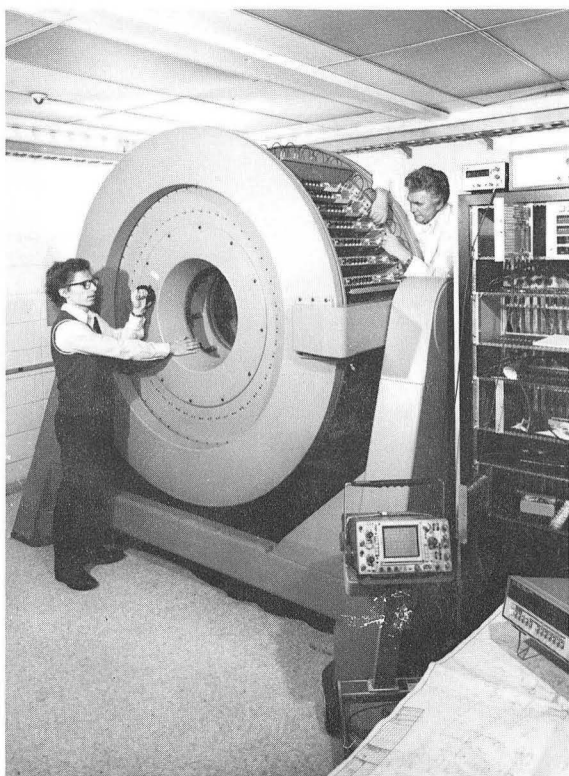


Figure 1. Donner 280-crystal positron tomograph. The surrounding ring of crystals and phototubes makes 14,700 measurements of the internal distribution of a positron-emitting compound. Computer processing reconstructs images that tell how vital organs are functioning.



Figure 2. Donner 280-crystal tomograph tilted to show detector assemblies. One of the two adjustable side shields with its 3-mCi transmission source is shown in the foreground.

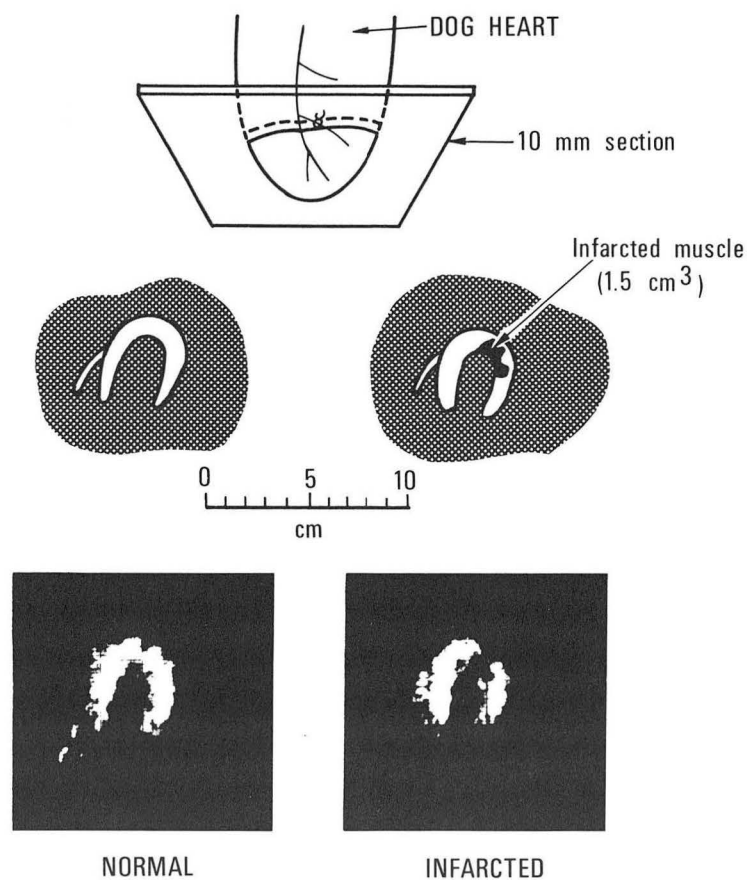


Figure 3. Images of normal and infarcted heart muscle taken after i.v. injection of 5 mCi of rubidium-82 ($t_{1/2} = 75$ sec). For the normal heart image 250,000 events were collected in 3 min. For the infarcted heart image 600,000 events were collected in 4 min.

METABOLISM OF BRAIN DISORDERS

T. W. Sargent

Our program is concerned with investigations of brain metabolism in central nervous system disorders. We are developing metabolically specific radiopharmaceuticals for use with specially designed instrumentation available only at LBL. Our interest is currently focused on the catecholamine neurotransmitters, which have been implicated in diseases such as schizophrenia and other psychoses. This technique will also be applied to determine the effects of pollutants (especially ozone) on catecholamine metabolism.

We are developing radioisotope methods for investigation of brain metabolism *in vivo*, with the aim of eventually applying these methods to human patients. We synthesized

the radioiodine-containing dopamine analog, 4-I-DPIA, and studied its brain uptake in dogs and monkeys. This compound is of interest in the study of mental function because it is structurally similar to dopamine and to amphetamine, both of which are implicated in schizophrenia—the former as a neurotransmitter, and the latter as an exogenous inducer.

The distribution of 4-I-DPIA in animals was studied by whole-body scanning, sacrifice and organ counting, and three-dimensional reconstruction tomography of the brain. After administration of iodine-123 labeled 4-I-DPIA in the monkey, the rate of accumulation of ^{123}I in the brain was rapid, with a half-time of 8 sec. The most unusual finding was the

observation of uptake of radioactivity in the eyes of both dog and monkey. The three-dimensional reconstruction of this study is shown in Figure 1. Dissection of the retina away from the lacrimal glands and the other eye tissues showed that the activity in the retina was ten times that in the surrounding tissues. The concentration of activity in the retina on a per-gram basis was about five times that in other central nervous system tissues, and was exceeded only slightly by that of the lung.

This new radiopharmaceutical, 4-I-DPIA, is of interest not only as an agent for positive imaging of the normal brain, but also for studies of the metabolic basis of schizophrenia. We are presently developing synthetic techniques for labeling the naturally occurring amino acid precursors of brain catecholamines, dopa and tyrosine, with two short-lived isotopes, 20-minute carbon-11 and 10-minute

nitrogen-13. With these compounds and the positron ring camera, we will be able to obtain quantitative images of the distribution in the brain as it changes over time intervals as short as 10 sec.

Using a different method of measuring radioisotopes, we have applied the established technique of measuring $^{14}\text{CO}_2$ expired from animals given compounds labeled with ^{14}C . Our new application consists of injecting ^{14}C -carboxyl-labeled tyrosine and dopa into the brain of rats and using the output of $^{14}\text{CO}_2$ as a direct measure of the rate of production of dopamine. Various drugs were found to inhibit or enhance dopamine production, and we have developed a hypothesis for a mechanism of failure in catecholamine metabolism that could be the cause of schizophrenia. We are presently designing experiments to further test this hypothesis.

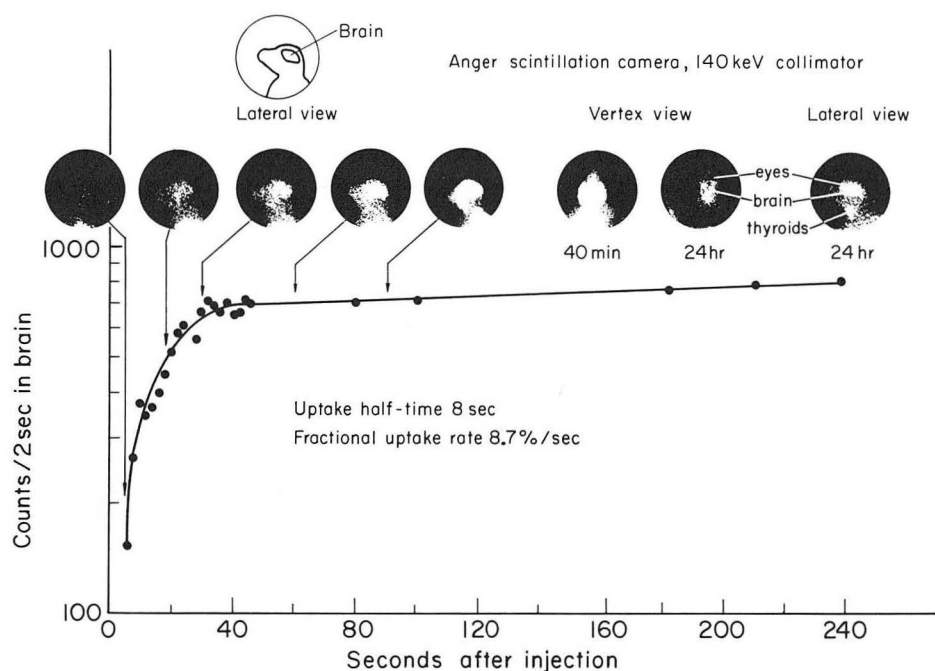


Figure 1. Brain uptake of ^{123}I in monkey (*Macaca radiata*) after administration of iodine-123-labeled 4-I-DPIA. The uptake curve was obtained at 2-second intervals from the area of interest shown in inset. Early pictures are keyed to curve at the time they were obtained. Later images, with different views, are also shown.

DEVELOPMENT OF RADIONUCLIDES AND RADIOPHARMACEUTICALS FOR EXPERIMENTAL MEDICINE

Y. Yano

Radionuclides and radiopharmaceuticals are developed in this program for use in scintigraphic and dynamic quantitative studies, which allow investigation of human physiology and metabolism by noninvasive procedures. The value of these studies in the early diagnosis of cancer, heart disease, brain disorders, and other metabolic abnormalities has long been recognized, and today we are becoming increasingly aware of their important role in evaluating the effects of various environmental factors on man's physiology. Our activities include the production and chemical separation of accelerator- and reactor-produced radionuclides; the development of radioisotope generators from which a short-lived daughter radionuclide can be "milked" from its long-lived parent; and the development of labeling methods or synthesis techniques for the preparation of radioactive chemical compounds, which either are selectively taken up in various tumors and organs or provide information on metabolism and perfusion rates.

The recent advances in positron cameras and positron ring detectors for transverse-section tomography have created renewed interest in positron-emitting radionuclides. We have been involved with the cyclotron production of carbon-11, nitrogen-13, and fluorine-18 for chemical synthesis of labeled amino acids, fatty acids, sugars, or other biochemical compounds of interest to biomedical investigators.

Carbon-11 as $H^{11}CN$ is being produced for the synthesis of ^{11}C -valine by the Oak Ridge National Laboratory "bomb" method. Many millicuries of amino acid are being used in animal distribution studies. Carbon-11 dioxide will be produced for the synthesis of ^{11}C -methionine, ^{11}C -palmitate, and for the possible β -carbon labeling of ^{11}C -dopa.

Nitrogen-13 is being produced by the proton irradiation of an H_2O target. The target vessel, methods for the automated transfer of $^{13}NO_3^-$ in the H_2O target and methods for the distillation and collection of $^{13}NH_3$ have been developed. Nitrogen-13 has been used in joint studies with A. Gelbard for the enzymatic synthesis of ^{13}N -glutamate and ^{13}N -valine. The distribution of the ^{13}N -amino acids in

animals under different conditions of diet, fasting, and so forth, is currently studied. A comparison of the ^{13}N -amino-acid and ^{11}C -amino-acid distributions in animals will also be done.

Investigators in the myocardial infarction imaging program at Donner Laboratory were interested in merging the benefits of the rubidium-82 generator system with the high-efficiency positron imaging system. The ^{82}Rb generator (see Fig. 1) will undergo improvements in column design, valving, and ion exchanger to deliver up to 30 mCi of ^{82}Rb per elution with less than 10^{-6} breakthrough of ^{82}Sr under long-term use involving many elutions. This is a very simple and highly effective system. Both bolus and continuous infusion studies will be done to measure uptake and washout over specific areas of interest such as the brain, heart, and kidneys.

Distribution studies of zinc-62 thioglucose

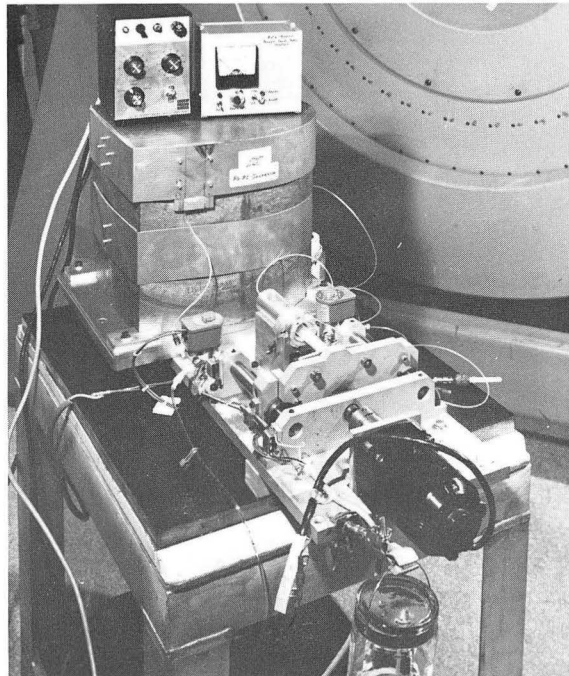


Figure 1. Semiautomated radionuclide generator for the separation of rubidium-82 (half-life 75 sec) from strontium-82 (half-life 25 days). ^{82}Sr is prepared at the Berkeley 88-Inch Cyclotron or Los Alamos Scientific Laboratory. The ^{82}Sr is loaded on a weakly acidic cation exchange resin. Pure ^{82}Rb is obtained by eluting the column with 2-3% saline solution.

in mice, with Dr. H. L. Atkins of Brookhaven National Laboratory, gave a pancreas-to-liver ratio of 3.5. This ratio was enhanced to 4.4 when porcine growth hormone was given intraperitoneally at the time of thioglucose injection. The kinetics of zinc-62-labeled histidine distribution were determined in male beagle dogs. Uptake was noted in the prostate of the dog 17 hours after intravenous administration of the compound, as shown in Figure 2. Further studies will be done using zinc-62 in pancreas and prostate studies.

An electrolytic system for Sn(II) reduction of $^{99m}\text{Tc(VII)}$ to $^{99m}\text{Tc(IV)}$ has been developed and used to label radiopharmaceutical agents such as: (1) formycin and formycin B, to compare uptake in transplanted tumors of the two compounds; (2) folic acid for evaluation as a tumor agent and for possible use as a pancreas or gall bladder agent; and (3) $^{99m}\text{Tc-TRH}$

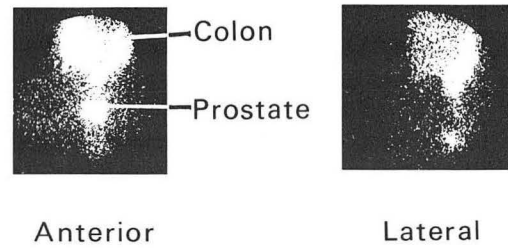


Figure 2. Uptake of zinc-62-labeled histidine in prostate of beagle dog 17 hours after intravenous administration of 200 μCi . Anger positron-camera image shows uptake in prostate and colon, in anterior and lateral views. Identification of prostate was made at necropsy.

(thyrotropin releasing hormone) for *in vivo* studies of hypothalamic pituitary function.

EPIDEMIOLOGY OF THE EFFECTS OF MAGNETIC FIELDS ON HUMAN BEINGS

T. F. Budinger

Because of the confusion and uncertainty regarding the biological effects of varying exposures to magnetic fields, the present recommended safety standards for workers in our country, and elsewhere, can only be regarded as tentative. Carefully designed and adequately documented studies are needed in this field, and we have initiated an epidemiological study of exposed personnel at the DOE national laboratories and other institutions to look into this problem.

This past year, substantial progress has been made at our initial study site, Lawrence Berkeley Laboratory. Magnetic field strengths were determined in the work environment for the Bevatron, the 184-Inch Synchrocyclotron, the 88-Inch Cyclotron, and the Heavy-Ion Linear Accelerator. On the basis of exposure to requisite magnetic field strengths, 250 employees have been selected as subjects for this study. Matching controls, or unexposed personnel were selected on the basis of age, sex, years of service, and similar job duties. The medical and personnel records have been

encoded on all subjects and controls using an anonymous coding scheme to protect individual identities for the entire period of their employment. The program has been designed so that the data may be translated from coded form into various tabular formats and statistical analysis routines. Preliminary statistical analyses have been done for the parameters of cardiovascular disease and cancer.

Site visits were made to the Los Alamos Scientific Laboratory (LASL) and to Brookhaven National Laboratory (BNL). The facilities of BNL are expected to provide a substantial population of personnel with cyclotron-level exposure of 5 G for four working hours per day, as well as some long-term exposures.

The understanding of magnetic field effects has value not only for determining reliable safety standards for those who work around magnetic fields, but also for applications in medical diagnostic studies. High magnetic fields may become an important tool for measuring tissue characteristics and blood flow using nuclear magnetic resonance principles.

KINETICS OF MEGAKARYOCYTE AND PLATELET TURNOVER

S. N. Ebbe

We are carrying out various studies of the megakaryocytic cell system in an attempt to understand the way it responds to homeostatic controls, the nature of those controls, and the responses of this cell system to cytotoxic agents.

Experimentally induced thrombocytopenia is known to stimulate individual megakaryocytes to become hyperpolyploid and larger than normal (megakaryocytic macrocytosis). It is thought that this change is mediated, in part, by a humoral thrombopoietin, the secretion of which is stimulated by a low platelet count. In an attempt to shed some light on the possible mechanisms involved in this phenomenon, we have studied three situations in which megakaryocytic macrocytosis occurs without the presence of thrombocytopenia in an effort to understand how reduced numbers of megakaryocytes can maintain normal platelet production.

Two strains of genetically anemic mice (Sl/SI^d and W/W^v) show megakaryocytic macrocytosis without thrombocytopenia. There are severe reductions in numbers of megakaryocytes, but there are normal complements of circulating platelets; both the platelet number and platelet mass are normal. Parabiotic experiments carried out with Sl/SI^d mice and their normal +/+ controls demonstrated that the prominent macrocytosis of megakaryocytes characteristic of Sl/SI^d mice is due to a humoral factor that can be transmitted to a normal parabion. This humoral factor may prove to have some of the characteristics of thrombopoietin. In the control parabiotic study with two normal +/+ mice, in which the stimuli to megakaryocytopoiesis would have been of the "nonspecific" type (i.e., physical trauma, stress, inflammation, and so forth), it was noted that a modest degree of megakaryocytic macrocytosis did develop, showing this change may occur in response to intense nonthrombocytopenic stimulation.

Sublethally irradiated mice (650 r, cesium-

137) developed and recovered from radiation-induced thrombocytopenia during the first three weeks after irradiation; megakaryocyte numbers were reduced to 10% of normal. Then, during the subsequent seven weeks, platelet counts remained normal, or were only slightly below normal; there was partial recovery of megakaryocytes, but their number in the marrow reached only about 50 to 60% of normal. During this latter period, when platelet production was maintained at normal or nearly normal levels by reduced numbers of marrow megakaryocytes, the megakaryocytes showed an increase in size of about 50%. This finding suggests that there was stimulation of megakaryocytopoiesis and substantiates the notion that autoregulation may occur, independent of the level of circulating platelets. The extent to which splenic megakaryocytopoiesis may compensate for the deficiency in the marrow is not clear; to investigate this further, experiments are currently being done to study the effect of sublethal dose of radiation on platelet counts in splenectomized mice.

We also observed an increase in megakaryocyte size after administration of hydroxyurea to normal mice—another situation in which a normal platelet count is observed with a reduced number of megakaryocytes.

All of these studies, considered together, raise the strong possibility that stimulation of megakaryocytopoiesis may be initiated by reduction of megakaryocytes themselves, independent of the platelet count. Health problems to which these studies may have relevance include a broad spectrum of hematopoietic dysplasias, thrombocytolytic states, and nonspecific thrombocytoses.

We are also developing an assay for thrombopoietin (following the techniques of Evatt et al.) so we will be able to measure thrombopoietin in genetically anemic mice and other states of perturbed thrombocytopoiesis in animals.

Donner Clinic

DONNER CLINIC OUTPATIENT FACILITY

S. N. Ebbe

As part of a program to determine the long-term effects of therapeutic use of radioisotopes (^{32}P and ^{131}I), the clinic has continued to monitor patients with hematological and thyroid disorders. In addition, the clinic has maintained the morally responsible position of providing consulting services and medical care for patients who have been referred for study because of the investigative interests of scientists at the Donner Laboratory and the availability of unique tools or procedures for study of their disease.

During calendar year 1977, 243 patients were seen 1,013 times by clinic physicians; 27 of these patients were new referrals. In addition, there were 157 clinic visits to the nursing and technological staff for treatment or tests. Patients were seen for the following conditions:

	No. of patients
Polycythemias	96
Other myeloproliferative disorders	21
Other leukemias and lymphomas	11
Anemias	10
Miscellaneous hematological disease	7
Hemochromatosis	16
Carcinoma of the thyroid	39
Other thyroid disorders	<u>43</u>
	243

During the same period, over 4,200 laboratory tests and treatments were performed by clinic personnel (non-M.D.). Of these procedures, only 65% were directly related to patient care while the remaining 35% were performed for research projects.

Continuing projects being conducted include the following.

1. The data collection for the long-term clinical science of thyroid cancer and its treatment was completed and is now being prepared for publication.

2. The clinic has participated in the evaluation of treatment for polycythemia vera by the Polycythemia Vera Study Group (Mt. Sinai Hospital, New York) and has continued to contribute research data to this group.
3. A study of the association of viral particles with leukocytes in 68 blood samples from patients with polycythemia, leukemia, or Hodgkin's disease, and normal individuals is well under way. The purpose of the study is to utilize stereoscopic high-voltage electron microscopy (EM) to search for viral clusters as possible etiologic factors in the diseases under study. Low-voltage EM has been completed on 10 subjects, and the first high-voltage studies have started. The tissues have been coded and will be identified only after analysis is complete.

New projects now in progress include the following.

1. Studies of human blood platelets. Essential items of equipment are being acquired and preliminary tests are being done in animals. Platelet survival studies, using ^{111}In -oxine as a label, have been started in rabbits. Donor platelets are labeled *in vitro* then injected into recipients. Survival is measured from platelet-bound radioactivity in serially obtained blood samples. Distribution of the label in the recipient's plasma and red cells is determined. Whole-body imaging is being done to determine if the organ distribution of platelets can be evaluated in this way. A platelet sizing technique, utilizing the Coulter principle with hydrodynamic focusing, has been tested.
2. Evaluation of residual thyroid function in individuals treated for hyperthyroidism more than five years ago. Patients are being asked to participate in studies of thyroid hormone and antibody levels, thyroid uptake and scintillation photography with ^{123}I , and response to thyroid stimulating hormone.

3. A program for the collection of large amounts of urine from two patients with severe hypoplastic anemia for preparation of human urinary erythropoietin (EP) for research use has been initiated.
4. The medical records of patients with polycythemia, dating back more than 35 years, are being analyzed to determine the effects of different forms of therapy (³²P, chemotherapy, phlebotomy) on the course of the disease and the development of

complications (myelofibrosis, leukemia, nonhematological disorders, thrombosis).

The Research Medicine Outpatient Clinic provides medical services for research projects throughout Donner Laboratory. The nurse, medical secretary, licensed clinical technologists, staff physicians, and medically equipped facilities are available to all researchers in the Donner Laboratory.

3. DONNER PAVILION

Donner Pavilion, which houses the metabolic facility, is directed by Dr. John A. Linfoot. Since 1958, high energy 910-MeV alpha particles have been used to suppress pituitary function in treating patients with disorders of the pituitary gland and with diabetic retinopathy. This treatment of pituitary tumors has become an internationally recognized therapeutic procedure. The long-term follow-up on these patients makes possible a unique investigation of the biological properties of the human pituitary. These data provide a valuable source of information regarding the acute and long-term effects of localized heavy ions on the central nervous system, on normal and tumor tissues, and on peptide hormone secretion. This project continues to make significant contributions to the understanding of the endocrinopathies associated with the pituitary.

Our ongoing work continues to assess the effectiveness and consequences of alpha

particle pituitary irradiation (APPI) as therapy of pituitary tumors, and to evaluate the long-term effects of APPI on the vascular complications of patients with diabetes mellitus. In addition, an understanding of the endocrine pathology associated with tumors of the pituitary is being sought by evaluating the molecular changes (heterogeneity) in pituitary peptide hormones and the influence of hypothalamic releasing factors. Dr. E. Wiedemann, who joined the Donner Pavilion staff in the fall of 1976, has started an investigation of somatomedins in patients with pituitary tumors. He has also developed an application of a radioimmunoassay of human beta-lipotropin, a pituitary hormone which hitherto had been poorly understood.

The highlights of our research effort over the past year are summarized in the following reports.

TREATMENT OF PITUITARY TUMORS WITH ALPHA PARTICLE IRRADIATION

J. A. Linfoot and E. Wiedemann

At the Donner Pavilion, three types of pituitary tumors are treated in the alpha particle pituitary irradiation (APPI) program.

TREATMENT OF ACROMEGALY

Two hundred and ninety-nine patients with acromegaly have been treated in the past 20 years. Although there is no general agreement on the optimum goal of therapy in the treatment of acromegaly, tumor control as well as adequate lowering of the elevated growth hormone (hGH) concentrations and the associated metabolic changes were the ultimate goals. Ninety percent of the patients have shown a significant fall in hGH, which has been associated with improvement of physical features and metabolic changes, which include glucose intolerance, loss of insulin resistance, and fall in serum phosphorus. Figure 1 shows the changes in serum growth hormone, measured by radioimmunoassay, following treatment with

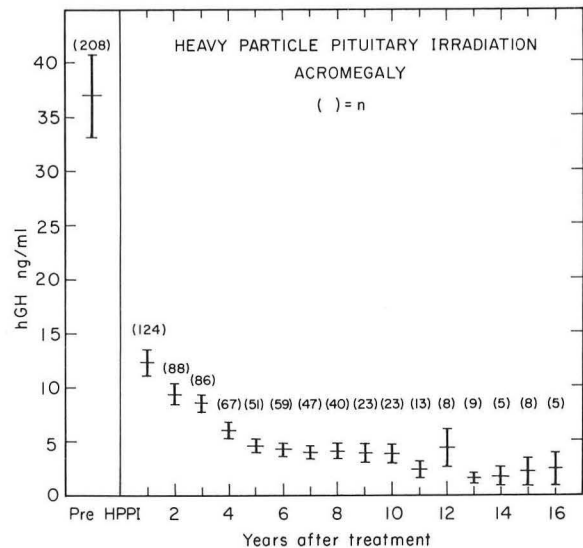


Figure 1. The chronological decrease in fasting growth hormone (hGH) levels ($\bar{x} \pm \text{SEM}$) following 910-MeV alpha particle therapy in pituitary tumor patients with acromegaly [() = n].

APPI. Excluded from this evaluation are those patients who have been treated recently and for whom we have no follow-up information, and all patients who had unsuccessful surgery prior to APPI. These data show that there is a 50 to 60% fall in growth hormone level within 6 to 12 months; values continue to fall to what we consider the normal range of 5 ng/ml within five to six years.

TREATMENT OF CUSHING'S DISEASE

Since 1959, we have treated 64 patients with Cushing's disease due to bilateral adrenocortical hyperplasia. The patients were treated with 6,000 to 15,000 rads administered in one to two weeks. Following treatment, there was not only a fall in cortisol levels but some tendency for the abnormal circadian rhythm to return to normal (see Fig. 2a). Prior to treatment, the overnight dexamethasone suppression studies (see Fig. 2b) demonstrate a lack of suppression of plasma cortisol to a level less than 5 $\mu\text{g}/\text{dl}$ in all

the patients. Following APPI, the normal suppressibility returned in the successfully treated patients. Several patients have undergone total adrenalectomy because of relapse or delayed response. Some of these patients were treated prior to currently available adjunctive drug treatments and may have been subjected to adrenalectomy prematurely. Three patients received insufficient radiation by our current criteria. The overall response of is significantly better than that described by conventional radiation (33% in adults).

TREATMENT OF PROLACTIN-SECRETING PITUITARY TUMORS

Prolactin-secreting adenomas were the last group of pituitary tumors to become part of the pituitary irradiation program. By 1977 a sufficiently large number of patients with this type of tumor had been treated to warrant a comprehensive review of the results. Nineteen patients (13 females, 6 males), of whom 6 had

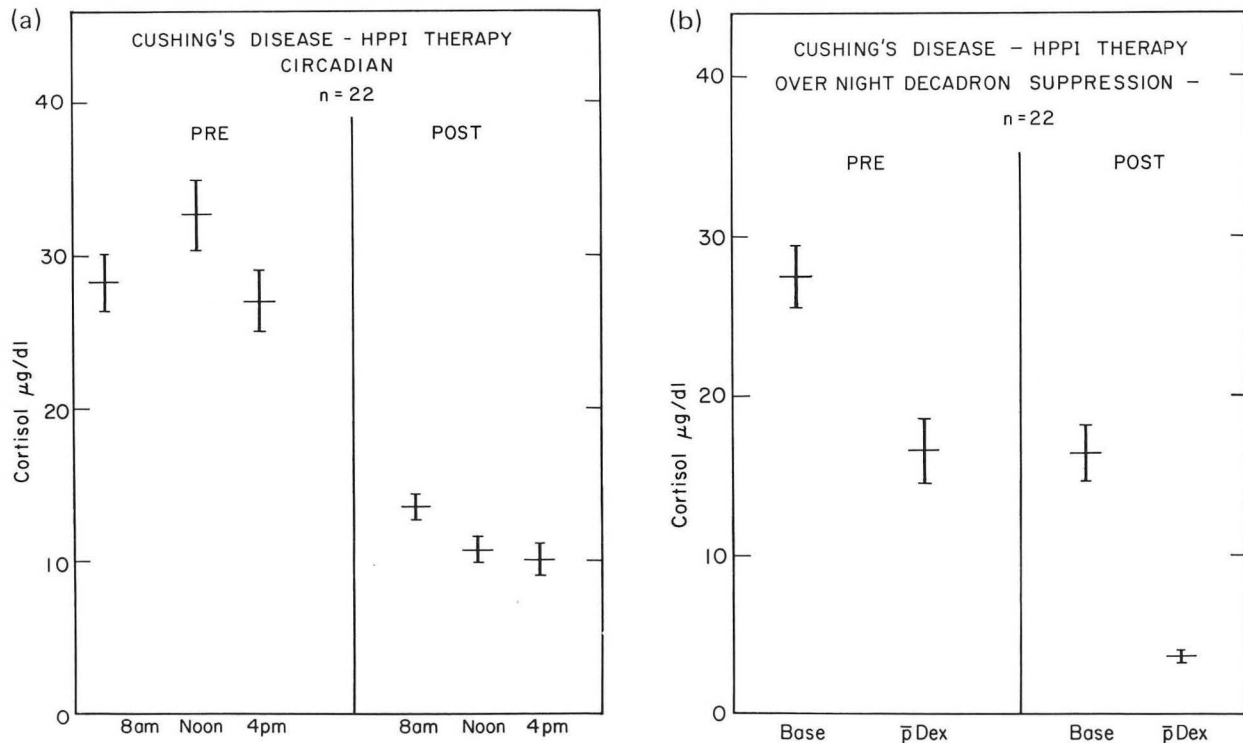


Figure 2. Changes in plasma cortisol levels in 22 patients with Cushing's disease due to bilateral adrenal hyperplasia before and after treatment with 910-MeV alpha particle pituitary irradiation (paired data). The left figure shows the subsequent fall in cortisol levels and shift in circadian rhythm toward normal. The right figure shows the fall in baseline cortisol levels to normal range and a return of normal dexamethasone suppression of the base value to less than 5 $\mu\text{g}/\text{dl}$ after treatment.

previously undergone unsuccessful pituitary surgery, were treated with doses ranging from 3,200 to 10,000 rad given in one to two weeks; all have now been followed for periods of one to seven years after APPI. Basal plasma prolactin concentration decreased in all except one patient. Pre-treatment prolactin concentration ranged from 27 to 2,526 with a median of 90 ng/ml, and post-treatment levels were 5 to 1,169 with a median of 25 ng/ml. Patients who had exaggerated prolactin responses to provocative stimuli prior to APPI developed blunted

responses after APPI. In 13 of the 19 patients, prolactin levels returned to the normal range after APPI; furthermore, in many female patients the lowering of plasma prolactin was associated with a cessation of galactorrhea and the return of menses. No neurological side effects were observed; hypopituitarism developed in 25% of the patients. These results demonstrate that APPI is comparable to or superior to transsphenoidal microsurgery or conventional photon therapy in patients with prolactin-secreting pituitary adenomas.

EFFECT OF HEAVY PARTICLE PITUITARY IRRADIATION ON VASCULAR COMPLICATIONS OF DIABETES MELLITUS

J. A. Linfoot and J. S. Nakagawa

A recent review of the long-term effects of alpha particle pituitary irradiation (APPI) revealed an apparent improved survival in many patients with proliferative retinopathy and diffuse diabetic microangiopathy. A favorable influence on diabetic nephropathy might explain these findings. Little data are available on the rate of progression in nephropathy, however. It has been reported that diabetes with constant proteinuria demonstrated a mean rate of decline in glomerular filtration rate (Δ GFR) of approximately 1 ml/min/month. To determine the Δ GFR in patients treated with APPI, Δ GFR was measured using endogenous creatinine clearance before and one, two, and three years after treatment. Three groups of patients were defined: Group (A) included 10 patients with proteinuria <1 gm/24 hrs., Group (B) included 23 patients with proteinuria between 1-4 gm/24 hrs., and Group (C) included 16 patients with proteinuria >4 gm/24 hrs. The data are presented in Table 1. All groups showed slower decline in GFR than predicted. Using paired t-tests the differences between observed and predicted GFRs were all significant ($p \leq 0.05$). Lesser significance was observed in Group (C) which had more advanced nephropathy than (A) and (B). The percentage of patients in each

group at various times after treatment who had less deterioration of GFR than predicted were: Group (A)—70%, 90%, 80%; Group (B)—65%, 72%, 83%; and Group (C)—46%, 67%, 83% respectively.

We conclude that APPI appears to have had a positive effect on diabetic renal disease and may be responsible for the improved survival of these patients, especially those with milder degrees of proteinuria and potentially reversible renal lesions.

Table 1. Changes in glomerular filtration rate (Δ GFR), using endogenous creatinine clearance, in patients with diabetic retinopathy treated with alpha particle pituitary irradiation.

Group	Pre-treatment proteinuria	Δ GFR (ml/min/mo.)		
		Years after treatment		
		1	2	3
A	<1 gm/24 hr	0.28	0.35	0.50
B	1-4 gm/24 hr	0.30	0.69	0.48
C	>4 gm/24 hr	0.95	0.42	0.46

INVESTIGATIONS OF SOMATOMEDIN IN PITUITARY TUMOR PATIENTS

E. Wiedemann and J. A. Linfoot

Somatomedins are a group of at least four hormone-dependent serum growth-factors believed to mediate the growth-promoting action and possibly other metabolic actions of pituitary elevated growth hormone (hGH). Because of their hGH dependence, the study of somatomedins in patients with pituitary disease can provide valuable insight into the physiology of these peptides. We have therefore begun an investigation of serum somatomedin activity in patients with pituitary tumors. We are using two assay systems, namely an *in vitro* bioassay recently introduced to the Donner Pavilion laboratory; and a radioreceptor assay performed in collaboration with Drs. Uthne and Martin Spencer at U.C. San Francisco. Three important results have emerged from the initial phase of the investigation:

First, the two assay methods are not exactly equivalent; they cannot substitute for each other but rather complement each other. Bioassayable somatomedin activity does not correlate well with plasma immunoreactive hGH concentration but is positively correlated with the fasting blood glucose concentration ($p < 0.01$). The bioassay therefore appears to be particularly sensitive to somatomedins, the concentration of which is increased in patients with chemical or frank diabetes mellitus. The radioreceptor detectable somatomedin activity, on the other hand, is not different in acromegalics with or without diabetes mellitus, but correlates very well with hGH concentration. These results could perhaps explain why only a minority of the acromegalics have diabetes mellitus and why the occurrence of diabetes is not clearly related to the degree of hGH hypersecretion.

Second, although radioreceptor-assayable somatomedin activity correlates well with plasma hGH concentration, it apparently reflects clinical remission of acromegaly following heavy particle pituitary irradiation better than plasma hormone levels. More extensive studies are required to confirm this finding. If verified, much time and effort could be saved in the follow-up evaluation of treated

acromegalic patients because somatomedin activity can be determined in a single serum specimen whereas evaluation of growth hormone secretion requires the assay of multiple samples obtained during more elaborate pituitary stimulation and suppression tests, because plasma hGH levels fluctuate considerably.

Third, among patients with other types of pituitary tumors, bioassayable somatomedin activity was found to be either normal or elevated in patients with Cushing's disease (Fig. 1) and normal in patients with prolactin-secreting pituitary tumors. Radioreceptor assayable somatomedin activity was normal in most patients with either disorder. Since hGH secretion is markedly impaired in most patients with active Cushing's disease and many with prolactin-secreting tumors, these results indicate that pituitary factors other than hGH are also involved in the regulation of the somatomedins.

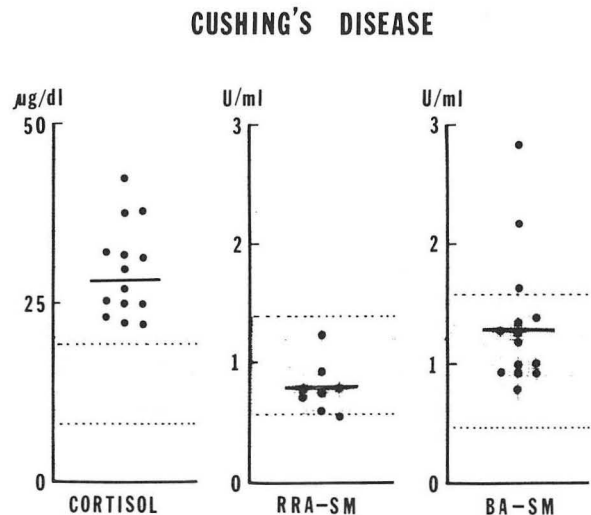


Figure 1. Comparison of fasting plasma cortisol concentration with radioreceptor-somatomedin (RRA-SM) and bioassayable-serum-somatomedin (BA-SM) activities in patients with untreated Cushing's disease. The cortisol levels are elevated, but the RRA-SM levels are normal; the BA-SM levels are elevated in some patients with Cushing's disease. (Normal ranges lie within dotted lines.)

DEVELOPMENT AND APPLICATIONS OF BETA-LIPOTROPIN ASSAY FOR PITUITARY TUMOR PATIENTS

E. Wiedemann and J. A. Linfoot

Beta-lipotropin (β -LPH) is a pituitary hormone, whose biological function is unknown although its chemical structure has been elucidated. Circumstantial evidence suggests that it may always be secreted together with ACTH (adrenocorticotrophic hormone). The recent demonstration that β -LPH may be the precursor or "pro-hormone" of the endorphins and enkephalins has aroused great interest, since these peptides act like morphine although they are produced *in vivo* by the brain and are believed to play key roles in pain perception, narcotic addiction, regulation of pituitary function, and mental disease. Investigation of the physiology of β -LPH has been hampered by the lack of a suitable assay method. Using a specific antiserum prepared in Dr. C. H. Li's laboratory, we have succeeded in developing the first specific and sensitive radioimmunoassay for human β -LPH in unextracted plasma. This assay has opened the way for a systematic investigation of the role of β -LPH in health and disease.

Initial results have already cast doubt on the assumption that β -LPH secretion always parallels ACTH secretion. For example, we were surprised to find elevated concentrations of β -LPH in plasma of a majority of patients with acromegaly, a disorder caused by hGH-secreting tumors (Fig. 1). This finding raises the intriguing question of whether increased β -LPH secretion could be involved in the pathogenesis of some cases of acromegaly, since endorphins and enkephalins, thought to be derived from β -LPH, have recently been shown to stimulate hGH secretion.

Another important result was the discovery that β -LPH may be a tumor marker in patients with pituitary Cushing's disease. We found β -LPH invariably increased in patients with radiographical evidence of pituitary tumors, but

was usually normal in spite of elevated ACTH levels in patients with Cushing's disease without significant x-ray abnormalities of the sella turcica. Although more experience is needed, it is clear that the β -LPH radioimmunoassay is a valuable tool to distinguish between pituitary hyperplasia and pituitary tumor in patients with Cushing's disease. Short of surgical exploration of the pituitary, this distinction presently can be made only if unequivocal abnormalities of the pituitary region are seen on x-ray films. This is not the case in perhaps as many as one-fourth of all patients with Cushing's disease. Because in these cases pituitary surgery does not cure the disease, these patients could be spared surgical pituitary exploration and be referred for pituitary irradiation instead.

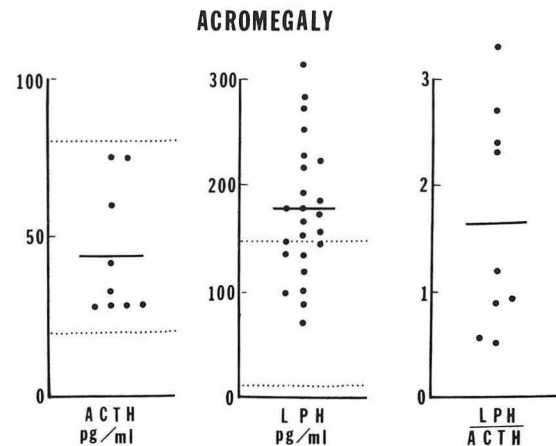


Figure 1. Comparison of plasma ACTH (adrenocorticotrophic hormone) and β -LPH (β -lipotropin hormone) levels in patients with untreated acromegaly. The mean ACTH levels were normal, but the mean β -LPH levels were significantly elevated. (Normal ranges lie within dotted lines.)

4. PERALTA CANCER RESEARCH INSTITUTE

The Peralta Cancer Research Institute (PCRI), directed by Dr. Adeline J. Hackett, was formed in May 1974 as an association of Peralta Hospital, Oakland, with the University of California, Berkeley. The Institute's goal is to encourage mutually beneficial interactions between basic researchers and clinicians practicing oncology. Thus, the tumor biologist gains clinical information needed to design new and perhaps more relevant model systems, and the clinician can be provided with important new and effective tools for the early diagnosis of disease and improved patient care. Since July 1977, PCRI has been affiliated with the Biology and Medicine Division of Lawrence Berkeley Laboratory.

PCRI's first research program, the Breast Cancer Studies Group, is concerned with developing techniques for early diagnosis of breast cancer and studying the biology of breast cancer cells, with the hope of developing improved therapeutic methods. This project requires the cooperation of women from the community who donate breast fluid samples,

which are examined for the presence of abnormal cells. Research studies are carried out with breast cell cultures developed from these samples. In addition, reports of the findings are sent to the donor's physician. Since the program's initiation, over 2,000 women have been studied, and early cancers have been detected in three women. In three other instances, lesions likely to become cancerous were detected and the women's physicians were alerted. These tumors were removed with only minor surgery.

The program of the Cell Culture Studies Group is concerned with the characterization of tumor cells derived from various human malignancies. These cells are maintained as cultures in the laboratory, thereby making it possible to investigate the growth properties, nutritional requirement, and hormone responsiveness of malignant cells and compare them with normal cells. The increased understanding of malignant cell behavior may lead to the development of new therapy protocols.

HUMAN MAMMARY TUMOR VIROLOGY

A. J. Hackett, H. S. Smith, and E. L. Springer

The elucidation of biological processes which cannot be feasibly studied in intact animals, as well as many types of controlled experiments on populations of human cells require the development of appropriate tissue culture systems. In the study of breast cancer, many unperformed experiments await the development of cell cultures which represent the different stages of tumorigenesis. An understanding of the parameters involved in the genesis of neoplastic mammary epithelial cells may aid in the prevention, detection and/or treatment of breast cancer.

We are studying the biology of human mammary epithelial cells as a basis on which to build effective measures for control of breast cancer. Clinical studies have demonstrated the usefulness of the breast Papanicolaou test in the detection of breast disease in asymptomatic women. Figure 1 illustrates one cell type found in breast fluid aspirates.

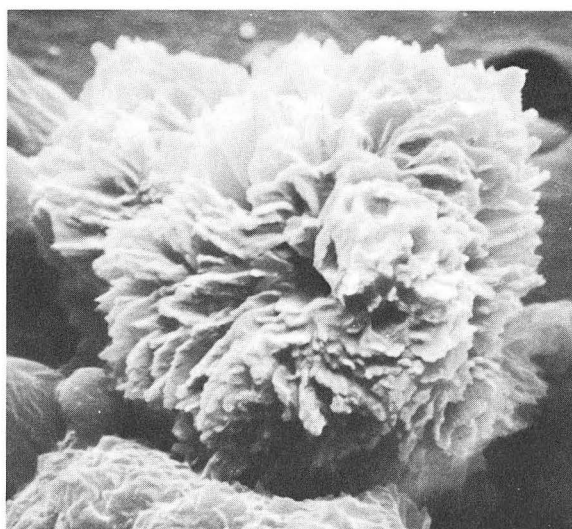


Figure 1. Scanning electron micrograph showing the undulating membrane of a foam cell or vacuolated histiocyte which is frequently found in breast fluid aspirates.

One breast tumor metastatic to bone and one metastatic to skin are in early stages of cell line development. Short term cultures of normal, benign and malignant mammary cells have been achieved from frozen pools of ductal and alveolar "organoids" isolated from breast tissue.

A quantitative analysis of expression of ultrastructural markers for malignancy has been developed which distinguishes normal, pre-malignant and malignant human breast cells.

Studies on cell-to-cell interactions show promise to develop into an approach for understanding the role of myoepithelial cells in the normal functional activity of the breast and in benign and malignant disease processes. Figure 2 illustrates observation of cell topography to identify morphological characteristics.

Preliminary study of lactate dehydrogenase isoenzyme patterns show correlation of

altered isoenzyme (L5/4) ratios in malignant mammary epithelial cells both in culture and from breast fluids.

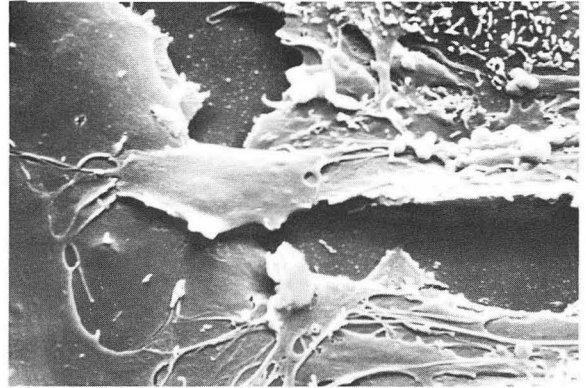


Figure 2. Scanning electron micrograph showing a cultured human mammary myoepithelial cell with a characteristically smooth surface interacting with a villous mammary carcinoma cell via a cytoplasmic bridge.

5. ENVIRONMENTAL PHYSIOLOGY

This group, led by Dr. John Schooley, studies the changes in physiological activity that occur as a living organism attempts to maintain homeostasis—the constant internal environment required for good health. For many years Donner investigators have studied and contributed significantly to the understanding of changes that take place when disease mechanisms alter homeostasis. Today, with the current interest in effects of environmental pollutants, these investigators are using their acquired knowledge and expertise to study changes that take place when pollutants, which arise primarily from nonnuclear technologies, exert their effects on the body's internal environment. They hope to provide screening tests for detecting the early effects of such pollutants and a scientific basis for successfully treating these effects.

Investigators have studied internal metabolic processes in several body systems of rodents to assess quantitatively the effects of representative types of environmental pollutants. Reported here are results of their investigations of pollutant effects on (1) the hematopoietic (blood-forming) system including studies of white cells, red cells, and platelets; (2) the metabolism of several protein and polypeptide hormones of the anterior pituitary gland, with the possible use of plasma levels of such hormones as early biological

indicators of pollutant exposure; and (3) the steroid hormone mechanism, looking at the effect on testosterone metabolism in mice.

The lung is the biological interface to the atmospheric environment, and some studies were directed at understanding environmental pollutant effects on growth and differentiation of lung tissue. Pulmonary macrophages, the large cells in the lung that engulf foreign material and thereby comprise the chief line of defense against inhaled bacteria, viruses, and inert particulates, come into contact with environmental agents at the lung interface. Investigators are studying subsequent changes in these cells, looking for agents that cause a decrease in the number of macrophages and/or change in their biological activities, which would have grave consequences for health.

Plutonium metabolism is being studied in monkeys to estimate the behavior of this heavy element in man. Investigators are also looking for biological effects of plutonium at low exposures such as might be encountered by individuals during the operation of nuclear power facilities. These investigations are directed toward developing appropriate protection standards for persons employed in the nuclear industry and for the general population.

EFFECTS OF ENVIRONMENTAL POLLUTANTS ON THE HEMATOPOIETIC SYSTEM

J. C. Schooley and M. E. Barker

The cells of circulating blood differentiate from several continuously renewing populations in the bone marrow. Distinct blood cell types have specific functions, but ultimately all are derived from primitive stem cells. Homeostasis in the hematopoietic system is delicately regulated by feedback mechanisms mediated in some instances by circulating hormones and, in other instances, apparently by cell-cell interactions. Proliferation of stem cells and their subsequent differentiation into the recognizable cells of the circulating blood involve complex interactions among mature

circulating cells, the humoral regulators, and the various pools of immature precursors. Thus damage resulting from disease, radiation or exposure to energy-derived pollutants can affect this diverse system at many levels.

Although a number of stem cell candidates have been suggested, the stem cell itself is not morphologically recognized within the bone marrow. The same is true for intermediate cell populations before the acquisition of specific components within the cell which characterize the mature form seen in the circulating blood. Thus measurements of proliferation and

differentiation of primitive stem cells as well as of intermediate populations cannot be done on morphological grounds; functional criteria must be utilized.

Our objectives have been to determine the direct effects of irradiation, of heavy metals such as lead, or of pollutant oxidizing gases as exemplified by ozone on the formation of red cells, white cells, and blood platelets. In our initial studies we have followed, as a function of time during or after exposure to the particular pollutant, the changes in numbers of circulating cells of various types, as well as their progenitors within the bone marrow. These measurements utilize either *in vivo* or *in vitro* cloning methods, which give an estimate of the activity of a particular progenitor. For example, the most primitive progenitor, termed CFU-S (colony-forming unit—in the spleen), is a cell which produces colonies within the spleen of lethally irradiated animals following the injection of suitable numbers of bone marrow cells. Other progenitors, already committed to a certain path of differentiation, produce colonies under *in vitro* conditions. Erythroid precursors, known as BFU-E (burst-forming unit—erythroid), and CFU-E (colony-forming unit—erythroid), as well as the precursor of megakaryocytes and platelets, the CFU-M (colony-forming unit—megakaryocyte) are grown in plasma clots. The progenitor of granulocytes and macrophages, termed CFU-C (colony-forming unit—in culture), grows in soft agar. It should be emphasized that, at the moment, the CFU-S is believed to be the precursor of all of the other CFU types mentioned; that is, it is a pluripotential progenitor, a primitive cell which, under suitable conditions, gives rise to all of the other cell lines.

In mice continuously breathing ozone at 1 ppm, we have found that CFU-S populations of the circulating blood, as well as of the spleen and bone marrow, are dramatically decreased. Our data suggest that circulating CFU-S cells are destroyed as they traverse the lung, via the pulmonary circulation, and are exposed to the ozone within the alveoli. The mechanism of this destruction is not known, but we intend to investigate it more thoroughly utilizing an isolated perfused lung preparation, which has been developed in the laboratory during the last year. The CFU-C population is also decreased in the ozone-exposed animal (Fig. 1).

In contrast to the action of ozone on the hematopoietic system, the acute administration of lead causes, within a day or two, a dramatic increase in the CFU-S concentration of the circulating blood and of the spleen. The same is true of the CFU-C cells in the bone marrow (Fig. 2). The mechanism of this increase is at present a mystery, particularly since it is well known that lead is toxic to precursors of circulating red cells. This observation with lead appears to us to be of considerable importance, because it suggests a model that can be used in studying factors regulating the proliferation

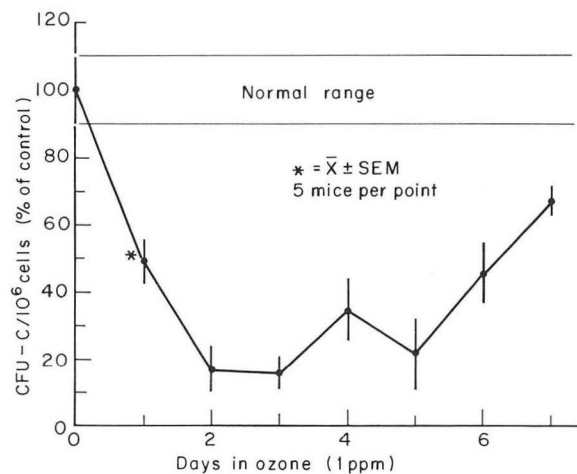


Figure 1. Effect of serum from ozone-exposed mice on the growth of bone marrow CFU-C from unexposed adult mice.

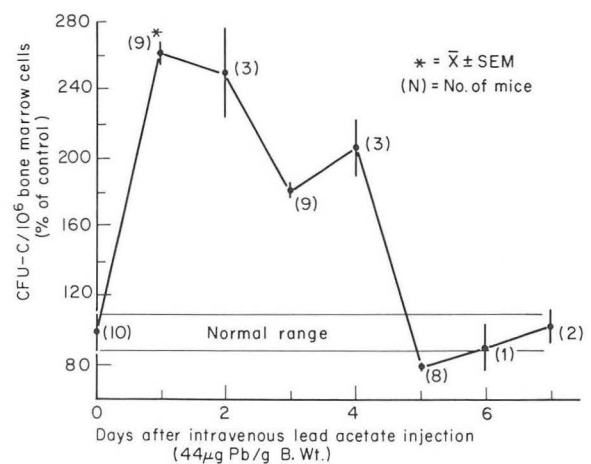


Figure 2. Injection of lead acetate on CFU-C in marrow from female mice.

of CFU-S cells. It is the presence of this progenitor cell which appears to be absolutely essential if the hematopoietic system is to survive, regardless of the agent initiating damage to the blood-forming tissue.

We have also conducted some pilot studies on the effects of ozone exposure on the circulating platelet levels. Our preliminary results indicate that after two to three days exposure to 1 ppm ozone, platelet counts are increased by 40-50%; at later times, the platelet levels show considerable cyclic fluctuation. Such fluctuations are not normal and could cause problems because platelets are so essential for the maintenance of vascular integrity and hemostasis.

Very little is known about the physiological mechanisms involved in the production of platelets in either man or animals, although there is some evidence that a circulating hormone is involved. Many of our experiments have been designed to elucidate the basic control mechanisms of platelet formation from the megakaryocyte of the bone marrow. Our approach in this case has been to depress the circulating platelet levels in mice by irradiation and/or the injection of antisera prepared against platelets. The rationale for this approach is the common observation that decreased platelet levels stimulate megakaryocyte proliferation and differentiation. Our experimental results have shown that when CFU-S cells are injected into a lethally irradiated animal, the restoration of platelet levels some 10-12 days later is proportional to the number of CFU-S cells transplanted. However, we have found it extremely interesting that the actual level of platelet restoration depends on both the conditions within the host itself, as well as the kind of CFU-S cells injected (Fig. 3). For example, platelet restoration appears to be much more efficient following the injection of CFU-S cells from the spleen than from the bone marrow. CFU-S cells taken from the fetal liver are much better than either CFU-S from the spleen or the bone marrow. This implies

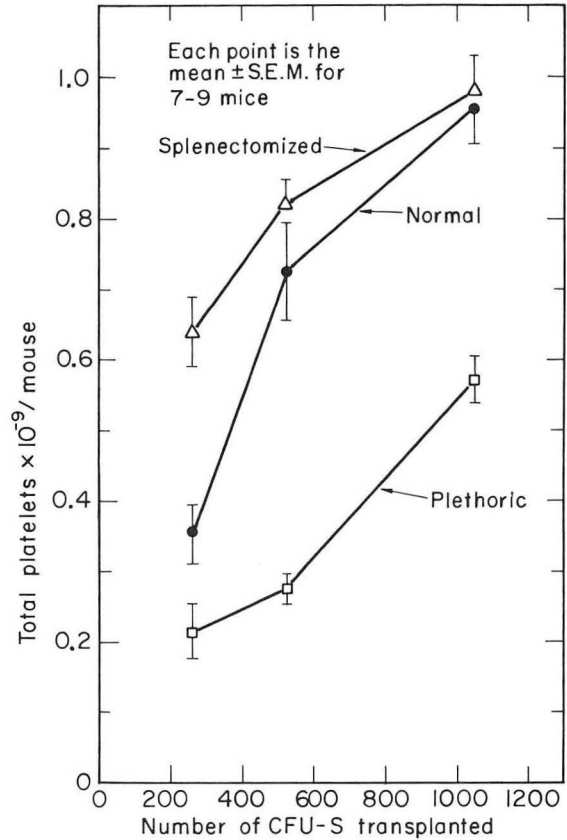


Figure 3. Platelet repopulating ability of normal, plethoric, and splenectomized mice after irradiation and transplant of bone marrow cells. (Counted on day 12.)

that the CFU-S or stem cells are, in fact, heterogeneous, and that their multiplication and differentiation can be altered by the milieu in which they develop. Behavior of these transplanted bone marrow cells in lethally irradiated animals with or without exposure to pollutants, or of bone marrow derived from pollutant-exposed animals, provides extremely potent tools for analyzing the physiological alterations initiated by pollutants on the hematopoietic system, a system so important in maintaining health.

EFFECTS OF ENVIRONMENTAL POLLUTANTS ON PROTEIN AND POLYPEPTIDE HORMONES

J. F. Garcia and G. K. Clemons

This research is concerned with the effect of nonnuclear energy pollutants on the production, secretion, and metabolism of protein and polypeptide hormones in laboratory animals. These studies are being carried out in rats both acutely and chronically exposed to a variety of gaseous and metal pollutants. For several reasons, we will be initially concerned with the hormones of the anterior pituitary; however, in later work we will extend our studies to other hormone systems.

The pituitary is functionally as well as anatomically linked to the central nervous system (CNS). Many influences on the CNS will result in effects on pituitary function. A variety of stressful environmental changes, such as cold and hypoxic exposure, and even more subtle changes, such as noise, light and handling, will alter pituitary function. Also, many of the metal pollutants are known to result in CNS pathology, and it can be expected that such pathological changes will be reflected by alterations in pituitary function. Our main tool in this work is the radioimmunoassay technique, which is very sensitive (picogram-nanogram range) and allows for the measurement of hormone con-

centrations in very small samples of plasma (100 μ l or less). One of the hopes is that changes in plasma hormone levels may serve as an early biological indicator of pollutant exposure before irreversible pathological changes can occur. Studies so far indicate a profound depressing effect on the pituitary-thyroid axis of rats following ozone exposure. The depression in thyroid-stimulating hormone (TSH) blood level is very sensitive and responds to an 8-hr ozone exposure of 0.8 ppm. Thyroxine levels are also moderately depressed, while prolactin levels are increased (Fig. 1.). The basic mechanisms involved in these pituitary-thyroid changes are being actively pursued.

In the past, Donner Laboratory has played a significant role in researching another hormone system, that is, erythropoietin, the hormone controlling red cell production. The recent acquisition of NIH support has rekindled our interest in this hormone. The measurement of normal blood levels for erythropoietin has heretofore been impossible because of inadequate assay systems. Recently, we have accomplished a major breakthrough in the application of the radioimmunoassay procedure to the

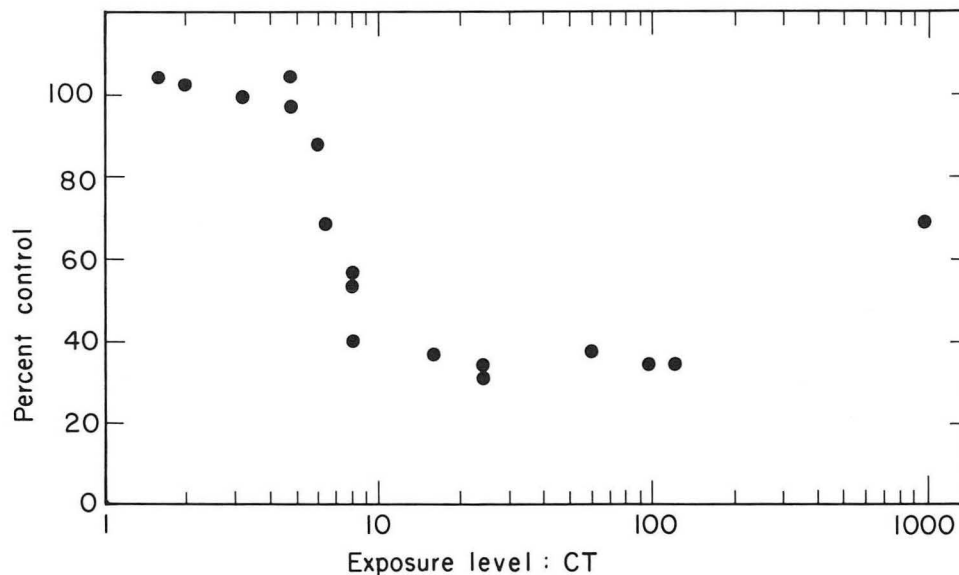


Figure 1. Plasma TSH levels in male rats after continuous ozone (O_3) exposure. The exposures are calculated as CT values (concentration in parts per million times the hours of exposure). There is a significant fall in TSH levels, to 40% of the control level, after an 8-hr ozone exposure of 0.8 ppm.

measurement of the concentration of this hormone in blood. Anemia is a common underlying factor in many clinical situations, including malignancy, infection, and endocrine and nutritional states. Using this radioimmunoassay

for erythropoietin, we hope to study many clinical as well as experimental laboratory situations, including the effects of metal pollutants such as lead and cobalt, which are known to have an effect on red cell production.

EFFECTS OF ENVIRONMENTAL POLLUTANTS ON STEROID HORMONE MECHANISMS

G. M. Connell

The primary objective of our research is to identify harmful physiological effects of common environmental pollutants generated by various energy-producing technologies. The energy pollutants that concern us include ozone, hydrocarbons, oxides of nitrogen and sulfur, and certain trace metals. The effects which interest us are those specifically related to steroid hormone mechanisms. These mechanisms can range from general environmental adaptation, which may be affected through the hypothalamic-pituitary-adrenal system, to possible reproductive complications that would be evidenced by ovarian or testicular dysfunction.

A variety of methodologies exist whereby one can study environmental effects. During the past year we have stressed the intact-animal response rather than isolated-cell-culture systems because we believe it more accurately represents the natural environmental sequelae. For our introductory studies, we have chosen a common atmospheric pollutant, the oxidant gas, ozone. Ozone is a common atmospheric pollutant near urban and industrial centers; during unfavorable conditions ozone concentrations can reach 0.2-0.7 ppm. Therefore, in our initial experiments laboratory animals were exposed to a controlled atmosphere which contained ozone at 0.8-1.0 ppm. These experiments suggested that female rodents could adapt to this toxic environment much more readily than male rodents. Recent experiments have confirmed these observations. Exposing mice of three different age groups (immature, young adult, and adult) to ozone (1.5 ppm) demonstrated that males were significantly more sensitive to this oxidant gas (Fig. 1). Of the three groups, the adult mice tolerated this stressful environment with greater success than the two younger groups. Prior to death these animals showed labored breathing and lethargy.

At autopsy the lungs were much enlarged and edematous. Biochemical studies indicated a greater protein and DNA content in the lungs than was observed in normal mice. Our current experiments are attempting to understand this intriguing sexual difference in mortality; it may be that the female sex steroids enable the females to adapt more successfully to this ozone challenge.

We also noted that immature and young adult mice that have been exposed to ozone have diminished reproductive capacities when returned to a normal atmosphere in our animal colony. Long term or permanent sterility was observed in mice exposed at very early ages. Young adults were generally fertile after ozone exposure, but frequently parturition was difficult or delayed. On examination, uterine horns showed fetal resorption. Survivors of the adult group of mice showed normal reproductive patterns when returned to the animal colony. These reproductive changes are currently under further investigation.

The effect of ozone exposure on the steroidogenic potential of the rat testis has been studied. Utilizing the decapsulated rat testis model we have demonstrated a diminished production of testosterone—the male hormone—in testes from ozone-exposed rats. The reason for this is unknown at present but this phenomenon clearly demonstrates that the harmful effects of ozone can be measured in organs distant from the lung, which is the biological interface with the atmospheric environment.

Lung tissue contains many enzymes and some of these enzymes will metabolize steroid hormones. We have demonstrated an ozone effect on the 11-beta-hydroxysteroid dehydrogenase, the enzyme that effects the conversion of cortisone to cortisol. Preliminary experiments suggest testosterone metabolism is also altered in ozone-exposed animals.

It has been apparent that a variety of steroid hormone mechanisms are affected by

oxidants in the atmosphere and we plan to explore the nature of these changes.

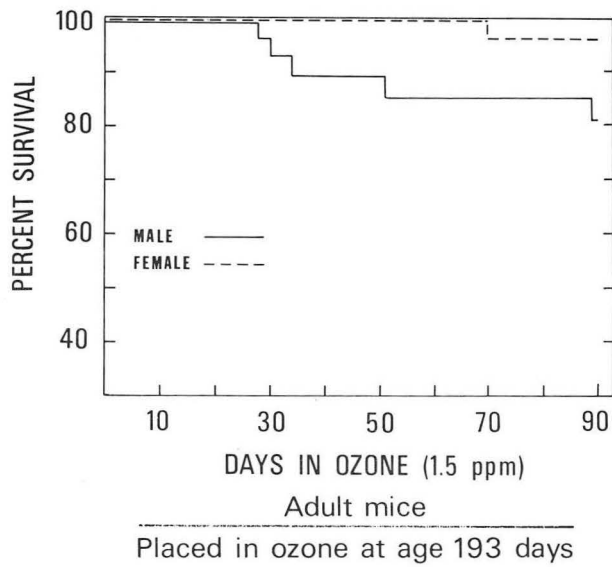
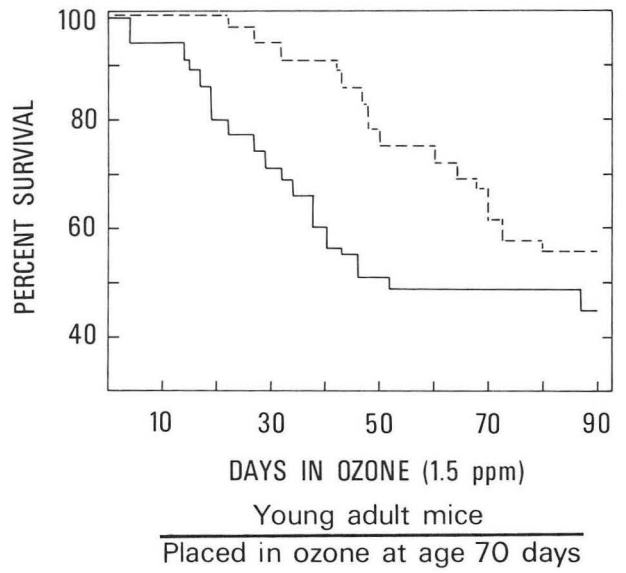
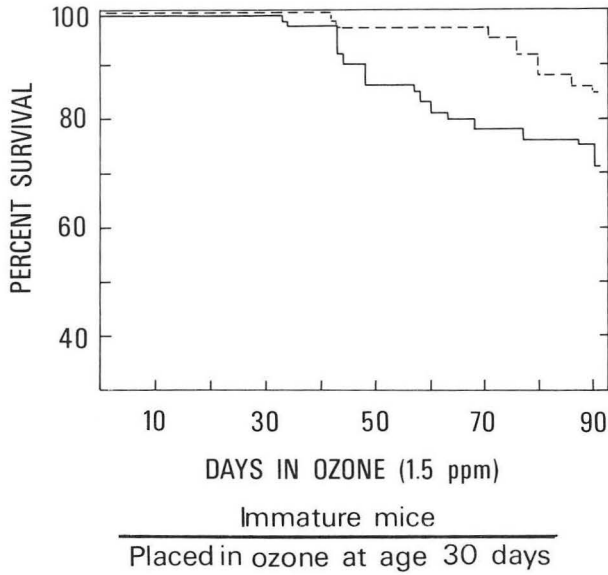


Figure 1. Survival rates of male and female mice, representing three different age groups, that were chronically exposed to ozone (1.5 ppm) for 90 days. In all three age groups, male mice (—) were more susceptible to the toxic effects of ozone than female mice (---). Immature and young adult mice demonstrated a greater susceptibility to the toxic effects of ozone than the adult mice.

EFFECTS OF ENVIRONMENTAL POLLUTANTS ON PROTEIN METABOLISM IN SMALL ANIMALS

J. S. Dixon and J. C. Schooley

This work is one aspect of a more extensive group effort aimed at investigating the impact of environmental pollutants on the health of humans. It is designed to evaluate the adverse effects of exposure to known amounts of pollutants by observing changes produced in small animals. Our premise is that pollution damage will lead to metabolic changes in the target organs such as lung, liver, kidney, and spleen and will also be reflected in changes measurable in the blood. We will make detailed biochemical and morphological observations of these effects and then select some changes that can be quantitated against levels of pollutant and detected by changes in drawn blood or in urine samples. Changes manifesting the early effects of pollutants will indicate the kinds of measurements that can be made to screen large numbers of individuals. Such screening procedures will facilitate setting acceptable levels of exposure and enhance the value of therapeutic treatment in humans.

Using ozone (0.4-0.5 ppm) as the pollutant, we have carried out a detailed study on the long-term exposure (39 days) of both male and female buffalo rats. Among the findings in animals was clear cut evidence of differing effects according to sex and age. More females than males survived. In other experiments involving the exposure of buffalo rats to 1 ppm for 59 days, no males older than 35 days at beginning of exposure time survived. Three females out of six of age 127 days, and five out of six of age 92 days, survived. Lung weights were enhanced over those recorded for unexposed control rats; the percentage increase in males was greater. Electrophoretic patterns prepared with soluble lung proteins differed according to sex.

Collaborative studies with others involved an investigation in which mice, already sensitized by injection with lead salts, were also exposed to ozone. The findings indicated that the considerable elevation of colony forming units (CFU-S), which were detectable in mice seven days after a single injection of lead, was much diminished in animals that, in addition to receiving lead, were also exposed to ozone during the last four days of the seven-day experiment. One hypothesis for this behavior

postulates that the CFU-S are destroyed in a single passage through the lung.

Stimulated by interest in this phenomenon and a desire to have a more isolated and controllable working system, we have developed an isolated ventilated perfusable lung system which is useful for investigating the CFU-S behavior and other metabolic processes in the lung.

Among the first lines of defense in the lung exposed to inhaled pollutants are the alveolar macrophages. Another system acutely affected by ozone is the lipid surfactant material which, through a lowering of surface tension, facilitates breathing. Both macrophages and surfactant may be conveniently removed from the lung by lavaging (flushing out) the lung with physiological saline or other solutions. Studies on the effects of exposure to ozone on the metabolic processes are continuing, including changes in enzyme levels in alveolar macrophages taken from mice by lavage. Ozone oxidizes the phospholipids and fatty acid residues of the surfactant materials, thus causing profound changes in lung processes; investigations on the effects of changing arachadonic acid (a fatty acid) levels as they relate to metabolic processes in the lung and in the blood are under way.

An investigation involving a model study designed to test our ability to detect and measure a lysosomal enzyme in pollutant- or otherwise-exposed small animals is nearing completion. Whereas others have postulated that the lysozyme measured in the blood is largely a measure of the rate of destruction of neutrophils, our measurements, carried out on lethally irradiated mice long after all neutrophils have been destroyed, indicate that lysozyme levels remain high. This finding reflects the fact that other cells, most likely macrophages, are continuously synthesizing and secreting this enzyme into the blood.

Recently, through a grant from NIH, our effort has been expanded to include investigations on the purification of the hormone erythropoietin. This substance is responsible for control of red blood cell formation, a process intimately related to lung function and to the environment of the animal, and

thus of vital concern in relation to the effects of inhaled pollutants.

The primary material under investigation is a crude preparation isolated from the urine of anemic patients and supplied by the NIH. Our purification methods involve the application of classical procedures such as fractional precipitation, ion exchange, and gel chromatography. Other, newer methods applicable to the purification of erythropoietin, known to be a glycoprotein, include isoelectric focussing and conventional electrophoresis, the preparation of affinity chromatography

systems, and the application of antigen-antibody techniques. We expect to achieve a level of purity such that the material will be suitable for testing its relationship to the effects of inhaled or heavy metal pollutants and for investigating a variety of other pathological conditions. Obtaining material of sufficient purity for fundamental structural studies is of considerable importance in ultimately understanding the mechanism by which this important class of compounds, the glycoprotein hormones, exercise control of biological systems.

STUDIES OF GROWTH AND DIFFERENTIATION OF LUNG IN FETAL MICE, ADULT MICE, AND REGENERATING LUNG TISSUE

J. C. Schooley, W. J. Vaughan, and D. A. Pointer

The general concern of this project is with the molecular basis of lung function and the changes that may occur as a result of chronic exposure to gaseous pollutants. The lung is the immediate and major site of damage by agents such as ozone, oxides of nitrogen and sulfur, and aromatic hydrocarbons.

Because many lung diseases are reflected by changes in serum proteins, this past year we have been monitoring these serum proteins using high-resolution SDS-gel electrophoresis in control and ozone-exposed mice, looking for any marked changes which could be used to assess an animal's previous exposure to ozone. Specific proteins of interest included lipoproteins. Previous work by Vaughan used the SDS-gel technique to compare serum protein levels in patients with cystic fibrosis (Fig. 1). In this disease, the major cause of death is respiratory insufficiency due to lung damage. He observed a major change in lipoproteins. Thus, using ozone-exposed mice, a change of serum lipoproteins may indirectly indicate a change in lung function—a reasonable expectation since serum lipoproteins carry exogenous lipids to the lung for surfactant production.

We exposed 13-week-old LAF₁ female mice to 1 ppm of ozone for periods of up to 14 days. During the first day of O₃ exposure, mouse activities were very subdued. Minimal activity, eating, and drinking were observed. Weight loss occurred. However, after the first day, mice seemed to adapt to ozone. After 14 days,

activities seemed normal, and body weights were within the normal range.

Serum lipoproteins as studied by SDS-gel electrophoresis, analytical ultra-centrifugation, and electron microscopy showed no change between chamber controls and ozone-exposed mice. However, statistically significant changes were measured by agarose gel electrophoresis. In contrast to the other techniques, agarose gels are treated with lipid specific stains (Fast Red).

Since the other methods clearly indicate that high-density lipoprotein (HDL) levels do not change, we interpret the agarose gel results to mean that different lipids with different affinities for Fast Red contribute to an apparent change in HDL. In other words, the lipids carried by HDL in ozone-exposed mice may be different than those from the control mice.

In addition, analytical ultracentrifuge scans suggested that low-density lipoprotein levels were elevated in ozone-exposed mice. The 1-ppm exposures and subsequent lipoprotein measurements are being repeated in male guinea pigs. These animals have higher levels of low-density lipoproteins and males at least appear to be quite sensitive to ozone—more so than female mice.

Many lung diseases have also been correlated with uncontrolled proteolytic activity in the peripheral airways of the lung. Irritation to the lung tissue by gaseous pollutants results in edema, inflammation and the concomitant influx of leucocytes. It is believed that the

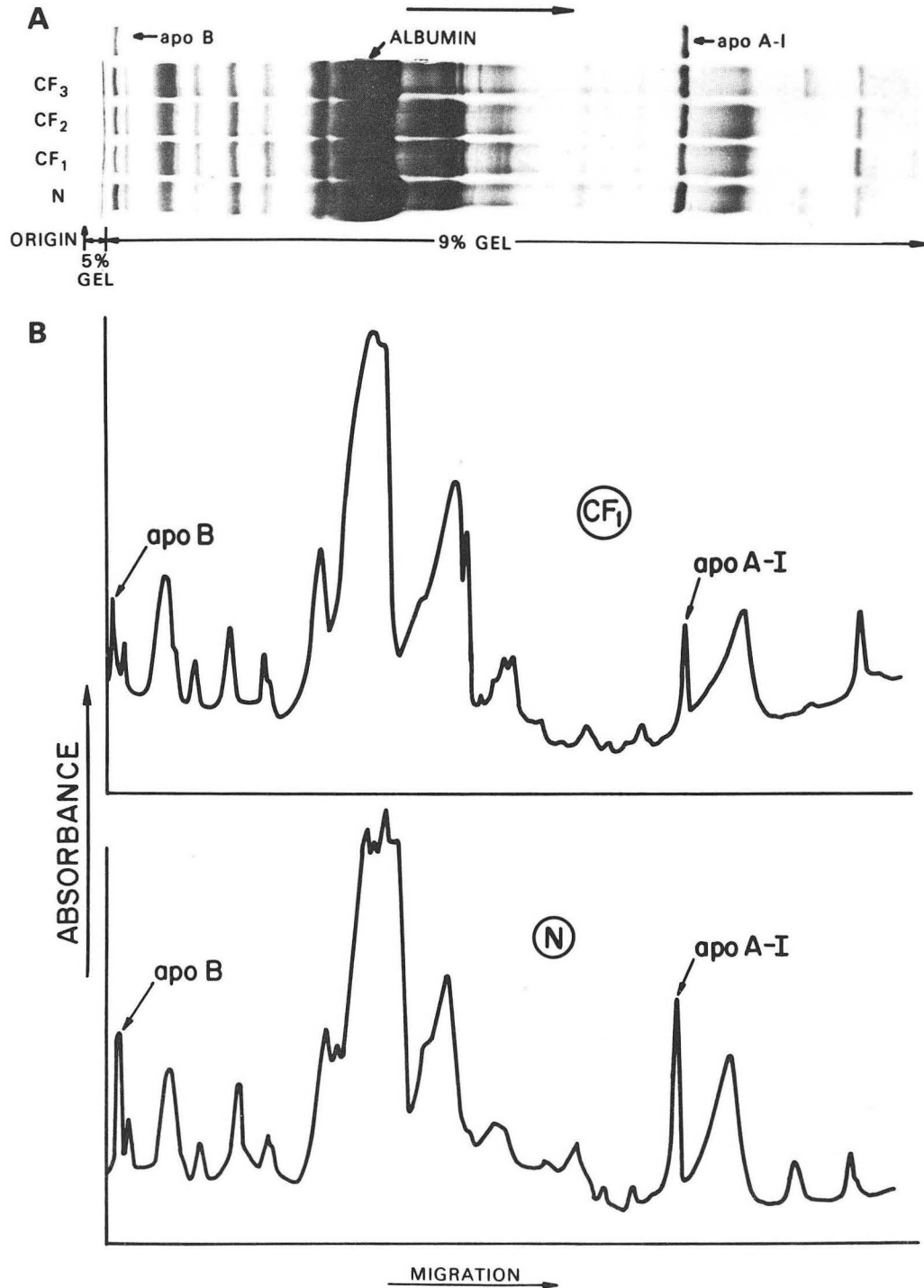


Figure 1. High-resolution electrophoresis on SDS-polyacrylamide gel to compare serum proteins of three cystic fibrosis patients (CF₁, CF₂, CF₃) and one normal control (N). In this separating gel, the protein migration distance is a function of protein molecular weight. The upper figure (A) shows that the visual intensities of two bands (apo B and apo A-1) were consistently lower in the gel patterns from the CF patient serums. Densitometer scans for CF₁ and N (shown in B) quantitate this observation; note the lower peaks for apo B and apo A-1 in the scan for CF₁. Apo B and apo A-1 are major protein components of low-density and high-density lipoproteins, respectively. Subsequent measurement of lipoproteins using agarose gels and analytical ultracentrifugation determined that serum lipoprotein concentrations were depressed in patients with CF.

proteases secreted by the eucocytes cause major damage to the connective tissue of the lung, thereby attracting more leucocytes. Normally, the extracellular proteases are controlled by a naturally occurring protease inhibitor (PI) system consisting of a series of proteins circulating in the blood.

It is postulated that proteolytic damage to the lung occurs when the PI is overwhelmed by the massive secretion of enzymes such as collagenase and elastase by invading leucocytes. We are in the process of monitoring the changes in the PI level in the blood of animals exposed to ozone. In addition to general destruction of lung morphology, the proteases may also release polypeptides into the circulation where these fragments could trigger an immune response to the animal's own lung tissue, as has been observed in lung diseases

such as emphysema. This attack by the immune system would enhance the general destruction of the lung and loss of function. Experiments are under way to try to demonstrate that perhaps some of the chronic disease resulting from ozone exposure can be attributed to this immune response.

The body's attempts to heal lung damage often results in morphologically similar but non-functional lung tissue. The ability to resynthesize or rebuild the proper extracellular matrix at the air/blood interface, the surfaces for gas exchange, is in question. Presently, we are examining these extracellular structures at the electron microscope level in normal and ozone-damaged lung, as well as regenerated lung tissue. An examination of fetal lung tissue is also planned.

EFFECTS OF TOXIC AIR POLLUTANTS ON TUMOR INCIDENCE IN MICE

M. R. White

INTRODUCTION

These studies relate to airborne contaminants from mining, combustion, and industrial processing of fuels, some of which may be carcinogenic. We hope to evaluate the risks of environmental carcinogens that occur at levels too low for direct testing by superimposing the action of air pollutants on tumor induction by other carcinogens and studying the effects of latent periods. We are also studying the possibility of multiplicative effects on the total tumor incidence.

The mouse lung adenoma induced by urethan is similar to that induced by polycyclic hydrocarbons such as benzpyrene, an atmospheric pollutant arising from the combustion of fossil fuels. We superimpose the action of a suspected carcinogen on the effects of urethan, and then study tumor yield and latent period.

NO₂ EXPOSURE

The experimental plan was to test NO₂ alone as a possible carcinogen, then with urethan as a possible cocarcinogen. A total of

1,550 female A/Jax mice were randomized into 180 groups. Those treated with urethan received an intraperitoneally administered dose of 0.5 mg per gram of body weight. Exposure to NO₂ preceded or followed a single dose of urethan. At 5 ppm, mice were exposed for eight days; at 10 ppm, four days; at 20 ppm, two days; controls were kept in the air-only chambers for four days. Total doses were approximately equal in all exposed groups, assuming that respiration was not greatly altered by the presence of NO₂. The animals were supplied with water and their usual food in open-mesh stainless steel cages. Mice were sacrificed at 12, 16, 20, and 24 weeks after treatment with urethan and NO₂. There were 15 to 18 mice in each sacrifice group with a specific treatment (Fig. 1). From tumor counts in the NO₂ experiment (see Table 1), we conclude:

1. NO₂ alone, under these conditions, is not a carcinogen; the incidence of lung tumors of unexposed controls and mice exposed only to NO₂ was identical and low.
2. NO₂ exposure for eight days at 5 ppm decreases urethan carcinogenesis. The

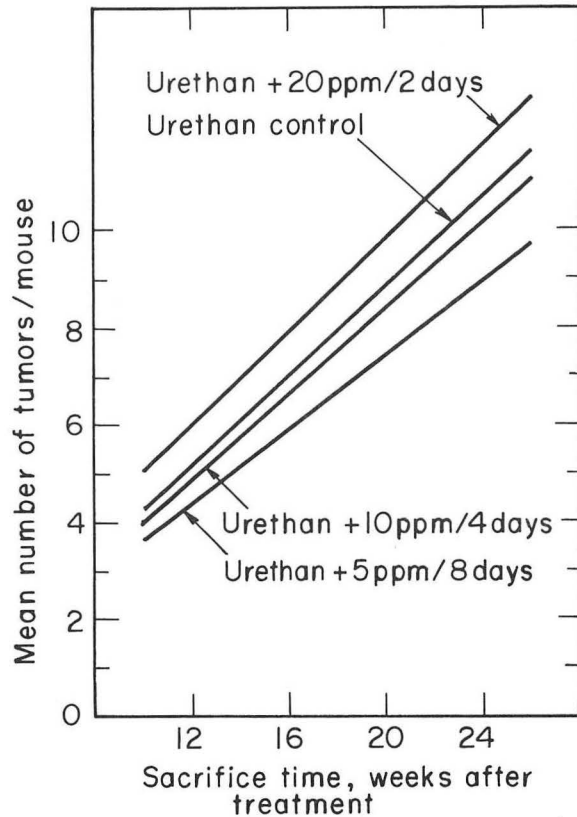


Figure 1. Regression of lung tumor incidence against sacrifice times in mice, comparing a control group (urethan only) and three groups given urethan plus exposure to three different levels of NO_2 (20 ppm for two days; 10 ppm for four days; and 5 ppm for eight days). Sacrifice times were from 12 to 24 weeks after treatment. There were 15 to 18 mice per sacrifice group, with four sacrifice groups used to calculate each mean (total 60 to 72 mice).

incidence of lung nodules was significantly less than in mice not exposed to NO_2 . (Reduction of 16%; sign test 8/0, $p = 0.005$).

- NO_2 has an effect on urethan carcinogenesis. It must reach the same cells (type 2 cells) affected by urethan.
- From 5 to 20 ppm NO_2 exposure, urethan carcinogenic response increases with NO_2 level, $p = 0.005$. (Note: exposure at 5 ppm was for eight days; at 10 ppm, for four days; at 20 ppm for two days). The rate of appearance of lung nodules increased from an average of 0.38 tumors per mouse per week at 5 ppm NO_2 to 0.51 at 20 ppm.
- The effect of NO_2 was the same whether its exposure occurred before or after urethan administration. The effect, therefore, is likely to be on a number of type-2 cells (the precursor cells to lung tumors).
- In comparing tumor incidence at 5, 10, and 20 ppm, the NO_2 concentration correlated with the increase in lung tumor risk.

The lungs of sacrificed mice are being examined microscopically, using both scanning electron microscope and light microscope. No data adequate for analysis are yet available on these tissues.

Some mice shipped from Bar Harbor Laboratory included groups afflicted at arrival

Table 1. Effect of NO_2 exposure on urethan carcinogenic response in mice as determined by incidence of lung tumors.

		Parts per million NO_2 in air			
		0	5	10	20
Lung tumors/mouse, mean*	(\bar{x})	7.990	6.651	7.620	8.840
Weeks of observation, mean*	(\bar{y})	18	18	18	18
Standard deviation of x	(S_x)	2.160	1.885	2.234	2.654
Standard deviation of y	(S_y)	4.78	4.78	4.78	4.78
Correlation coefficient	(r)	+0.981	+0.952	+0.922	+0.911
Tumors appearing/mouse/week	(b_{xy})	0.45	0.38	0.43	0.51
Calculated incidence of Lung tumors/mouse at 24 weeks		10.68	8.91	10.20	11.87

*Based on 15 to 18 mice per sacrifice group; four sacrifice groups used to calculate each mean (total 60 to 72 mice).

by an epidemic of viral lung disease. Since many humans have similar lung disease from smoking, viral pneumonia, or emphysema induced by atmospheric pollution, we seized the opportunity to study the effect of urethan and NO₂ exposure on affected mice that recovered from the infection. Comparison of animals with pneumonia-damaged lungs with those that had no symptoms of respiratory disease shows no difference in lung tumor incidence.

SO₂ EXPOSURE

SO₂ studies are under way. The experimental design is the same in the NO₂ experiment except that the SO₂ exposures are 40 ppm for three days, 20 ppm for six days, and 10 ppm for twelve days, with controls exposed only to air in the chamber for six days. Final results are pending.

SCANNING ELECTRON MICROSCOPY

Our background studies with the scanning electron microscope cover what we believe are the earliest stages in tumor formation that

are likely to be used as end points in our quantitative studies.

LATENT PERIOD

To test our hypothesis that latent period in carcinogenesis depends on an inverse power of the dose of carcinogen, we are trying to define more precisely the beginning of urethan-induced lung tumors. As one approach, we are measuring the size of tumors at various times after treatment with urethan, in order to establish a tumor growth curve. The preliminary findings at this time are:

1. The diameter of tumors at a given time after treatment increases significantly with dose of urethan. A graph of the data suggests that tumor diameter varies as the ninth root of the dose. This would be consistent with assumptions that tumor mass is proportional to the cube of tumor diameter and to the cube root of the dose.
2. Tentative extrapolation of the data indicates that tumors probably start forming at the same time regardless of dose.

METABOLISM OF TRANSURANIC ELEMENTS IN NONHUMAN PRIMATES

P. W. Durbin

Radiation exposure limits for radionuclides, which may enter and be deposited in the body, are met by limiting intakes. Intake limits are calculated, in turn, from a metabolic model for each element. When human data are not available or are incomplete, the best animal data are those from animals phylogenetically close to man.

The goal of this project is to develop in *Macaca*, a genus of Old World monkeys, complete metabolic models for the three most biologically hazardous radioelements generated in nuclear power production. A complete metabolic model is a quantitative description of the biological behavior of an element—its transport into and within the body, its gross and microscopic distribution in tissues and bones, and the temporal changes of those distributions. A simian model for ⁹⁰Sr can be used to verify or modify current models of alkaline earth metabolism in man. Simian

models for plutonium and americium can be used along with available human data to construct more reliable models of actinide metabolism in man.

METHODS

Classic metabolic balance methods were used, and each monkey was followed as an individual case. Procedures include the following: (1) sampling of blood for radiochemical analysis and hematologic examination; (2) collection of excreta (continuously for 6 to 18 months depending on the isotope under study) followed by quarterly two-week collections; (3) both timed early sacrifices and observations for lifespan; (4) careful gross autopsy and microscopic examination of tissues; (5) radiochemical analyses of all tissues and bones; (6) preparation of gross and detailed autoradiographs of selected tissues and bones to provide

information on microdistribution; and (7) refinement of analytical techniques until close to 100% of injected nuclide can be accounted for in each animal.

⁹⁰STRONTIUM STUDIES

The ⁹⁰Sr studies were begun in 1954 because of concern about the health hazards of ⁹⁰Sr in fallout from nuclear weapons tests. Between 1954 and 1967, 40 immature or adult rhesus monkeys (*Macaca mulatta*) of both sexes were each given a single injection of 5 to 14 $\mu\text{Ci}/\text{kg}$ of ⁹⁰Sr in citrate buffer. The highest dose is about one-half of the ⁹⁰Sr dose that has been shown to induce bone tumors in some beagle dogs within 10 years. Some monkeys were killed at short post-injection times to examine skeletal deposition patterns, and others were kept for long-term observation. As of January 1, 1978, six monkeys were alive 11 to 18 years after injection. Some important results include:

1. Skeletal uptake and retention and intraskeletal distribution of ⁹⁰Sr are related to growth status at time of injection—immature monkeys take up and retain more ⁹⁰Sr than adults, and a larger fraction of the ⁹⁰Sr is deposited in cortical bone or its precursor structures.
2. Body (skeletal) content of ⁹⁰Sr can be reconstructed from excretion curves, and the main components of exponential excretion rate curves can be correlated with ⁹⁰Sr loss from trabecular, and later, cortical bone.
3. Ten- to fifteen-year post-injection skeletal retention of ⁹⁰Sr in injected adolescents is less than 8% of the dose, and of injected adults, less than 4%.
4. No biological effects (changes in either blood or bone or neoplasia) have been observed that can be unequivocally related to ⁹⁰Sr-⁹⁰Y beta-radiation at an injected dose ranging from 5 to 14 $\mu\text{Ci}/\text{kg}$.
5. No gross changes in urinary or fecal clearance of ⁹⁰Sr from blood occur with age in the monkey. However, in some animals daily ⁹⁰Sr excretion rises (or fails to continue declining) late in life, presumably because of bone atrophy associated with aging and/or the prolonged inactivity of cage confinement.

²⁴¹AMERICIUM STUDIES

The ²⁴¹Am studies were begun in 1960 to provide metabolic information on an important but poorly studied nuclear byproduct. Between 1960 and 1967, 20 adult female cynomolgous monkeys (*Macaca fascicularis*) were each given a single injection of 0.44 to 0.87 $\mu\text{Ci}/\text{kg}$ of ²⁴¹Am(III) in citrate buffer. Metabolism (excretion, blood levels, tissue and bone contents) of ²⁴¹Am was studied in 17 monkeys from 1 to 735 days p.i. and in three animals for three to six years. At injected doses of 0.3 $\mu\text{Ci}/\text{kg}$ of ²⁴¹Am or more, all beagle dogs develop bone tumors in three to six years. Recently three adult monkeys have been injected intramuscularly with 0.3 $\mu\text{Ci}/\text{kg}$ of ²⁴¹Am citrate to study uptake and deposition kinetics using *in vivo* nuclear medical techniques to trace the patterns of internal redistribution, if any, of ²⁴¹Am initially deposited in either bone or liver. Equipment used was (1) a fixed-position, four-detector photon system, (2) an Anger whole-body camera, and (3) conventional large NaI crystal. Some important results include:

1. The initial liver burden of ²⁴¹Am is cleared via bile and GI tract with a half-time of about 70 days. Thus, in the monkey, initial bone burden can be estimated from the relationship [100% - (total fecal excretion + urinary excretion in first week)].
2. Some variability was observed in the apparent initial partition of ²⁴¹Am between bone and liver. That this variability was *not* caused by internal redistribution of ²⁴¹Am after injection was demonstrated using the *in vivo* techniques.
3. Intraskelatal distribution of ²⁴¹Am favors trabecular bone structures located within active marrow.
4. Daily urinary excretion is about 10 times greater than that of ²³⁸Pu reflecting the lower stability of complexes of Am(III) with serum proteins.

²³⁸PLUTONIUM STUDIES

The plutonium studies were begun in 1973 after a literature review revealed that the data on metabolism of plutonium in man were both incomplete and unsatisfactory. An animal model was needed with which to evaluate the

available human data. The ^{238}Pu isotope is being used because its high specific radioactivity permits use of small masses of plutonium and the abundance of the 17-keV x-rays of ^{238}Pu permits accurate measurements of photons, which requires less effort than alpha-particle measurement techniques.

Since 1973, 16 adult macaques have been injected at a dose level of $0.3 \mu\text{Ci}/\text{kg}$ of $^{238}\text{Pu}(\text{IV})$ citrate. (At that dose level ^{239}Pu induced bone tumors in all young adult beagle dogs within five years.) Three macaque species have been used—*mulatta*, *fascicularis*, and *arctoides*—and they range in body size from 3 to 11 kg. A mixed population is being used because of the great difficulties in obtaining adequate numbers of a single species of a specified sex and age.

A one-week distribution study in six monkeys has been completed as an approximate match to the human cases who were injected with plutonium in the early 1940s and died of their diagnosed illnesses shortly thereafter.¹ Four of six monkeys have been introduced into a 5-year group and one of six into a 1.5-year group. The 1.5-year group will provide a match for the longest-surviving human injectees; the 5-year group will provide long-term metabolic data, and some toxicologic information. Other animals have been killed at 2 and 20 hours after injection to study intramuscular absorption and the characteristics of early liver deposition. Still others have been killed at 56 to 106 days after injection for testing purposes; one of those animals also received about $4 \mu\text{Ci}$ of ^{237}Pu for *in vivo* measurement of uptake kinetics. Subsequent radiochemical analyses of both ^{237}Pu and ^{238}Pu in all dissected tissues and bones, blood samples, and excreta of that animal verified the accuracy of the techniques used routinely to detect ^{238}Pu . Some important results include:

1. A significant variability in initial skeletal deposition was demonstrated as shown in Table 1. Variations were not related to sex, age, or route of injection.
2. ^{238}Pu was cleared from the simian liver at a rate comparable to that of ^{241}Am . Thus in monkeys the initial deposit of ^{238}Pu in the skeleton can also be estimated from cumulative excretion.
3. In gonadal and endocrine tissues ^{238}Pu was generally associated with connective

Table 1. Distribution and excretion of ^{238}Pu in adult macaques killed 7 or 8 days after parenteral injection of $^{238}\text{Pu}(\text{IV})$ citrate. Values are expressed as percent of absorbed dose* corrected to 100% recovery.

	Percent of Absorbed Dose	
	Mean	S.D.
Skeleton [†]	29.0	8.3
Teeth	0.11	0.049
Liver	60.7	10.3
Spleen	0.20	0.096
Kidneys	0.63	0.25
Muscle	1.46	0.28
Pelt	0.76	0.14
Other soft tissues	1.15	0.81
Tissue balance [‡]	0.45	0.18
Bile	0.024	0.02
Urine	2.38	0.50
Feces	2.06	1.35

*The amount remaining at the site of injection (where applicable) and the amount in all blood samples drawn before sacrifice are considered to be unabsorbed. Absorbed dose = % dose recovered - (injection site + all blood samples). Correction factor = $100/\text{absorbed dose}$.

[†]Includes costal cartilages and hyoid bone.

[‡]Includes surgical swabs and blood from dissection, hip pads, paw pads, ears, fat, and connective tissue.

tissue structures at one week, except that in ovary, some of the ^{238}Pu was initially also associated with the follicular liquor of maturing ova and with the degenerating corpus luteum of menstruation.

4. The intraskeletal distribution of ^{238}Pu was even more skewed (than that for ^{241}Am) to trabecular structure surrounded by active marrow.

REFERENCE

1. Durbin, P. W. Plutonium in man: a new look at the old data, *in* Radiobiology of plutonium. Salt Lake City, J. W. Press, pp. 469-530 (1972). Also LBL Report UCRL 20850, 141 p.

6. RADIATION BIOPHYSICS

This group, led by Dr. C.A. Tobias, is studying applications of accelerated heavy ions in biology, medicine, and health protection, with particular emphasis on radiation therapy of cancer. Beams of carbon, neon, and argon nuclei are accelerated up to 90% of the speed of light using the Bevalac, a combination of the SuperHILAC and the Bevatron. The nuclear physics of high-energy heavy ions is just beginning. Heavy ions are expected to improve significantly the ratio of tumor dose to normal tissue dose, and investigators are systematically studying the physical, chemical, and biological characteristics of heavy-particle beams so that radiotherapists will have the information required to select the most appropriate heavy particle beam to achieve maximum benefit in a specific therapeutic situation.

Nuclear interactions of the penetrating beam result in lighter fragments and a corresponding modification of biological effect. Investigators are studying the production of fragments as a function of depth in tissue-equivalent absorbers, and are also developing calculational methods to incorporate these results along with cross-section measurements by other physics groups to predict the effect of nuclear interactions on dosimetry. A spin-off of this work is a channel-plate time-of-flight detector that can measure particle velocities with a resolution of approximately 10^{-10} sec.

Other investigators are studying the radioactive fragments of the heavy ions in the beam. They have developed a new biomedical detector called the Positron Emission Beam Analyzer (PEBA), which allows measurement of the gamma rays emitted in the decay process when energetic radioactive beams stop in the tissue. Such studies are used for localizing the Bragg peak and accurately positioning the treatment beam; they can also be used for tracer studies by following the radioactivity of the metabolic products in a manner similar to that used for radioactive pharmaceuticals.

Several cellular radiobiological parameters for charged-particle beams at the Bevalac and the 184-Inch Sychrocyclotron are being measured using the transplantable rat rhabdomyosarcoma, a tumor system in a specific pathogen-free strain of female rats. These studies are helping to develop a comprehensive model

of tumor response to high-energy charged-particle radiation.

Cell survival studies, using human kidney T1 cells and Chinese hamster cells to investigate effects of heavy-ion exposure, are aimed at understanding the basic mechanism involved in cell killing by ionizing radiation. These studies also analyze the radiobiological properties of cells in culture with reference to high-LET (linear energy transfer) particles and the relationship of these properties to the goal of optimal therapeutic use.

Other investigators are studying the long-term effects of high-energy radiation on normal tissue systems in small animals. The early and delayed responses in the function of organ systems of the various test animals are used as significant end points.

The sharpness of the range of high-energy heavy-ion beams has led to their use for radiography. Division scientists have demonstrated that heavy-ion radiography can resolve smaller differences than the best available x-ray techniques, and at a much reduced dose.

A major program is that exploring the use of heavy-ion beams in the treatment of tumors. A clinical trial to evaluate the use of helium and heavy-ion radiotherapy in the treatment of human cancer was initiated in July 1975. Patients have been treated with fractionated doses of helium ions at the 184-Inch Synchrocyclotron. Late in 1977, following extensive investigations to characterize suitable configurations of the neon and carbon beams from the Bevalac, the first irradiations of cancer patients with these heavy ions were carried out.

Some investigators are studying the effects of magnetic fields on living organisms. They have designed and constructed the required laboratory facility to study biological effects of stationary and time-varying magnetic fields on selected molecular, cellular, and whole-animal systems. These investigations will develop a fundamental understanding of magnetic field interactions with biological systems, and will provide quantitative baseline data for the establishment of exposure guidelines for workers at fusion reactors, magnetohydrodynamic systems, and other energy-related technologies that utilize intense magnetic fields.

Another group is carrying out biophysical

studies on cell membranes, looking especially at populations of red blood cells. Using a new, rapid automated method called resistive pulse spectroscopy (RPS), they have characterized cell-membrane systems according to size, form,

deformability, fragility, and membrane kinetic responses. The variations in patterns of RPS response have been used to study cells in both normal and abnormal conditions.

Bevalac Studies

RADIOLOGICAL PHYSICS AND CHEMISTRY OF HEAVY PARTICLES

A. Chatterjee and J. L. Magee

There is considerable medical and scientific interest in the development of a radiation therapy program using beams of energetic heavy charged particles. Before these particles can be used with maximum benefit in a given therapeutic situation, it is important to understand the physical, chemical, and biological characteristics of various heavy particle beams. The purpose of this project is to study these characteristics in a systematic manner. It is hoped that the results of such studies will be of prime importance to therapists who must choose one particular heavy particle beam over another.

It is generally believed that energy is deposited through electronic interaction by heavy particles in about 10^{-16} sec. There is a lapse of about five orders of magnitude in time before free radical chemistry starts. In this project we are mostly interested in the radiolysis of water, since water is a major component in a cellular medium (80% by weight). Radiation interaction produces various products through decomposition of water as given by the following equation:



How much of a particular product is produced is dependent upon the geometrical pattern of energy deposition, which varies with particle energy and particle charge. Some of the products cause biological damage, generally attributed to the indirect effect of radiation.

We have developed a model that attempts to determine the detail of the chemical effects of heavy particles on aqueous systems, using the

microdosimetric concepts of "core" and "penumbra." The core is a cylindrical region within which the resonant energy losses of the heavy particle are degraded to create radicals. The penumbra is the region that surrounds the core; it contains the tracks produced by the energetic electrons created in knock-on collisions. The tracks in the penumbra are, to a good approximation, physically and chemically independent of each other. (In biological systems, radicals such as OH and H react in the nanosecond time scale and to this extent the tracks are quite independent.) Calculations were performed on the Fricke dosimeter, as a test system, to evaluate molecular and radical yields in water. Both the core and the penumbra yields have been calculated separately, and then added through proper energy partition fraction between the two regions of the track.

A study was made of the radiation chemistry of aqueous systems under irradiation with carbon, neon, and argon beams from the Bevalac. Preliminary evaluation of the data indicates that the present track structure model for heavy particles quite adequately describes the observed yields of radicals and molecular products including ferrous to ferric conversion (see Fig. 1). We are continuing to refine the track model for heavy particles to account for microscopic and submicroscopic details. Information obtained from the chemical stage of our theoretical calculations will be correlated qualitatively with biological effects. When thoroughly understood, these considerations can be quantitatively evaluated.

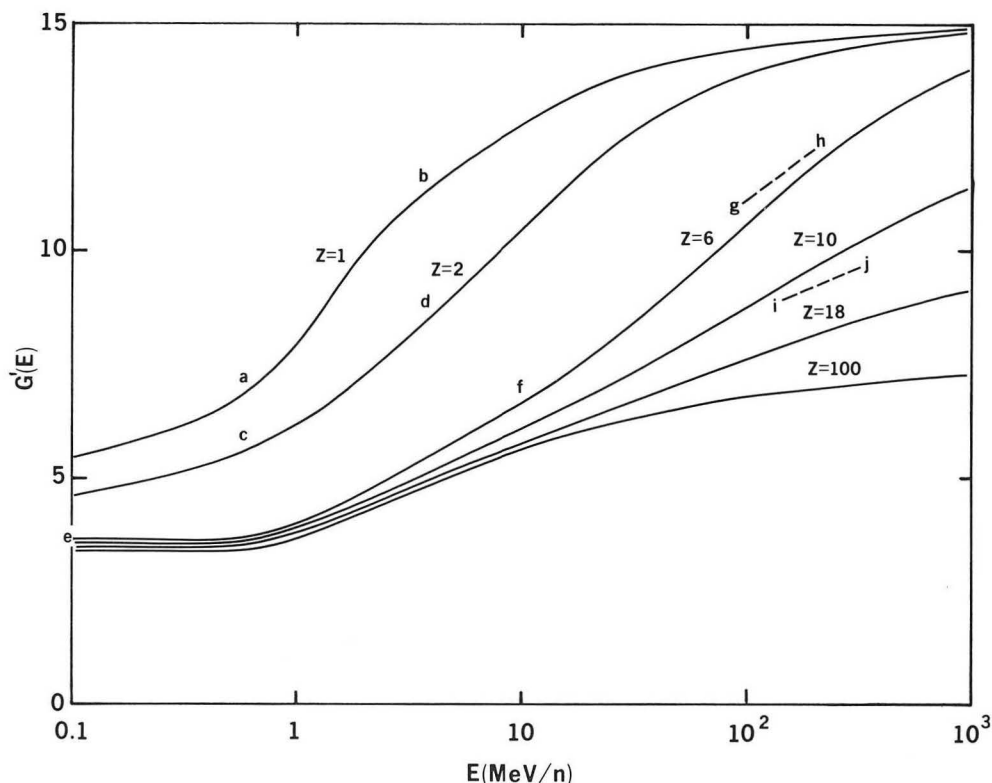


Figure 1. Differential ferric yield for various incident particles ($Z=1$ to $Z=100$) based on heavy particle track model. The core yield and the penumbra yield have been calculated separately and added according to their respective contribution to energy partition. In order to calculate the ferric yield, the radical ($-OH$, $-H$, $-HO_2$, etc.) and molecular (H_2O_2 , H_2 , etc.) yields were obtained from the basic principles known in water radiolysis.

TRACER STUDIES WITH RADIOACTIVE BEAMS

A. Chatterjee, C. A. Tobias, and J. Llacer

Our studies have important applications to the use of high-energy particle beams in therapeutic and diagnostic medicine. The favorable depth-dose characteristics (Bragg peak phenomenon) and increased biological efficiency of heavy particles provide major advantages in radiotherapeutic procedures. However, for effective use of Bragg peak therapy in cancer treatment, it is essential that the precise location of the peak be known so that the tumor area can be treated effectively with minimal damage to the surrounding normal tissues. The Bragg peak position cannot be determined accurately by mathematical calculations because it is not possible to adequately account for the contributing effects of intervening tissues with various densities (bone, blood, air, and other tissues), which lie between

the skin and the tumor. We have made an attempt to solve this problem by developing a new biomedical detector called the Positron Emission Beam Analyzer (PEBA) which allows us to measure the gamma rays emitted in the decay process when energetic radioactive beams stop in the tissue (which can be a location of the tumor). Even though this project was started with the purpose of localizing the Bragg peak, we discovered that the PEBA has many other diagnostic applications that are now impossible with conventional nuclear medical techniques. We are exploring these applications also.

The current PEBA, which is a preliminary version of a suitable detector device, was developed by Dr. Jorge Llacer of the LBL Engineering and Technical Services Division.

This device is operated in coincidence mode and consists of two moving banks of detectors with each bank containing 24 NaI (Tl) crystals (see Fig. 1). The crystals are 3 in. long and 0.75 in. in diameter, except for the outer ones which are only 2 in. long. [PEBA will eventually use a larger number of smaller NaI (Tl) crystals to achieve even higher sensitivity.] To bring the detectors as close as possible to the targets, which can range in diameter from approximately 8 to 30 cm, two moving banks of detectors separated by a variable distance are used. Each bank contains three movable modules, each containing eight crystals. For activity confined within a cylindrical volume along the axis of the heavy-ion beam trajectory, the detector banks are articulated so that the crystals are maintained parallel to the direction of the beam trajectory line.



Figure 1. Positron Emission Beam Analyzer (PEBA) in its present design along with Jorge Llacer who developed it. On the left bank the assembly of 24 crystals is clearly visible. (A similar arrangement is on the right bank.) There are three modules in each bank and each module contains eight crystals. The modules are so arranged that all the crystals are aimed at the beam line and can exactly locate the stopping region of the radioactive beam. Countings at various time intervals determine the translocation of radioactivity due to biological elimination processes.

PEBA was connected to the biomedical PDP 11/45 computer through a microprocessor. This computer is capable of acquiring a large amount of data in about 0.5 sec after each beam pulse, and all programs are now available for fast data acquisition. Facilities have been made for the immediate graphic display of the stopping distribution of the radioactive beam particles in the material of interest. (Figure 2 was drawn from such a printout.) In addition to the display of the activity, the distribution position of the highest activity is also immediately obtained; the entire operation takes only a few seconds.

Experiments have been carried out using a 400-MeV/n neon-19 beam. The distinctive 17-sec half-life of neon-19 made it distinguishable from other radioactive fragments produced in the reaction. Beryllium was used as a target for producing neon-19 from neon-20 accelerated in the Bevalac. With the present state of

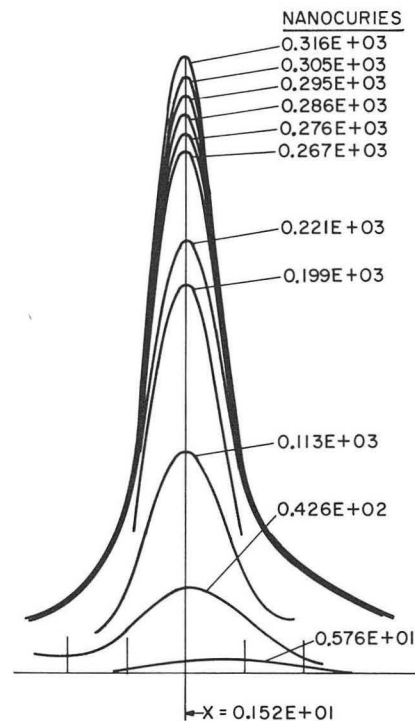


Figure 2. Deposition of activity at various depths along the target depth. The beam used was neon-19 and the target in which the activity was measured was a Lucite rod. The zero of the PEBA was at 9 cm position of the Lucite rod from the direction of the beam, and the highest activity was observed at 10.52 cm ($9 + 1.52$). At $t = 0$ the peak activity was 316 nCi. With the progress of time the activity dropped, which in this case was only due to the physical decay process.

development of PEBA, 40 to 50 counts/sec were sufficient to localize the Bragg peak.

We then replaced the beryllium target with a Lucite rod, and again we were able to detect the position of the Bragg peak almost instantaneously. In this situation, the detectors registered counts all along the target because of activity also produced in the target nuclei. But the target activity was much smaller than the activity in the stopping region of the neon-19 beam.

After verifying the position of the Bragg peak in these homogeneous objects, we attempted to make measurements in heterogeneous materials. We again used a Lucite rod, but in this case we replaced a thin section of the rod with a higher density material such as copper or lead, or in some instances a piece of bone. In each case the shift in the position of the Bragg peak location was exactly as predicted when compared with the location in a pure Lucite rod.

In another experiment, a thin section of the Lucite rod was replaced with a carbon disc

which, based on simple calculations, was the proper thickness to shift the Bragg peak by 1 mm only. Data from the activity measurement verified the calculation, and it was concluded that in the direction of the beam, the present device is sensitive enough to give a position accuracy of 1 mm.

We have produced a steady flux of radioactive beams through the phenomenon of autoactivation—a physical process in which the projectile particles undergo nuclear fragmentation when they collide with target nuclei. With the help of proper detection devices, these radioactive particles should allow the development of important new diagnostic procedures hitherto impossible. Measurements are in progress with different radioactive beams (neon-19, carbon-11, oxygen-15) with the present form of PEBA. A second version of PEBA, using a large number of small NaI (Tl) crystals is in the designing stage. When completed, we would like to use the PEBA to demonstrate the multiple diagnostic uses of radioactive beams.

PHYSICAL CHARACTERIZATION OF ENERGETIC HEAVY-ION BEAMS

W. Schimmerling

Beams of carbon, neon, and argon nuclei, accelerated up to 90% of the speed of light, are available from the Bevalac at LBL. These high-energy, heavy-ion beams are important in biological and medical fields because they have advantageous radiobiological properties. Our fundamental studies of the various beams will advance understanding of the nuclear physics of high-energy heavy ions, will provide the information required to work out heavy-ion dosimetry for therapeutic applications, and will lead to their use in valuable diagnostic procedures.

One of the most important types of nuclear interaction when high-energy ions traverse an absorbing medium is the production of lighter fragments of the incident particle. These nuclear interactions of a penetrating beam will affect the Bragg peak dose because they cause a dilution of biological effect and an increased dose to tumorless tissues beyond the beam path. We are now studying the production of fragments as a function of depth in tissue-equivalent absorbers to determine their contribution to the

total energy deposited along the beam path. We are also developing calculational methods to incorporate these results and the cross-section measurements by other physics groups so we can predict the effect of nuclear interactions on dosimetry.

A series of preliminary measurements of the fragmentation of energetic heavy-ion beams traversing thick, tissue-equivalent targets were made. The experimental arrangement (see Fig. 1) consisted of several scintillation counters for beam definition and range discrimination, a multiwire proportional counter to define beam position, a time-of-flight telescope based on channel plate multiplier detectors, and a pulse ionization chamber. The Biomedical Computer Facility was used for on-line data acquisition, and a fairly sophisticated series of data-taking and analysis programs were developed by Dr. William Steele, on loan from another experimental group.

Measurements were made using beams of carbon, neon, and argon ions with energies in the range of therapeutic interest: 250-500

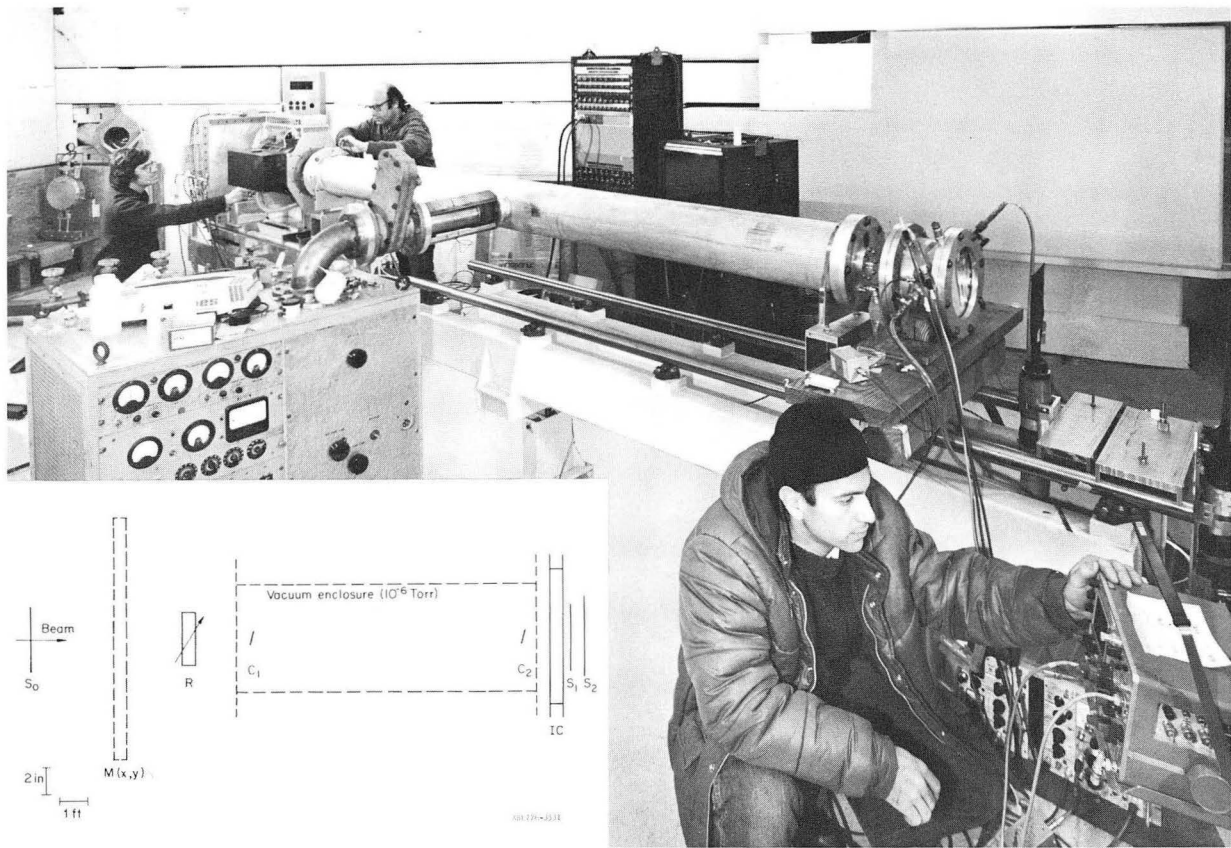


Figure 1. A view of the experimental arrangement used in Cave 1 for the physical characterization of heavy-ion beams. The beam is incident from the upper left. The large square box contains the multiwire proportional counter $M(x,y)$ (cf. insert, used for beam position measurements). The black box downstream of it is a vacuum enclosure for the time-of-flight telescope, followed by the ionization chamber (IC). Two scintillation counters (S_1 and S_2) are shown at the far right of the optical bench used to align the apparatus, in their black light-tight wrapping. The rack with dials connected to the middle of the vacuum pipe contains vacuum pumps and related equipment. Pictured with the apparatus are, from left to right, Douglas Ortendahl (Perez-Mendez Group), Walter Schimmerling (Radiation Biophysics Group), and George Gabor (Nuclear Instrument Techniques). Also participating in this experiment, but not pictured, were S. Kaplan (Nuclear Engineering), William Steele (now in CTR group), and Jack Ozawa (now at LLL).

MeV/nucleon. Preliminary results show that the apparatus performed as expected. The time-of-flight resolution of the telescope was of the order of 100 psec, and the charge resolution of the ionization chamber was of the order of 8%. The total mass of the particle identification detectors is of the order of a few hundred mg/cm^2 , and it was possible to explore the Bragg peak region in some detail.

A sample time-of-flight spectrum of a 500-MeV/nucleon argon beam after traversing $14.5 \text{ g}/\text{cm}^2$ of Lucite is shown in Figure 2. Data analysis of such spectra is in progress and will yield information on the spatial distribution of secondary fragments in biological absorbers. The measurements disclosed some beam characteristics that are not otherwise easily identifiable, such as occasional contamination and

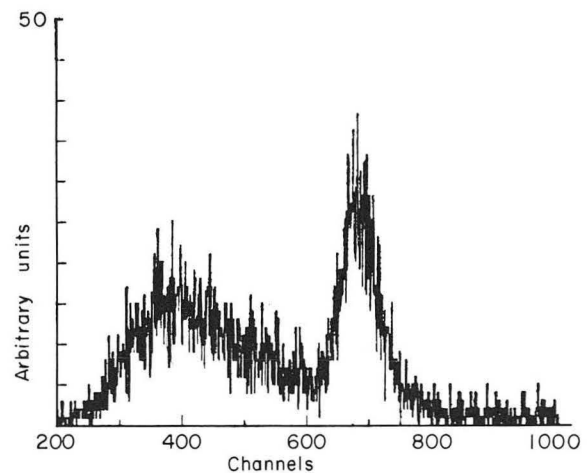


Figure 2. Sample time-of-flight spectrum of a 500-MeV/nucleon argon beam after traversing $14.5 \text{ g}/\text{cm}^2$ of Lucite.

increased energy spread due to mistuning and obstructions in the beam line. Preliminary analysis of the argon results shows that it is possible to separate at least three components of the emerging beam quite clearly—the primary beam, the lighter isotopes of the primary beam, and the (lighter) secondary beam fragments. This identification is possible because products of nuclear interactions that are heavier than the primary beam (nucleon pickup) are exceedingly rare. Most of the argon-induced fragments were in the region of neon to chlorine, with a clustering estimated to occur around phosphorus, although systematic effects that might be introduced by detection efficiency remain to be studied.

Detailed comparisons of calculated and measured velocity distributions will be made so that, eventually, accurate predictions of velocity and other distributions of interest to the radiobiologist and radiotherapist can be made. These basic physical data will then be used to estimate tumor response and assess the validity of models of cell killing currently under development by radiobiologists in our group.

In separate experiments studying neutron

production by high-energy heavy ions (funded by NASA), some results of interest were also obtained. Preliminary analysis of an initial data-taking run showed a significant difference between energy spectra of neutrons produced by 250-MeV/nucleon neon ions and proton spectra measured for the same configuration by other experimenters. At forward angles, the proton spectra show only a slight dependence on energy, while the neutrons seem to decrease exponentially with a greater proportion of low-energy neutrons. Data analysis of this work is also proceeding.

Finally, it is worth noting that the interdisciplinary environment of Donner Laboratory is conducive to applying research from one field to another. One such development currently in progress is an effort to apply the detectors used for time-of-flight measurements to the construction of x-ray imaging devices functioning at ultra-low doses. Medical radiographic procedures account for the bulk of the population exposure to radiation. Therefore, if the present project is successful, it would be an advance of major significance.

RESPONSE OF A RAT RHABDOMYOSARCOMA TO HEAVY-ION BEAMS

S. B. Curtis, T. S. Tenforde, W. Schilling, S. Daniels, and K. Crabtree

In order to develop a comprehensive model of tumor response to high linear energy transfer (LET) radiation, several cellular radiobiological parameters for charged particle beams at the Bevalac and the 184-Inch Synchrocyclotron are being measured using a transplantable rhabdomyosarcoma tumor system in a specific pathogen-free strain of syngeneic female rats. Experiments have been conducted with a helium ion beam produced at the 184-Inch Synchrocyclotron and with carbon-, neon-, and argon-ion beams accelerated at the Bevalac. These beams had the following initial energies and ranges in water: helium, 910 MeV/n, 22 cm; carbon, 400 MeV/n, 24 cm; neon, 400 MeV/n, 14 cm; and argon, 500 MeV/n, 12 cm.

IN VIVO TUMOR VOLUME RESPONSE AND TCD_{50} MEASUREMENTS: SINGLE RADIATION DOSES

Measurements of radiation-induced tumor growth delay were carried out for each of the four charged-particle beams. In these studies, the Bragg peak ionization region was spread out to a width of 4 cm by means of a variable-thickness absorber (ridge filter), and experimental tumors with volumes ranging from 0.4 to 1.0 cm³ (mean = 0.55 ± 0.09 cm³) were irradiated in the distal 1.5 cm of the extended peak. Tumor volume measurements were made with vernier calipers before and after the day of irradiation, thus producing a series of volume response curves displaying tumor regression and regrowth characteristics during the post-

irradiation period. From such curves, a determination was made of the radiation-induced growth delay, defined as the difference in time for irradiated and nonirradiated tumors to reach twice their volume on the day of irradiation. Plots of growth delay time vs. absorbed dose are shown in Figure 1 for R-1 tumors exposed to carbon-, neon- and argon-ion beams and to 220-kV x-rays. Using the growth delay curve for each charged-particle radiation modality, the relative biological effectiveness (RBE) was calculated by forming

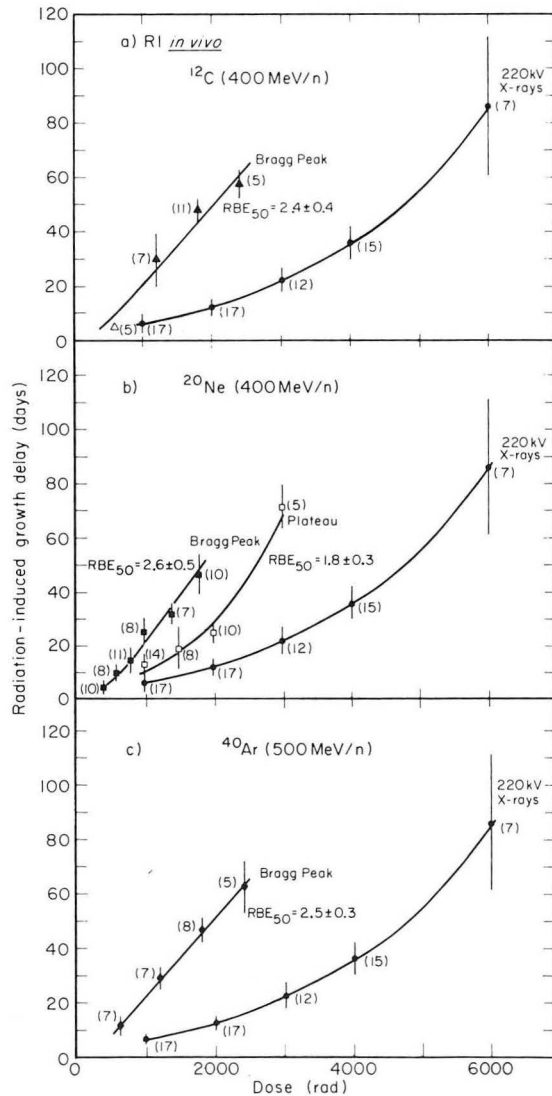


Figure 1. Radiation-induced growth delay is plotted as a function of absorbed dose for R-1 tumors exposed to 220-kV x-rays and to (a) carbon-, (b) neon-, and (c) argon-ion beams in the distal 1.5-cm region of a 4-cm spread-out Bragg peak. The growth delay curve for plateau neon ions is shown in (b). The number of tumors used for each dose is given in parentheses.

the ratio of x-ray to heavy-ion dose required to produce either a 20-day or 50-day growth delay (the RBE_{20} and RBE_{50} values). Values of RBE determined in this manner for the four accelerated ion species are summarized in Table 1 and demonstrate the following general results:

1. The RBE values for Bevalac-accelerated carbon-, neon- and argon-ion beams in the distal Bragg peak region do not differ significantly. The large values of RBE_{20} and RBE_{50} (ranging from 2.4 to 3.0) reflect the high LET of these charged particle beams and may also reflect the presence of a large hypoxic fraction of cells in the R1 tumor.
2. The RBE for Bragg-peak helium ions was significantly lower than the RBE values for the higher-Z ion species. This observation is consistent with the lower median LET in the 4-cm helium-ion Bragg peak region (15 to 25 keV/ μm) compared with the median LET in the spread-out Bragg peaks of carbon (40-120 keV/ μm), neon (80-250 keV/ μm), and argon (170-700 keV/ μm) beams.
3. The RBE values measured for plateau (high-energy) helium and neon ions were significantly less than the corresponding values for Bragg-peak radiation. This observation reflects the lower LET of the high-energy ions in the plateau ionization region (1.7 and 35 keV/ μm for helium and neon ions, respectively).

For Bragg peak helium and neon ions, measurements were also made of the 50% tumor-cure dose (TCD_{50}) assayed in a 180-day period (the $TCD_{50/180}$). As shown in Table 1, RBE values based on this endpoint did not differ in a statistically significant way from the RBE values obtained from tumor growth delay measurements.

IN VIVO TUMOR VOLUME RESPONSE MEASUREMENTS: FRACTIONATED DOSES

Six daily fractions of 250, 350 and 500 rad were administered to R-1 tumors positioned in the distal region of a 4-cm spread-out carbon Bragg peak. For comparison, R-1 tumors were administered six daily fractions of 650, 750 and 900 rad of 220-kV x-rays. The recovered dose per fraction calculated at the 50-day growth delay level was 6% for the Bragg-peak carbon ions and 10% for x-rays. At the 50-day growth delay endpoint, the RBE_{50} for the fractionated

Table 1. RBE values for radiation-induced growth delay of R-1 tumors *in vivo*.

Ion	Initial Energy (MeV/n)	Tumor Position*	RBE ₂₀ [†]	RBE ₅₀ [†]	RBE _{TCD50/80} [‡]
⁴ He	910	Bragg peak	1.5±0.3	1.4±0.3	1.4±0.2
¹² C	400	Bragg peak	2.8±0.7	2.4±0.4	—
²⁰ Ne	400	Bragg peak	2.9±0.7	2.6±0.5	3.1±0.6
⁴⁰ A	500	Bragg peak	3.0±0.6	2.5±0.3	—
⁴ He	910	Plateau	1.0±0.2	1.1±0.2	—
²⁰ Ne	400	Plateau	1.7±0.4	1.8±0.3	—

*The Bragg peak was spread to a width of 4 cm using a ridge filter, and tumors were positioned in the distal 1.5-cm region.

[†]RBE₂₀ and RBE₅₀ values were calculated as the ratio of the 220-kV x-ray dose to heavy-ion dose required to produce growth delays of 20 and 50 days, respectively.

[‡]RBE_{TCD50/180} values were calculated as the ratio of 220-kV x-ray dose to heavy-ion dose required to produce 50% tumor cures in 180 days.

carbon ions was 2.5 ± 0.3 , which is not significantly different from the RBE₅₀ of 2.4 ± 0.4 obtained for single doses. It is probable that the high RBE observed for the single-dose schedule resulted from the efficient sterilization of hypoxic cells by large doses of high LET carbon-ion radiation. In contrast, because of the previously demonstrated rapid reoxygenation in R-1 tumors, cell-killing with small fractionated doses occurred primarily in the oxygenated cell compartment. The high RBE for the fractionated schedule thus resulted, in all likelihood, from reduced repair of carbon-ion radiation damage relative to x-rays.

IN VIVO AND IN VITRO SURVIVAL CURVES

Survival curves for R-1 tumors exposed to Bragg-peak carbon and neon ions were measured after irradiation *in vivo*. REB_{10%} values in the distal position of a 4-cm peak were 2.0 and 3.0 for the carbon and neon ions, respectively.

IN VITRO RBE AND OER MEASUREMENTS WITH ACCELERATED HEAVY IONS

Extensive experiments have been carried out to determine cell survival characteristics and the magnitude of the oxygen effect at several positions in the plateau and extended Bragg-peak regions of carbon-, neon- and

argon-ion beams. In these studies, R-1 cells were irradiated in suspension under oxic and hypoxic conditions. With this technique, a cell suspension continuously gassed with either air or nitrogen is subjected to a series of prescribed radiation exposures; aliquots are sequentially removed, diluted to appropriate concentrations, and plated onto tissue-culture dishes for determination of colony-forming ability.

The x-ray survival curves obtained in this manner are in good agreement with those measured for R-1 monolayer cultures. The suspension technique has the advantage of permitting the acquisition of a large amount of cell survival data in a relatively short period of time. This factor is of considerable importance in accelerator experiments where beam time is both limited and costly. The principal disadvantage of the suspension technique is the thickness of the sample chamber (1.5 cm in our experiments), so that cell survival measurements must be regarded as an average over that depth within the radiation field. Using this technique, an OER₁₀ of 2.8 ± 0.2 has been obtained for R-1 cell suspensions irradiated with 220 kV x-rays.

Survival curves for R-1 cell suspensions irradiated at several positions along the Bragg curves of carbon- and neon-ion beams are reproduced in Figure 2. The Bragg peak region was spread out to a width of either 4 cm with a triangular lead ridge filter or 10 cm with a spiral

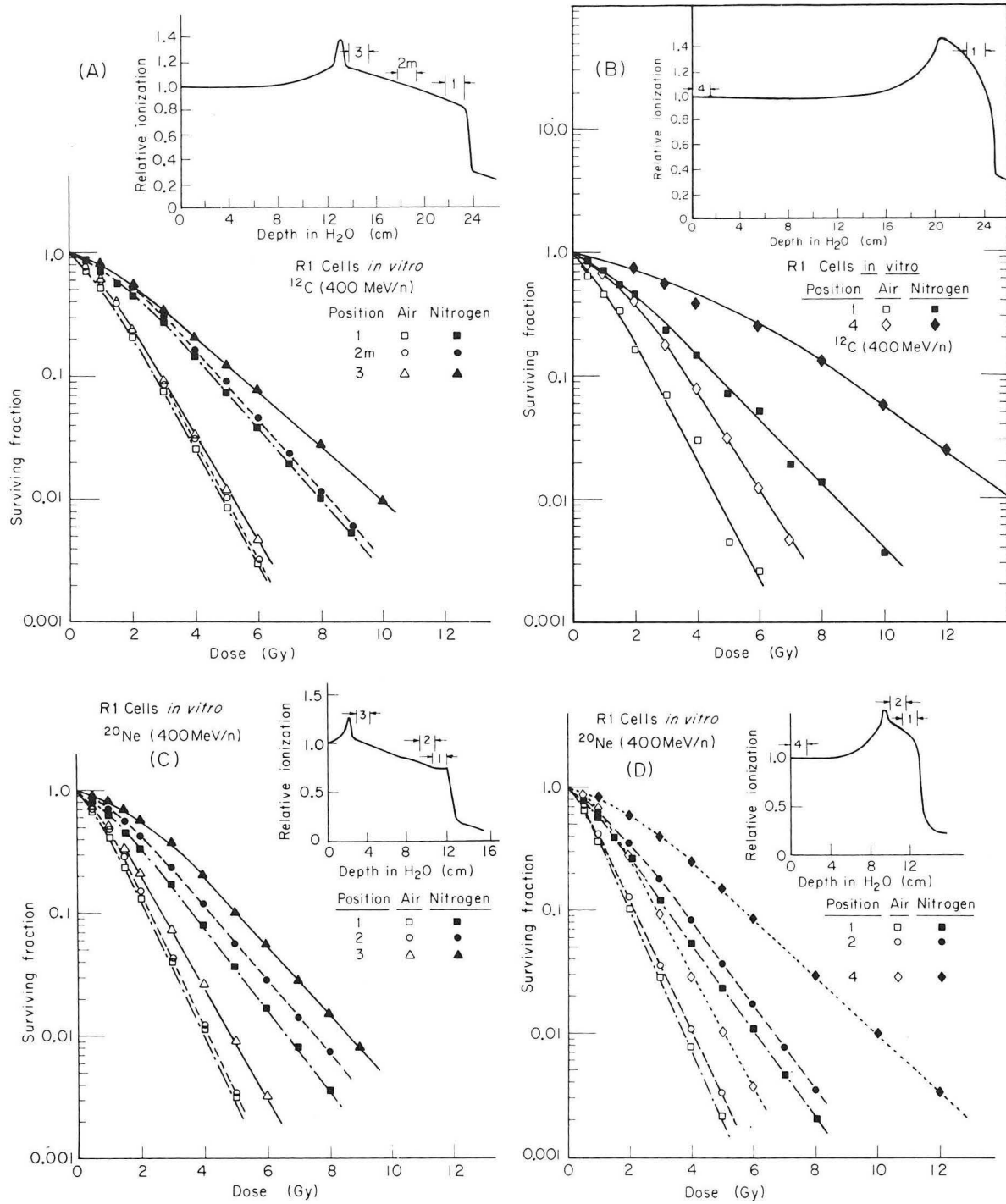


Figure 2. In vitro survival curves are plotted for R-1 cells exposed to carbon- and neon-ion beams at several positions along the Bragg curve. In the experiments shown in (A) & (C) the Bragg peak region was spread out to a width of 10 cm, and in (B) & (D) to a width of 4 cm. At each position, survival curves are shown for cells irradiated under oxic and hypoxic conditions. Each survival curve represents a composite of data obtained in two to four separate experiments.

brass ridge filter. A summary of RBE and OER data is given in Table 2. Several statements can be made on the basis of these results:

1. The values of OER obtained for plateau carbon and neon ions were higher than the OERs obtained in the extended Bragg peaks of these beams.
2. In the most distal region of the 4-cm and 10-cm spread-out Bragg peaks, the OER decreases from 1.8 for carbon and 1.7 for neon to 1.3-1.4 for argon ions. Because of the experimental error, the difference in OER values for the carbon and neon ions is not significant.
3. For both carbon- and neon-ion beams, the OER is higher in the proximal region relative to the distal region of a 10-cm spread-out Bragg peak. This observation reflects the higher median LET near the distal end of an extended Bragg peak.
4. The therapeutic ratio, RBE (spread-out Bragg peak)/RBE (plateau), is approximately the same for the carbon- and neon-ion beams.

In vitro RBE and OER measurements have also

been carried out for 910 MeV/n helium ions with 4-cm and 10-cm extended Bragg peaks. In addition, experiments have been performed with carbon- and neon-ion beams of different energies in order to compare RBE and OER values for these two beams under conditions of identical range. The results of these experiments are presently under analysis.

COMPUTER MODELING OF TUMOR RADIATION RESPONSE

A Tektronics 4012 graphics terminal was obtained and connected via telephone line to the Biomedical PDP 11/45 computer at the Bevalac. A computer code was written to accept measurements of tumor diameters and to calculate and plot tumor volumes and standard errors. This program permits intercomparison of the post-irradiation volume response of tumors that are subjected to different radiation modalities and to different doses. Data obtained in the experimental program described above are being incorporated into a model of tumor response to high LET charged-particle radiation.

Table 2. RBE and OER values for R-1 cells exposed to Bevalac-accelerated heavy-ions *in vitro*.

Ion	Initial energy (MeV/n)	Ridge filter (cm)	Position*	RBE _{10%} ^{oxic†}	RBE _{10%} ^{hypoxic†}	OER _{10%} [‡]
¹² C	400	4	Plateau	1.2	1.5	2.4±0.2
		4	1	1.7	2.8	1.8±0.2
		10	1	1.7	2.8	1.8±0.2
		10	2m	1.6	2.7	1.8±0.1
		10	3	1.6	2.3	2.0±0.1
²⁰ Ne	400	4	Plateau	1.6	2.2	2.0±0.3
		4	1	2.3	4.4	1.7±0.1
		10	1	2.1	3.4	1.7±0.1
		10	2	2.0	3.0	1.8±0.1
		10	3	1.7	2.5	1.9±0.2
⁴⁰ Ar	500	4	1	2.3	4.4	1.4
		10	1	2.1	4.2	1.3

*The positions labeled 1, 2, 2 m and 3 in the 4-cm and 10-cm spread-out Bragg peaks correspond to the positions shown on the Bragg curves reproduced in Fig. 2. Position 1 is located in the distal region of the extended peak, positions 2 and 2 m are in the mid-peak region, and position 3 is in the proximal region. The plateau position is denoted as 4 in Fig. 2.

†RBE values were calculated at the 10% survival level relative to 225-kV x-rays.

‡OER values were determined at the 10% survival level; OER values for carbon and neon ions represent the mean ±1 standard deviation calculated from two to four experiments; the OER values for argon ions were measured in a single experiment.

CELL SURVIVAL STUDIES WITH HEAVY-ION BEAMS

C. A. Tobias, E. A. Blakely, and F. Q. Ngo

Heavy ions are used in cellular radiobiological research to improve cancer therapy. Our present studies are based on a variety of findings gained from experiments at low energies, including the following properties of heavy ions: (1) they decrease the radiobiological oxygen effect at the cellular level; (2) they decrease sensitivity variations during the cell division cycle; (3) they reduce repair; and (4) they retain most of the depth-dose advantages of protons and helium ions. Aneuploid cells and cells with abnormally large nuclear cross sections (like those often found in cancerous tumors) have a greater sensitivity to heavy ions than do normal cells. Since the Bevalac was completed in 1976, a vigorous effort has been made to analyze the radiobiological properties of cells in culture and to relate these properties to the requirements of cancer therapy.

We have addressed two aspects of cell survival after exposure to heavy ions, and experiments at the Bevalac (using human kidney T-1 cells and Chinese hamster cells) have been designed accordingly. One aspect is aimed at understanding the basic mechanism involved in cell killing by ionizing radiation; the other is the analysis of radiobiological properties of cells in culture with reference to high-LET (linear energy transfer) particles and the relationship of these properties to the goal of optimal therapeutic use. Figure 1 shows a specially designed apparatus for heavy-ion studies at the Bevalac.

Extensive studies have been completed with unmodified carbon, neon, and argon beams (see Figures 2 and 3). These data have formed a basis for testing molecular and

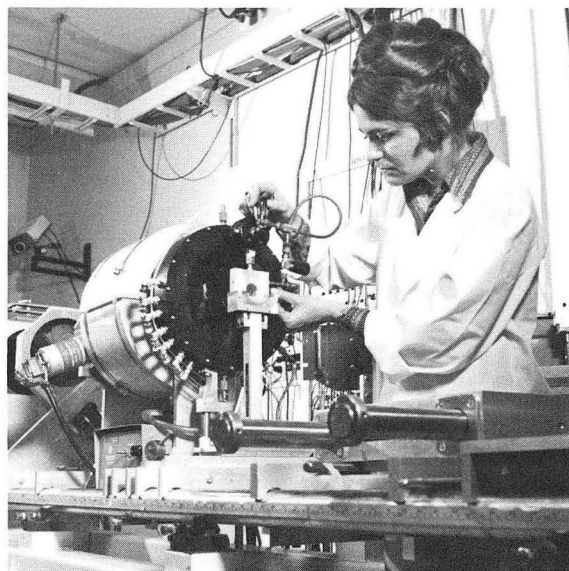


Figure 1. This specially designed apparatus is used to study the sensitivity of cell lines, under varying controlled environmental conditions, to irradiation with accelerated heavy ions from the Bevalac. The cells are grown in monolayer on a glass Petri dish, which is then inserted into the special chamber. Dr. Eleanor Blakely is shown here, positioning the cell chamber in the beam line. To study the oxygen effect, the chamber is filled with either oxygen or nitrogen during the heavy-ion beam exposure, and the survivals for the two conditions are compared.

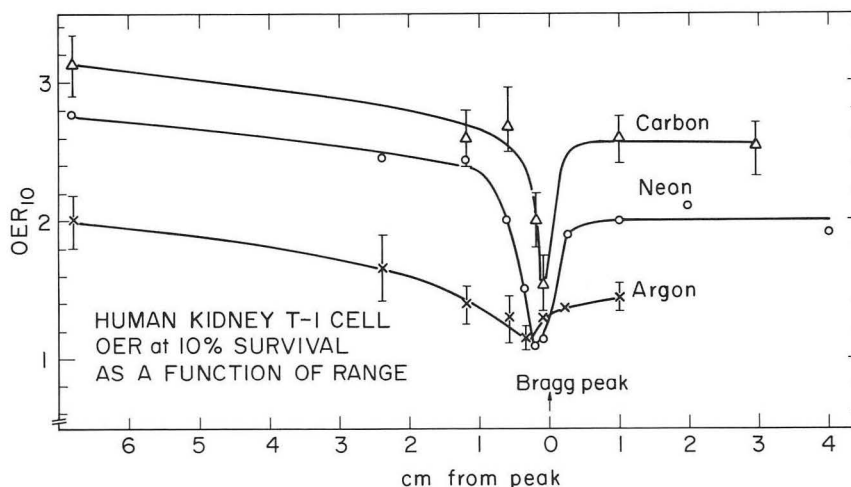


Figure 2. Summary of OER values for carbon, neon, and argon beams at 10% survival level. The beam enters from the left; fragmentation effects beyond the Bragg peak are seen on the right.

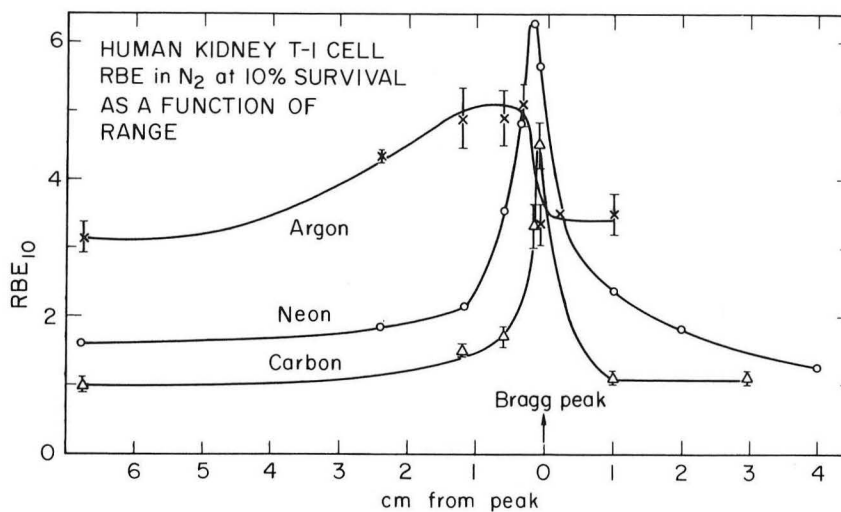


Figure 3. Summary of RBE values for T-1 cells at 10% survival level. The beams (C, Ne, or A) enter from the left; RBEs for fragments beyond the Bragg peak are recorded to the right.

physical models for the mechanism of action of high-LET radiations as a function of velocity, charge, and atomic number. However, a therapist would rarely treat a patient with monoenergetic heavy particles because the Bragg peak is very narrow. Hence, efforts have been made to adequately spread the energy (extend the Bragg peak) to cover a wider tissue volume. We have shown, for example, that the oxygen enhancement ratio (OER) for argon in the unmodified peak is 1.2 to 1.3 and increases to 1.3 to 1.4 over the cross-fired 4-cm extended peak. This is a lower OER than is currently available with any other modality. However, the peak-to-plateau relative biological effect (RBE) and physical dose ratios for the neon and carbon beams are more advantageous than argon, where saturation effects occur in the peak. Thus, consideration must be given to the characteristics of the tumor to be treated before a decision can be made on which beam is best for therapy. It is possible that the large reduction of the oxygen effect achieved by extended argon beams may be especially useful for tumors with hypoxic cells and may outweigh the slight loss of RBE and physical dose advantages.

One group of studies concerns the effects of external chemical modifiers on biological lesions. Besides playing a possible role in therapy, these studies are important to our understanding of molecular damage mechanisms. We are investigating whether the modifiers act on the initial fast radical reactions, on macromolecular long-lived states, or on the

repair mechanism.

An additional set of studies has been initiated that examines the cellular effects of combined heavy-ion and x-ray radiation. This combined radiation modality will provide new information on the nature of radiation damage due to heavy ions (such as sublethal lesions and repair), which would not be available from studying each radiation type separately. Our ultimate goal is to establish a radiobiological basis for the potential application of mixed radiation modality for therapeutic uses. It was often assumed that high-LET particles killed cells by causing radiation DNA lesions that were irreparable. In contrast to this hypothesis, we have showed that with the combined radiation modality technique, sublethal lesions are involved in the killing mechanism (see Fig. 4). In conjunction with these studies, dose-fractionation experiments with neon and carbon ions at the Bragg plateau region and at the peak region have led us to suggest a new parameter (called the fractionation gain factor, or FGF), which indicates that heavy ions may have special advantages for therapy.

In the past few months we have seen some of these studies come to fruition as the first patients were treated with the carbon and neon beams. We will soon be able to determine which beam is most advantageous for specific tumor types, and begin controlled therapeutic studies in which heavy ions are compared with more conventional radiological techniques.

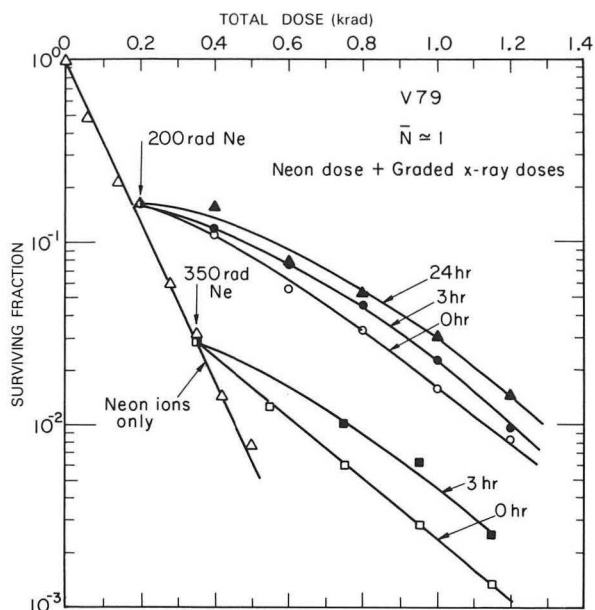


Figure 4. Survival data of V79 Chinese hamster cells exposed to graded doses of neon ions near the Bragg peak (initial energy 425 MeV/amu), or graded doses of x rays (225 kVp, 15 mA) preceded by a single dose of neon ions. The time indicated represents the interval at 37°C between the two modalities of radiation. These data suggest that sublethal damage is produced by neon ions and can be repaired.

HEAVY-ION RADIOGRAPHY

C. A. Tobias and E. V. Benton

The heavy-ion radiography project is continuing to develop methods for two- and three-dimensional reconstruction of radiographic images taken with high-energy accelerated particles (carbon and neon). The stopping points of these heavy ions can be precisely recorded in a stack of plastic nuclear detectors after they have passed through the object to be radiographed. The stopping point distributions can then be analyzed in terms of the electron density distribution of the object. The ability of heavy-ion beams to measure small density differences in tissue-like materials is more sensitive than any other known method. Thus far we have been able to obtain a 0.1-cm resolution laterally and 0.1% accuracy in depth. We find that carbon beams are practical to use in heavy-ion radiography; however, in the future it is possible that boron or helium beams will be used for a somewhat lower dose, or neon or oxygen for a better resolution. Heavy-ion radiography may extend beyond the sphere of biomedical applications; some preliminary radiographs have been taken of engineering apparatus where normal x-ray procedures cannot be used.

After radiographic studies of specimens, we initiated a series of heavy-ion human mammography studies. In the medical phases of

the work a collaborative arrangement exists with the staff of the Radiobiology Department, University of California, San Francisco; a group of Bay Area physicians also participate. In 1977 we performed mammographies for 25 patients referred to us through a group of San Francisco Bay Area physicians. Our goal is to perform an additional 40 mammographies in the coming year. Superior contrast was demonstrated for carbon ions for small-density differences in breast tissue; however, x-rays were better for detecting microcalcifications. On several specimens it was shown that the electron density of the carcinoma was greater than that of cysts, which was greater than that of fatty deposits. In 3 of these first 25 patients, densities were detected in the heavy-ion radiographs in the tumor region that were not seen in the x-rays.

Usually single exposures of carbon ions are at 80 mrad at the exit side. With experience, the dose levels were gradually lowered so that at 20 mrad we can obtain satisfactory mammograms. Figure 1 is a sample of one sheet of a high-dose mammogram (80 mrad) compared with a low-dose mammogram (19 mrad) of the same breast. The low-dose picture has more noise, but it has the essential information for the radiologist and for computerized scanning. By taking radiographs of the left and the right

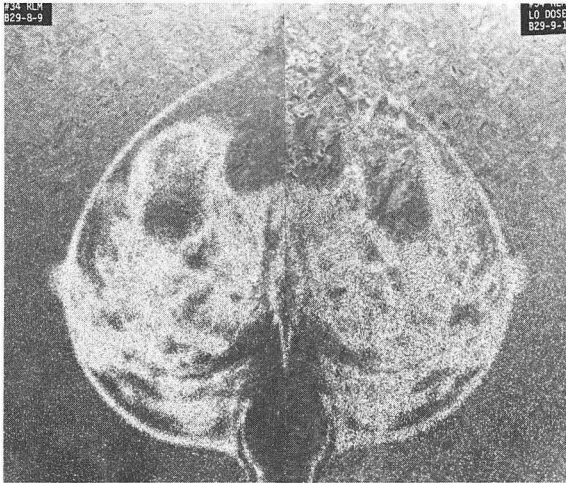


Figure 1. High-dose mammogram (80 mrad) compared with a low-dose mammogram (19 mrad) of the same breast. The low-dose picture has more noise, but it has the essential information for the radiologist and for computerized scanning. Standard x-ray mammography usually uses more than 0.5 rad (500 mrad).

breasts of the same individual, the radiologist can look for asymmetries in opposing breasts as indications of high density tissue. Figure 2 shows such a comparison. Early results of our program indicate that ductal carcinomas and other tumors usually have higher density than normal stroma or lipid tissues of the breast. A program is under way to test the significance of heavy-ion diagnosis by comparing the results to other diagnostic modes, surgery, and post-operative pathology.

In the comparative evaluation of heavy-ion radiographs with xerograms and mammograms, we gradually realized that the heavy ions furnish information not available from other methods (for example, quantitative density distributions), which often correlate with other findings. Carbon radiographs do not

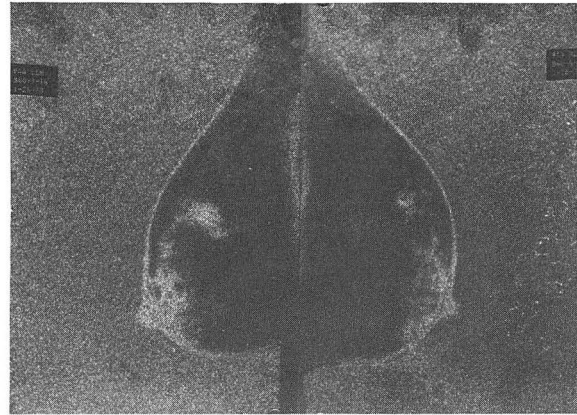


Figure 2. These are two carbon radiographs, taken laterally, one of the left and one of the right breast of the same individual. Radiologists look for asymmetries in opposing breasts as indications of high-density tissue. In these radiographs, the whitish region in the upper portion of the breast shows a high-density region.

pick out microcalcifications but high-density regions were identified in several cases in regions corresponding to microcalcifications. For objective evaluation, the isodensity contour maps, which carry quantitative information on the average density at each scanned location, appear to be of some value. However, in the analysis of fibrocystic disease or dense breasts it has become desirable to use density distribution plots which display the statistical distribution of the frequency of picture elements as a function of tissue density.

The computer can find and plot each area of a chosen density and a certain amount of correlation can be established between the various density distribution functions. We hope that as the number of cases accumulate and computerized assay methods improve, we can establish strong correlations between contour graphs, density distribution graphs, and the occurrence of cancer.

TREATMENT OF CANCER WITH HELIUM AND HEAVY IONS

J. R. Castro

This clinical radiotherapy project, which is evaluating the use of the helium-ion beam from the 184-Inch Synchrocyclotron and several heavy-ion beams such as carbon, neon, and argon from the Bevalac for treatment of human cancers, has been under way at LBL since July 1975. The key to successful radiotherapy lies in the ability to achieve a favorable therapeutic ratio—to be able to deliver an adequate radiation dose to an entire tumor volume while sparing the surrounding normal tissues. Heavy charged-particle beams have radiobiological and physical dose distribution giving them therapeutic advantages compared with conventional radiation techniques. In this situation, the volume of normal tissues within the target is reduced and the biological effect of the radiation on tumor cells is greater than on surrounding cells. Both these factors enhance the sparing of normal tissues and thereby improve the probability of an uncomplicated cure.

HELIUM-ION PILOT STUDY

The 184-Inch Synchrocyclotron and medical cave were modified to permit large-field, multifractionated 934-MeV helium-ion spread-out Bragg peak irradiation of a variety of tumor sites including brain, head and neck, esophagus, pancreas, stomach, and pelvis. A selected group of 55 patients with a variety of far advanced or locally recurrent tumors have been treated during the past 2½ years. No untoward effects have been noted in the acute phase or immediate follow-up period using our current dose schedule of 6,000 rads in 7 weeks, 4 fractions per week. Much has been learned concerning treatment techniques, tumor response, and normal tissue response in preparation for irradiations with heavier particles at the Bevalac.

BEAM STUDIES

A double scattering system has been implemented in the biomedical beam at the 184-Inch Synchrocyclotron, which will produce fields as large as 27 cm in diameter that are uniform to $\pm 2\%$ over 92% of the field. Secondary collimation of the expanded beam is accomplished by low-melting-point alloy collimators individually shaped for each patient.

The Bragg peaks of monoenergetic heavy-ion beams are narrow (less than 1 cm) and must be broadened in order to produce a more useful therapeutic depth-dose distribution. This modification of the dose distribution is usually obtained by using a range modulator such as a ridge filter. Using physical and radiobiological data, we have designed and fabricated a family of ridge filters to provide the clinical flexibility needed in radiotherapy. These will provide isosurvival regions (spread-out Bragg peaks) with widths between 4 cm and 14 cm (in 2-cm increments) to allow optimal therapeutic depth-dose distributions for a variety of anatomical sites.

Further evaluation of the radiobiologic parameters of the helium ion beam has been done to assist with planning and delivery of clinical radiotherapy. Radiobiologic studies continue with carbon, neon, and argon beams at the Bevalac to determine the most suitable heavy-ion beam for clinical studies.

TREATMENT PLANNING

Treatment plans have been calculated for sites of interest for heavy charged-particle therapy, taking into account the effect of inhomogeneities in the beam path. We have been using computer-assisted tomographic (CT) scanning techniques for tumor localization and for delineation of tissue densities. Drs. G. Chen and R. P. Singh have continued to modify the DOSEM computer code for radiation treatment planning to include tissue inhomogeneities, oblique beam entry, multiple coulomb scattering, and so forth. Wax bolus is frequently made for most of the patient treatments in order to provide at least a moderate compensation for inhomogeneities.

PATIENT SET-UP AND IMMOBILIZATION

The majority of patients treated with a horizontal beam are immobilized in an upright isocentric position. The major advantage of an upright position over a supine or prone patient orientation is the ability to deliver oblique fields accurately by rotating about an isocenter. This position also offers more patient comfort, ease of set-up, and better reproducibility. Accessories have been built to attach to the cyclotron

patient positioner Isocentric Stereotaxic Apparatus for Humans (ISAH) to allow treatments to be given in either a seated or standing position (see Fig. 1). Also available for use are a bite block head-holder assembly for head and neck therapy; both line and spot lasers to facilitate patient set-up; Lightcast (photosetting plastic resin) to make individual girdle-like belts that help fix the patient contour and also support bolus and compensators; and face mask technique, as used for pituitary irradiation therapy, to immobilize the head in some situations.

BEVALAC

The remodeling and outfitting of necessary clinical facilities for the heavy charged-particle irradiation at the Bevalac is under way, including

installation of a patient positioner. Heavy charged particles such as carbon, neon, and argon have the potential to improve physical dose distributions and increase biological effect on the tumor compared with helium ions, which mainly are valuable because of dose distribution advantages.

Pretherapeutic evaluation of carbon, neon, and argon beams from the Bevalac is well under way. Pilot clinical studies have been started with carbon and neon ions, using patients with advanced skin and subcutaneous nodules to establish clinical relative biological effect (RBE) for skin irradiation. Preliminary studies will be carried out over the next two years to evaluate which ions appear the most promising for clinical trials and to determine the feasibility of prospective randomized trials at the Bevalac.



Figure 1. Helium ion treatment room at 184-Inch Synchrocyclotron. "Patient" is shown in standing position, as for treatment of pancreas carcinoma, with the ISAH pedestal by the right leg. The monitoring microphone is by patient's head. A Lightcast immobilization girdle is in place, supporting the beam flattening bolus on the patient's abdomen. The beam line comes in from the left center.

CLINICAL TRIALS

The potential physical and biological advantages of using heavy charged particles must be tested in a clinical setting. An informal organization of interested radiotherapists and other scientists, the Bay Area Heavy Ion Association, was initially established several years ago in order to provide design of a cooperative clinical trial and assist in referral of patients. During the past few years the Northern California Cancer Program (NCCP) has been organized. The clinical trial group of NCCP is

the Northern California Oncology Group (NCOG), headed by Dr. Stephen Carter. LBL has been accepted as a special member of NCOG and the Radiation Therapy Oncology Group (RTOG) to facilitate coordination of its clinical heavy-ion protocols with other cancer protocols in the area. Prospective randomized helium-ion trials will begin this year, together with Phase I-II carbon and neon ion studies. The duration of patient accession for these clinical trials is estimated at five years for the helium trial, and two to three years for the pilot heavy-ion studies.

Magnetic Field Studies

BIOLOGICAL EFFECTS OF HIGH MAGNETIC FIELDS

T. S. Tenforde

Biological effects of stationary and time-varying magnetic fields are being studied in selected molecular, cellular, and whole-animal systems. The immediate goal of this investigation is to provide quantitative baseline data for the establishment of exposure guidelines for workers at fusion reactors, magnetohydrodynamic systems, and other energy-related technologies that utilize intense magnetic fields. A long-term objective is to develop a fundamental understanding of magnetic field interactions with biological systems.

Initial efforts have concentrated on the construction of a laboratory facility suitable for carrying out a broad spectrum of magnetic field studies. Figure 1 shows the completed research facility, which contains five electromagnets and an experimental staging area. A preliminary design has also been made of a large-volume magnet for future human subject research so that eventually we will be able to evaluate magnetic field effects on human health by performing functional studies on the visual, cardiovascular, respiratory, and nervous system of exposed individuals.

Another aspect of this program that has been under development is the design and fabrication of environmentally controlled exposure chambers for experimental animals and cellular and molecular systems. These chambers have been specially constructed with nonmagnetic materials and provide for rigorous

control of light, temperature, and humidity. The chamber for rodent experiments also contains a variety of transducers for automated monitoring of physiological parameters and activity patterns during exposure to magnetic fields.

A somewhat unique facet of this project has been the development of electronic devices that are operational in strong magnetic fields. The type of instrumentation problem that we have encountered is clearly exemplified by our efforts to develop a biotelemetry unit for the continuous monitoring of body temperature in exposed rodents. The essential element of this system is an implantable telemetry pill which contains a battery-driven thermistor and an oscillator circuit that radiates a signal (~ 100 MHz) proportional to body temperature. This signal is picked up by an antenna and decoded to give a pulse-interval-modulated signal, which is shown on the oscilloscope screen in Figure 2. The commercially available unit fails to function in a magnetic field exceeding 100 G because of an iron-core oscillator in the circuitry that produces the radiofrequency signal. We therefore worked with the Königsberg Instrument Company of Los Angeles to produce a telemetry pill containing an air-core oscillator. A totally nonmagnetic battery was also installed to prevent orientation of the pill in strong fields. With these modifications, the operation of the telemetry pill was found to be unaffected by fields as high as 15 kG.

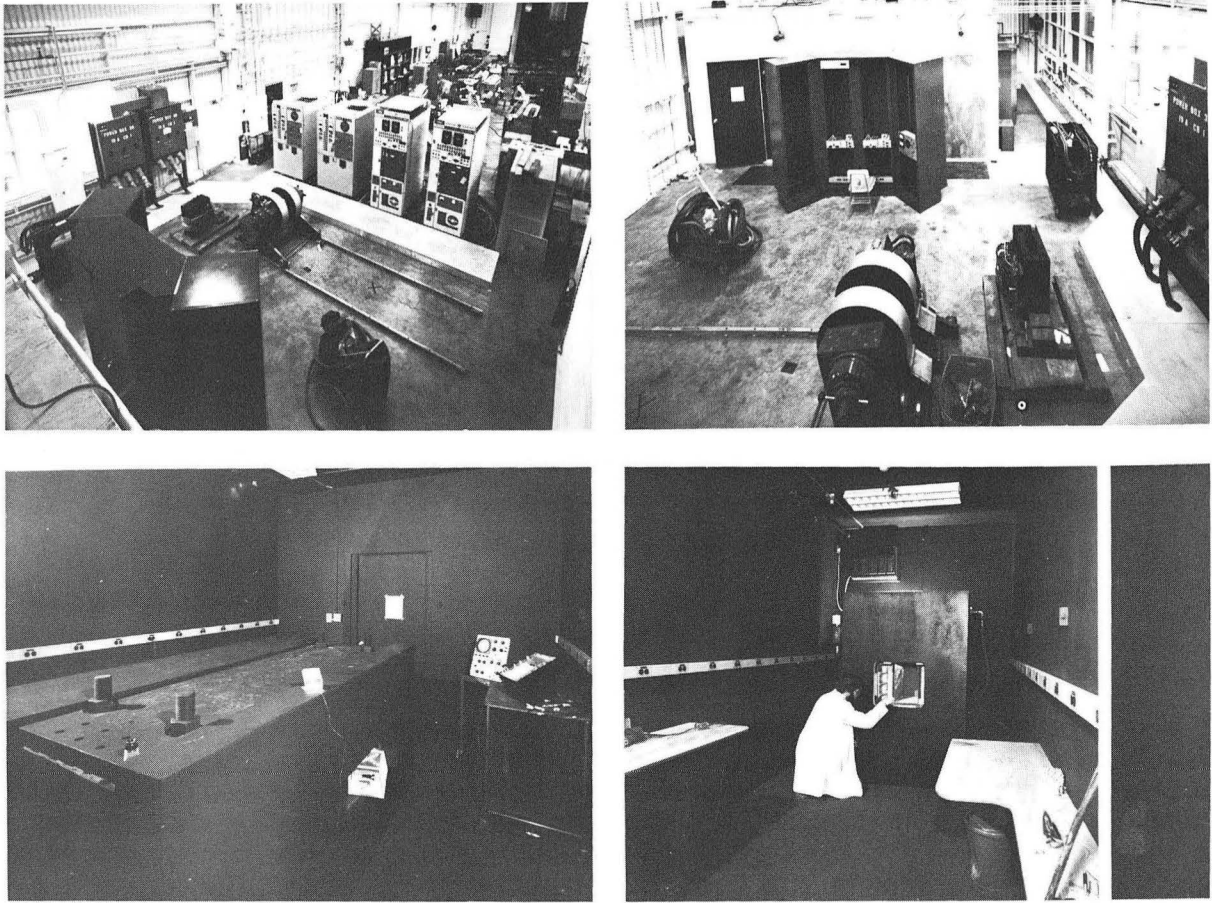


Figure 1. Four views of the biomagnetic facility built in the High Bay region of LBL Building 10 during 1977. Upper left panel: power supplies for five large-volume electromagnets. Upper right: 400-ft² magnet enclosure. Lower left: 17-kG DC magnet for animal physiology studies. Lower right: 18-kG DC magnet for electrophysiological measurements on neural and retinal tissues.

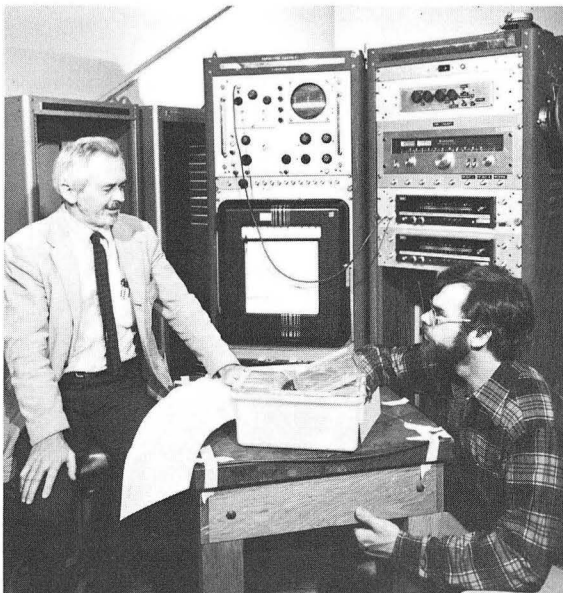


Figure 2. Consulting engineer Charles Dols (left) and research associate Steve Hurst (right) work with a temperature telemetry unit that will be used to continuously monitor the body temperature of rodents exposed to intense magnetic fields. The pulse-interval-modulated signal shown on the oscilloscope screen at the upper left is directly correlated with body temperature.

The magnetic effects project has four principal areas of experimental research. A list of these areas and the associated staff members follows:

Animal physiology (T. Tenforde, S. Hurst, G. Ryan). Magnetic effects in small mammals are being investigated by measurements of food intake, body weight, temperature, respiration, climbing activity, blood and urine composition, plasma hormones, cellular mitotic activity, and tissue pathology.

Visual and nervous tissues (M. Raybourn, C. Gaffey, G. Meyer). Electrical recording will be made from retinal photoreceptor cells, which contain photopigments that exhibit orientation in magnetic fields of approximately 1 kG intensity. Magnetic field effects on the electrical activity of rat brain neurons and the chemical activity of the neurotransmitter enzyme acetylcholinesterase will be examined.

Molecular studies (R. Roots, R. Farinato). Orientational effects of magnetic fields on macromolecules such as supercoiled DNA are

being investigated by electro-optical techniques.

Developmental studies (T. Yang, L. Craise). The development of the plant *Phycomyces* and the beetle *Tribolium* are being examined after exposure to intense stationary fields. To date, several experiments have been carried out to determine the influence of a 16-kG field (produced by permanent magnets) on the hatchability of beetle eggs. A wide range of incubation temperatures were used in these experiments to explore the possible combined effects of a strong magnetic field and an imposed thermal stress. Table 1 summarizes the results of studies carried out at 36.5°C, the upper limit of the temperature range in which *Tribolium* eggs can hatch. From these data, it is clear that no statistically significant difference occurred in the development of control and exposed eggs. These studies will be extended to the development of larvae, looking at parameters such as wing formation.

Table 1. *Tribolium* egg hatchability at 36.5°C in a 16-kG field.*

Time of exposure	Number of experiments	Total number of eggs per group	Percent hatched in control group†	Percent hatched with B = 16 kG†	Difference in percent hatched	p‡
3 days	8	1530	73.5±3.4	74.5±3.8	1.0	0.6 (N.S.)
4 days	9	1570	60.2±9.3	62.2±6.1	2.0	0.6 (N.S.)

*A uniform 15-kG field was applied by permanent magnets placed in an incubator regulated at 36.5±0.3°C.

†Errors represent one standard deviation.

‡Based on student's "t" test; "N.S." denotes that the difference in mean values for the control and the exposed groups is not significant.

Biophysical Studies

CELL-MEMBRANE BIOPHYSICS AND ENVIRONMENTAL AGENTS

H. C. Mel

Our group is interested in cell-membrane biophysics, particularly as it applies to populations of blood cells—their condition, their normal and abnormal production and destruction, and their interactions with agents such as environmental pollutants and drugs. The membrane is the cell's exterior barrier, which allows it to control its own internal environment. That is, the membrane protects the cell from the outside world while still permitting it to carry out its normal functions within a living animal or human, including exchanges and other interactions with its surroundings.

The group has been interested in several kinds of problems of blood cell populations. Our studies include: (1) determining the physical properties of the cells and how these can be related to cell condition; (2) understanding the nature and role of various subpopulations within a given population—in a sense, serving to delineate the “ecological” properties of the heterogeneous cell population; (3) investigating mechanisms of production and development of blood cells (in the bone marrow) and how these are altered under abnormal conditions; and (4) developing new methodology for separation and analysis of cell populations to aid in the above objectives.

With respect to cell physical properties, the group has been particularly interested in the size, density, and electric charge of cells (especially of red blood cells) because these factors have proved to be excellent markers of cell condition and change. More recently we have turned to some newer dynamic properties of blood cells, namely their ability to deform under stress (their deformability), the mechanisms and rates of their “self-destruction” when placed in dilute solution (osmotic hemolysis), and finally the subsequent self-repair undergone by their membranes as they recover their former integrity.

Some degree of deformability is vital to survival of red blood cells since in their continual circulation they must pass through capillary spaces considerably smaller than their normal dimensions. An inability to “flex” and pass through such microcirculation can not

only endanger the cell's existence (human red cells normally live about 120 days before being replaced by new cells) but also poses a threat to the life of the host individual. Sickle cell anemia is one disease in which this is the case.

In recent years we have developed a new, rapid automated method called resistive pulse spectroscopy (RPS) for measuring a new shock-response kind of deformability of the red cell, which depends particularly on the membrane. We have been using RPS to study cells in both normal and abnormal conditions. In essence RPS generates electrical pulses, collected into multi-cell spectra, from passage of individual cells flowing through a small orifice. By computer analysis of these spectra we are able to deduce the cell's deformability, to obtain a more precise measure of cell size, and to determine other useful properties of the cell-membrane composite system. A recent extension of the RPS work has permitted investigations of dynamic osmotic hemolysis, as will be described below.

An illustration of the use of RPS spectra is given in Figure 1(a), where “channel number” corresponds to apparent size. Native *deformable* red cells give a “bimodal” spectrum of apparent sizes. When the cells are rigidified under controlled conditions, the bimodality disappears. A mixture of two differently sized *rigid* subpopulations could give a bimodal curve similar to that for the native deformable cells. However, this situation would be easily distinguishable from that shown in Fig. 1(a), since the “fixed” spectrum for the second case would be identical with the “native” one. The RPS computer program readily analyzes the degree of bimodality of such spectra; for a deformable cell sample, it generates a numerical “deformability index” which serves as a new kind of characterizing feature for blood cells.

An additional important RPS measure of both size and deformability is obtained by reducing the rate at which the cell suspension flows through the small orifice. Under these conditions of reduced stress on the cells, they do not deform and they appear to be the same

size as their “ideally fixed” counterparts, as shown in Figure 1(b). Such spectra, in fact, now become the best available measures of red cell size “uncontaminated” by considerations of deformability and the normal red cell population is seen clearly to have a single, symmetrical distribution of size. For the other kind of case just mentioned, where a bimodal distribution might actually represent a mixture of different-size cell types, the “slow flow” mode of RPS reveals this also, and it provides a high-resolution measure of their individual sizes, as indicated in Figure 2.

A recent extension of RPS permits investigation of “dynamic osmotic hemolysis,” that is, the process of “explosion” of a red cell upon exposure to sufficient osmotic stress, and its subsequent recovery. This recovery may be likened to the repair of a perforated self-sealing fuel tank (or perhaps to the “repair” of a punctured piece of bubble gum). An illustration of the red cells caught in the nearly instantaneous act of hemolysis is given in Figure 3. The “blowout hole” covers roughly 20% of the membrane surface, and most of the cell’s hemoglobin escapes through it, leaving a resulting membrane sack called a ghost.

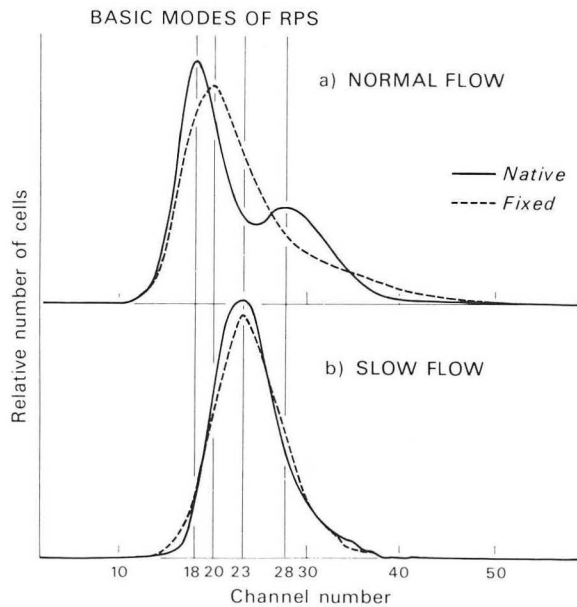


Figure 1. RPS spectra of native deformable, and glutaraldehyde-fixed human red blood cells: (a) normal flow, 0.008 ml/sec (curves are drawn through the 64 channel data points); (b) same preparation, analyzed at slow-flow rate, 0.0012 ml/sec.

Studies by Resistive Pulse Spectroscopy

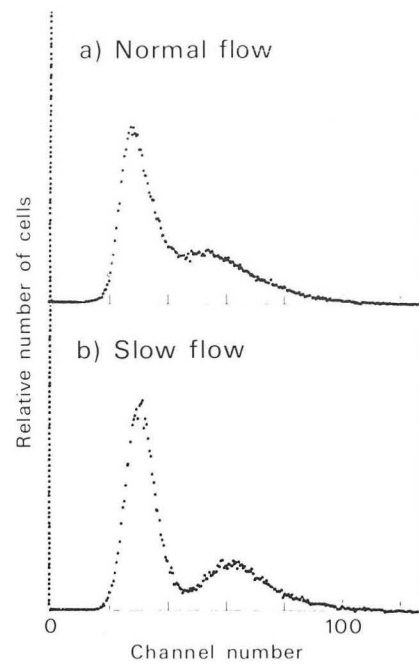


Figure 2. Mixture of glutaraldehyde-fixed human adult and fetal blood (X-Y plotter outputs of data points taken at 256 channel precision): (a) measured at normal flow; and (b) measured at slow flow.

RPS is also able to capture the red cells in this act. It was, in fact, by application of RPS methods that the conditions were determined which permitted obtaining a picture like Figure 3. Figure 4 shows selected spectra from RPS sequences taken during the 440 sec. immediately following initiation of the hemolytic process. The on-line computer, in analyzing the normal flow sequence, determines the rate at which new ghosts are produced (the increasing number of cells in the first peak) and the rates of recovery—for example, the rate at which the first peak moves upward to join the second peak (which represents resistant intact cells). Both the slow-flow sequence and the fixed spectra (dashed curves at 60 sec) indicate that the apparent small size of “young” ghosts results primarily from the very high deformability of these ghosts, rather than being a size-reduction effect as believed by previous workers. We conclude this from the fact that when the cells and ghosts are deformed little or not at all in the native state (that is, at slow flow) or when they

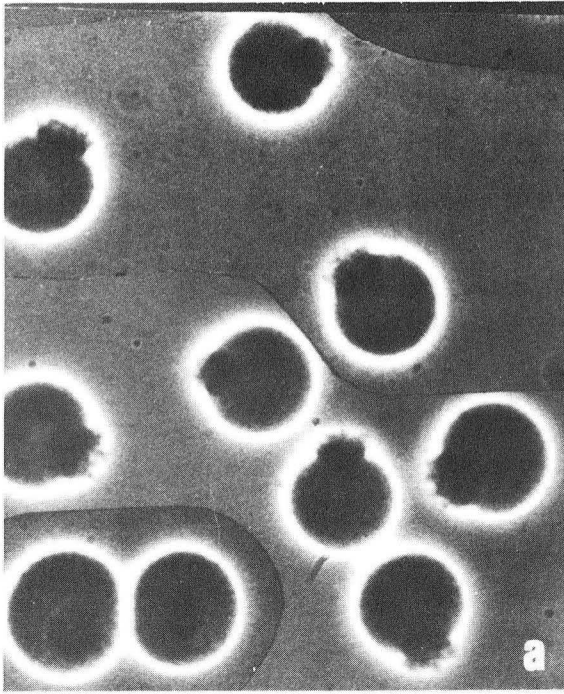


Figure 3. Views of normal red cells "exploding" during osmotic hemolysis.

are rigidified, the small "size" characteristic of the ghosts largely disappears.

How are such fundamental measures related to environmental or other agent effects and to other types of abnormal conditions? We have found, for example, that extremely small concentrations of contaminants such as mercury or lead alter the various RPS measures in a significant and complex way. That is, the rates of formation of ghosts, the rates of recovery of the membrane, and the ability of the cells to maintain their internal environment under normal conditions or when subjected to controlled stresses all show considerable alterations, which depend on the concentration and time of exposure to the contaminant. There is also evidence that different contaminants induce different patterns of alterations, depending on their modes of action at the cell membrane level. By studying and quantitating these effects, we hope to obtain a greatly improved knowledge of these actions, to evaluate means for counteracting adverse effects, and to develop convenient measures for detecting very low levels of noxious agents by their actions on living blood cells.

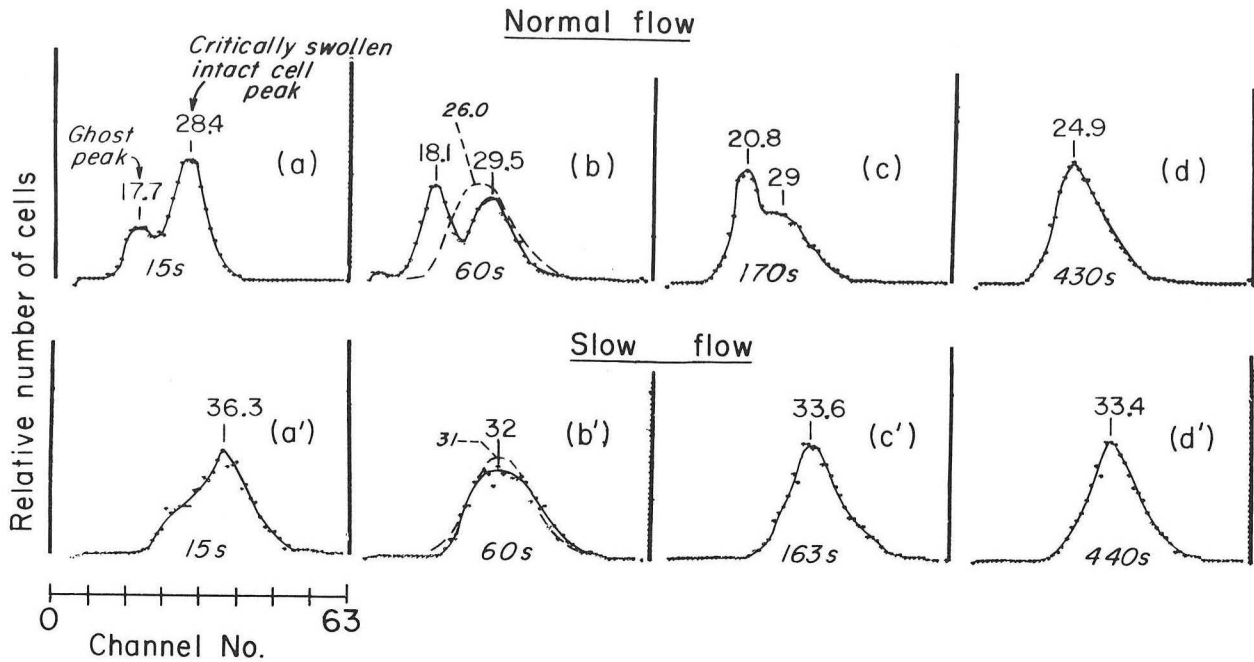


Figure 4. Dynamic osmotic hemolysis sequences of cells and ghosts.

In related studies we have also found that other less harmful (and even beneficial) agents affect some of the RPS measures in interesting ways, which lead to valuable insights on their actions on cells. Such agents include drugs (such as chlorpromazine, widely used as a tranquilizer and as a treatment for schizophrenia) and fats appearing in the blood stream from diet. In addition, cells from patients with anemias and other blood-related disorders also display interesting, and in some cases unique, patterns of RPS responses that may be useful in improving diagnosis of such conditions.

One other noteworthy result of recent work is the discovery, isolation, and characterization of a new type of red blood cell in one of the youngest forms, which is normally present in significant numbers only in the bone marrow where the blood cells are manufactured. Our work indicates that the property of cell

deformability (in this case “undeformability”) also plays a central role for this cell type in keeping it normally confined to its birthplace within the bone marrow. As it matures it apparently develops sufficient deformability to be able to squeeze out into the blood and embark upon its normal circulation. Under conditions of severe need (such as loss of blood) this “deformability control” appears to be bypassed, and some of these young red cells (called R-1 reticulocytes) are able to escape prematurely.

Present group members include Howard Mel, professor of biophysics; Jim Yee, Steve Akeson, Jon White, Tom Reed, Chris Cullander, Sarah Rabinovici, and Dr. Narla Mohnadas (collaborator from UCSF Medical School). Important assistance to the work has also been provided by Frank Upham’s electronic support group.

7. STRUCTURAL BIOPHYSICS

This group, led by Dr. Robert Glaeser, is composed of several subgroups that are carrying out a variety of studies involved with molecules, cell membranes, and intracellular contents, including the DNA-protein complexes within the cell nucleus. Special techniques have been devised to enable exploration of the finer structural details and to help understand the interactions taking place at the ultrastructural level.

Those working with high-resolution transmission electron microscopy have developed techniques eliminating two major problems, specimen hydration and radiation damage, and have carried out studies of macromolecular structure with a resolution of about 7Å. Scanning electron microscopy (SEM) has been used to measure the chemical elemental composition of individual fly-ash particles (an atmospheric pollutant associated with coal-burning power plants) at the site of the damaging action in cells and tissues. This single-particle single-cell analysis is important because damage to even a single cell is significant in assessing possible health effects of fly ash. Another interesting SEM study presents a membrane recycling hypothesis for gastric hydrochloride secretion by characterizing three stages of the ultrastructural changes following histamine administration.

Investigators in the lipoprotein group have used their microdensitometry computer system for quantitative lipoprotein microelectrophoresis to study serum lipid and lipoprotein distributions and how the subfractions of the different lipoprotein components differ or are changed under various conditions. Certain lipoproteins have been indicated as predisposing individuals to cardiovascular disorders,

and studies have been done with hypertensive individuals. An electron microscope study was done to investigate the nature of lipoproteins secreted by cultures of isolated hepatocytes from rat livers. This hepatocyte monolayer system is used for studying the synthesis of high-density lipoproteins (HDL) and may become a valuable tool for studying the effects of various agents on lipoprotein metabolism.

Genetic studies are being carried out by another group. The basic work in yeast genetics continues, using the yeast *Saccharomyces cerevisiae* to increase understanding of the eucaryotic cell cycle. Other investigators have used a newly developed synchrony system (which achieves excellent synchrony without the use of drugs) to examine the effects of various agents on synchronous cell populations. The DNA repair mechanism is being studied, and the investigator has developed a model for the role of gene product 32 (a DNA-unwinding protein) in DNA replication. Mutagenic, carcinogenic, and teratogenic effects of environmental pollutants and other agents have been studied by making quantitative observations on the growth of mammalian cells in culture. These studies identify those agents that pose a health hazard, determine the level of exposure at which the hazard is first detectable, and explore the mechanism by which cells are damaged.

Biophysical studies are being performed to examine experimentally the mechanisms of light excitation and energy transfer, photochemical energy transfer and storage, and subsequent electron-transfer and chemical-free energy production on both green-plant (chloroplast) and bacterial photosynthesis.

Microscopic Studies

BIOLOGICAL STRUCTURE ANALYSIS BY ELECTRON MICROSCOPY

R. M. Glaeser

The methods of molecular structure determination by high-resolution electron microscopy have been under development in this research group for several years. During this time we have developed methods to overcome the "specimen hydration" problem for unfixed, unstained specimens by the use of frozen thin specimens. We have also developed computer methods to superimpose and average the images of many unit cells in a crystalline object. This permits us to reduce the intensity of electron exposure given to the specimen to a "safe" level, from the point of view of electron-beam-induced radiation damage.

In the past year these developments have been applied to two problems of macromolecular structure. The first of these is the structure of bacteriorhodopsin, which is the photon-driven proton-pump of the "purple membrane" of *Halobacterium halobium* (Fig. 1). The

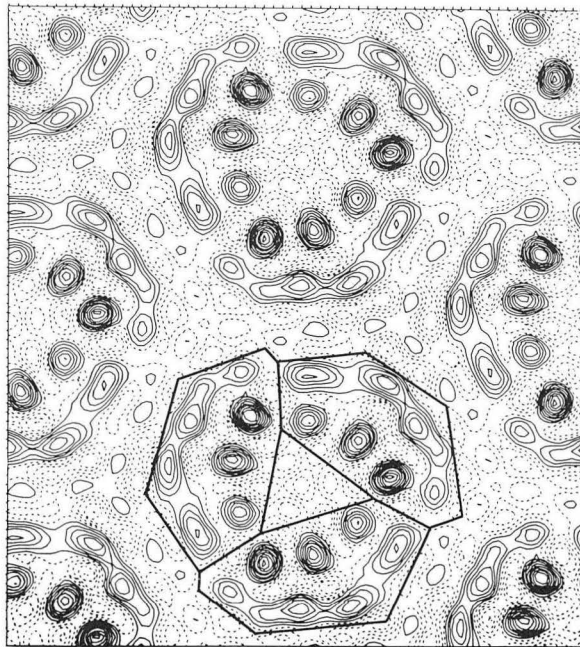


Figure 1. Projected structure of purple membrane at 7.1 Å resolution. Center-to-center spacing is ~ 62 Å. Three hypothetical monomers are delineated. This structure corresponds to the "right-handed" diffraction pattern.

second structural problem is that of a protein coded for by gene 32 of the T4 bacteriophage (Fig. 2). This is a DNA-binding protein that is known from genetic analysis to play a major role in DNA replication and in DNA repair.

While research applications on these and other biological problems are continuing, we are also moving ahead with improvements in instrumentation and in experimental technique. Thus, although the limitation on the resolution attained in our experiments is presently about 7 Å, we hope to reduce this to ~ 3.5 Å, at which time major instrumental advances will be required in order to achieve even higher resolution.

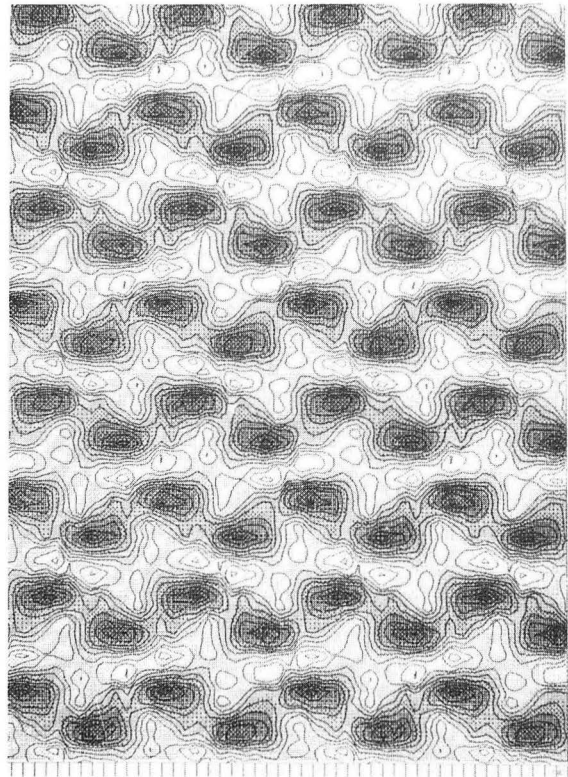


Figure 2. Projected potential map of gp32*1 (gene product-32) embedded in glucose-uranyl acetate, with partial data extending to 7.8 Å. This picture contains four repeats in each direction, and shows the pgg symmetry.

SCANNING ELECTRON MICROSCOPE STUDIES OF FLY ASH IN CELLS

T. L. Hayes and J. B. Pawley

Fly ash is a major atmospheric pollutant associated with coal burning power plants. Particles of fly ash interact with the lung at the cellular level (Fig. 1) and produce alterations in the morphology and function of individual cells. The response of a given cell such as a pulmonary macrophage depends, in part, on the burden of foreign chemical elements contained in the fly ash particles associated with that particular cell. It has been shown that the chemical composition of fly ash varies greatly from particle to particle. Individual cells, therefore, are exposed to a range of elements and concentrations depending on which set of particles they pick up (Fig. 2).

The chemistry of fly ash particles produced by coal-burning power plants has usually been characterized from data obtained from multiparticle bulk analyses. Although such averaged values are very useful in determining quantity and overall composition, the distribution of the chemical elements among individual fly ash particles is not revealed by these bulk analysis techniques; it can only be evaluated by the application of individual particle analysis methods. Scanning electron microscopy with x-ray elemental analysis can provide the required localization and particle identification for determining individual particle matrix chemistry (Fig. 3.). The results to date indicate substantial segregation of matrix elements among the particles (Fig. 4). This nonuniform distribution of matrix elements can alter the distribution of many of the trace elements found in fly ash, since it has been shown that sorptive behavior of the trace elements is associated with specific matrix composition of the particles. Trace element concentrations will be elevated in these particles above that estimated from multiparticle analysis. The existence of high-concentration particles plays a significant role in the biological effects of fly ash exposure. Single-cell exposure results

from interaction with only a few particles, and it would be greatly affected by the inhomogeneous distribution of the trace elements among individual particles. Some of the serious biological effects of fly ash (particularly the recently demonstrated mutagenic effect) may result from alterations in a single cell.

If we are to make an accurate correlation between the type and concentration of elemental exposure on the one hand and the cellular response on the other, it is helpful to apply scanning electron microscopic x-ray analysis. Such an analysis can provide data on individual cell exposure to foreign elements and can help us examine changes in cell morphology resulting from this exposure. By correlating light microscopic observations on the same cell prior to scanning electron microscope (SEM) analysis, certain cell functions not readily seen by SEM analysis alone (viability, phagocytic index) can also be determined on an individual cell basis. This is particularly important in cases where a single cell change can be amplified biologically, as in the recently demonstrated mutagenic effect of fly ash extracts.

The foreign chemical elements of fly ash are segregated and compartmentalized by the existence of the fly ash as heterogeneous individual particles. The biological response is also compartmentalized by the cellular nature of the biological system. It is not always possible to evaluate the exposure and response of biological systems on the basis of chemical bulk analysis of fly ash and biological response averaged over many cells. Single-cell exposure and response data are also needed. This project looks at the individual lung macrophage cell following exposure to fly ash and relates changes in its morphology and function to the specific chemistry of the particles found in that cell (Fig. 5).

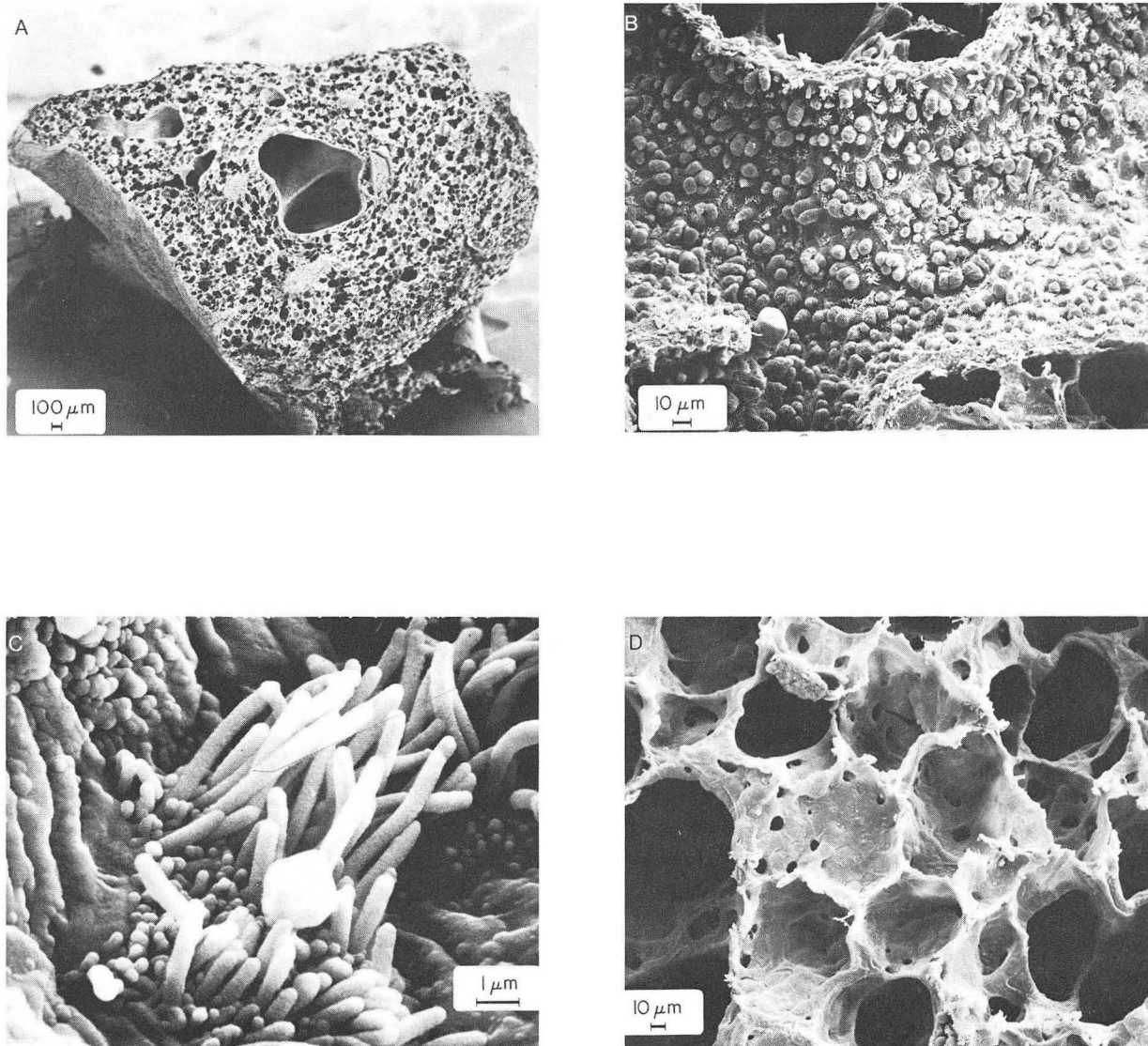


Figure 1. A, mouse lung showing several large airways and numerous small air sacs; B, airways in lung with tufted ciliated cells and mucous cells; C, cilia on cell lining an airway in the lung; D, air sacs (alveoli) with roaming, phagocytic pulmonary macrophage cells.

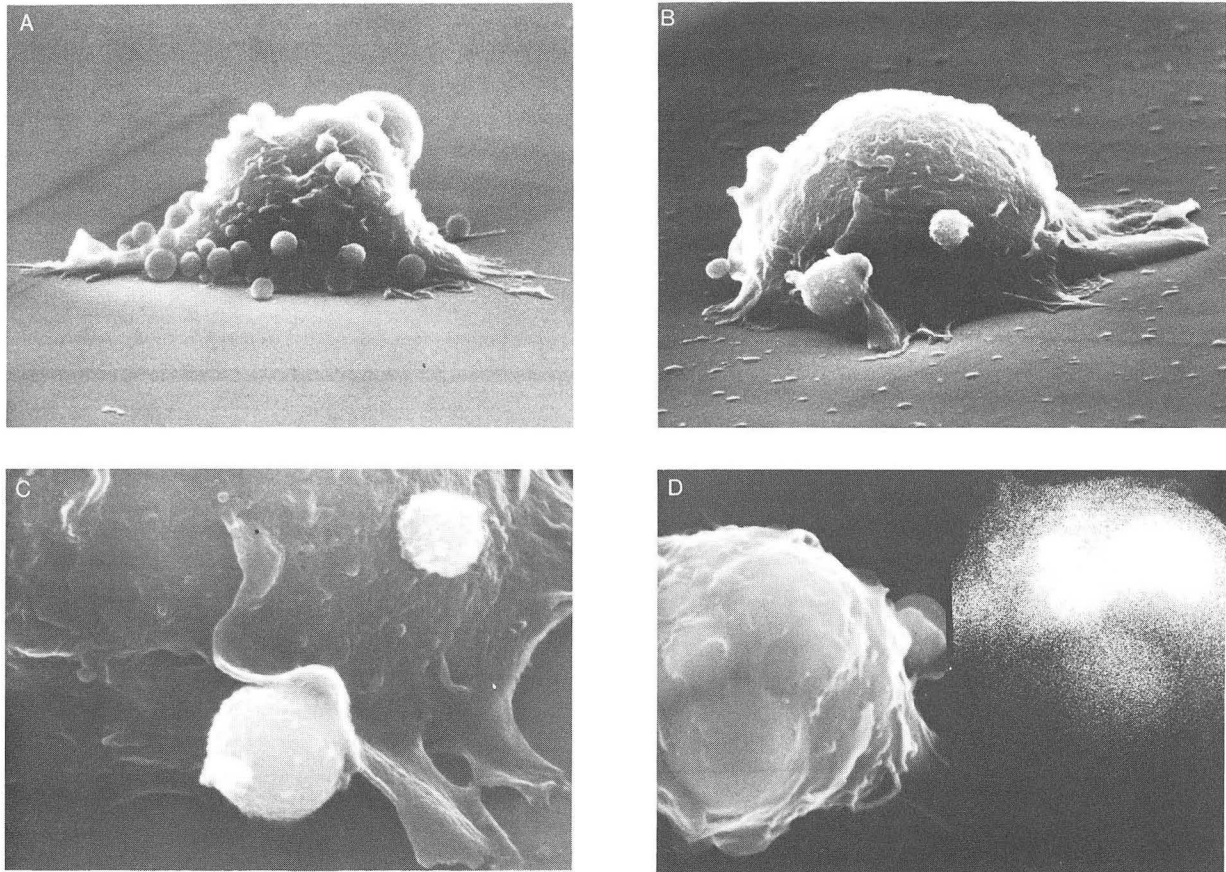


Figure 2. A, pulmonary macrophage with fly ash particles on surface and in interior (cell diameter equals about 10 microns); B, macrophage cell engulfs particle by throwing membrane over it (cell diameter is about 10 microns); C, higher magnification of phagocytic membrane over particle (large particle is about 2 microns); D, backscatter electron image can reveal particles deep within cell (cell diameter is about 10 microns).

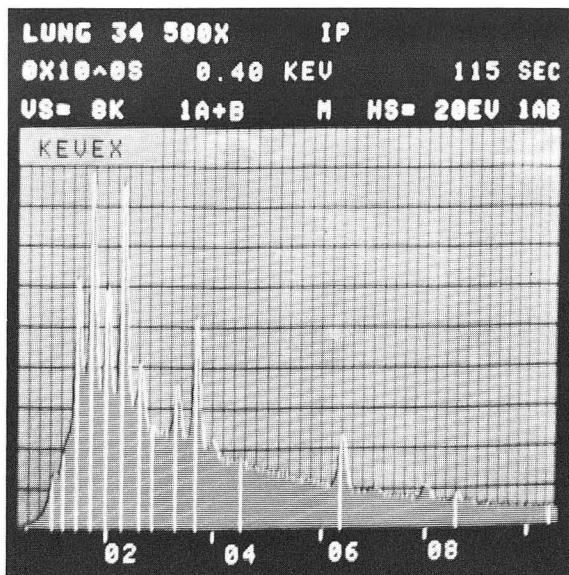


Figure 3. Spectra of complete chemical element composition can be obtained as well as three element maps.

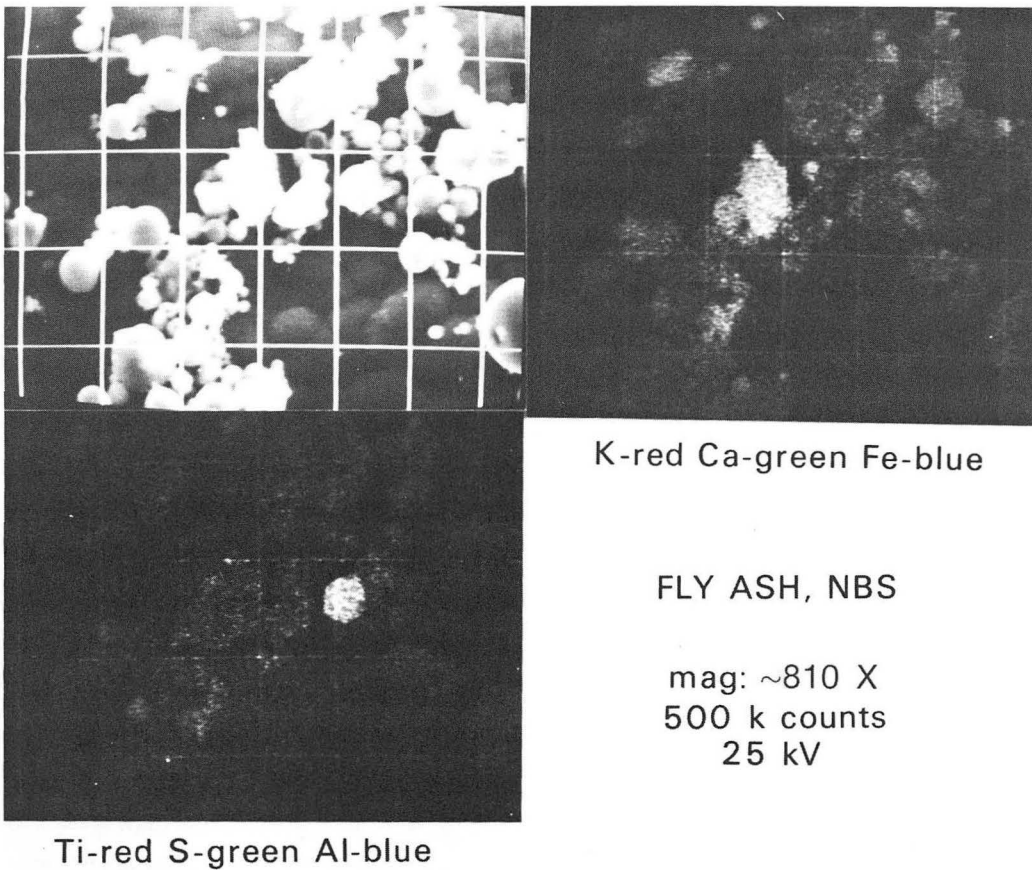
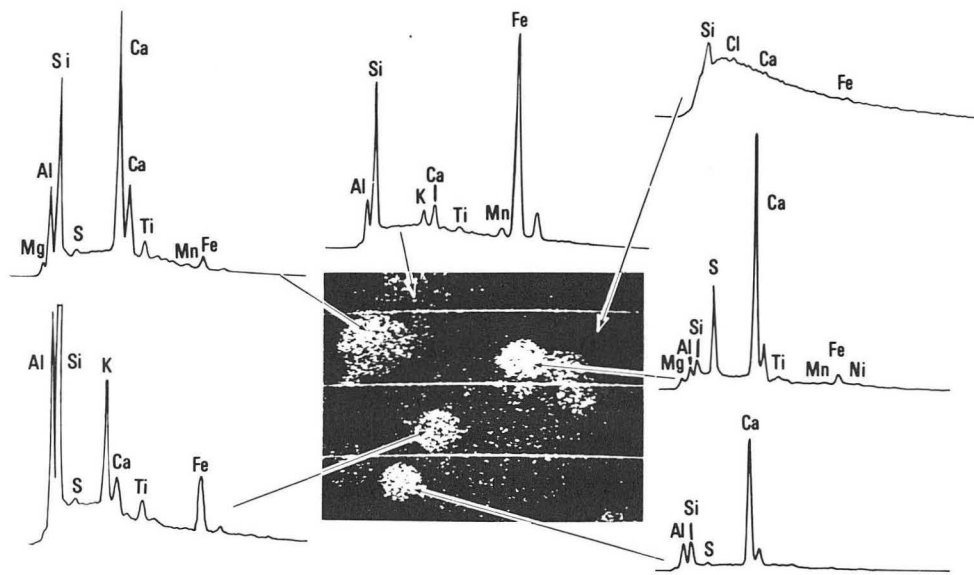


Figure 4. Top: heterogeneity among individual fly ash particles with respect to chemical composition. Bottom: field of approximately 100 fly ash particles showing nearly all of the titanium is contained in a single particle.

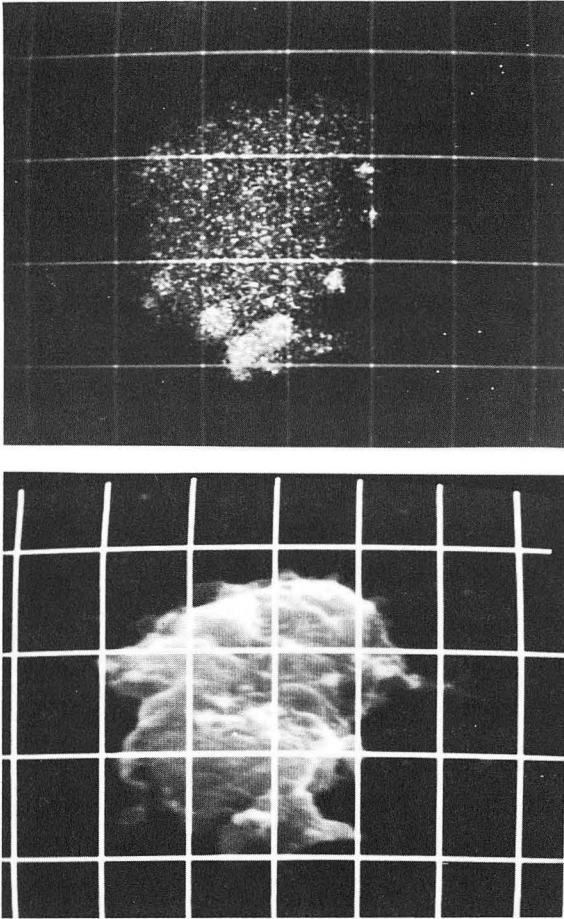


Figure 5. Top: particles mapped within the macrophage cell on the basis of elemental matrix composition (characteristic x-ray signal). Bottom: secondary electron image of surface of same cell.

MEMBRANE RECYCLING HYPOTHESIS FOR GASTRIC HCl SECRETION

T. M. Forte, T. E. Machen, and J. G. Forte

The nonsecreting gastric mucosal oxyntic (acid secreting) cell is characterized by short microvilli on its secretory surface and an abundant tubulovesicular (TV) membrane system within its cytoplasm (see Fig. 1). This latter membrane component is believed to play an important role in hydrochloric acid production by the stomach. We have analyzed time-dependent changes in oxyntic cell ultrastructure during active HCl secretion and recovery of cells after stimulus withdrawal. Paired halves of neonatal pig gastric mucosa were used as experimental tissue; one segment was used to monitor physiological activity and the other to study ultrastructural changes.

The stimulation phase, following administration of histamine, was divided into three

stages based on characteristic ultrastructural changes.

1. *Early stage.* At this time (approximately 3 minutes post histamine) there was no detectable H^+ secretion but a pronounced decrease in potential difference and resistance. Electron microscopy revealed small changes in proliferation of secretory surface. Microfilaments and microtubules appear to be involved in this early stage of membrane movement.
2. *Intermediate stage.* This occurs 5 to 20 minutes after histamine while H^+ secretion is increasing but has not plateaued. This stage is recognized by the fact that numerous tubulovesicles (TV) appear to be fusing with the secretory plasma

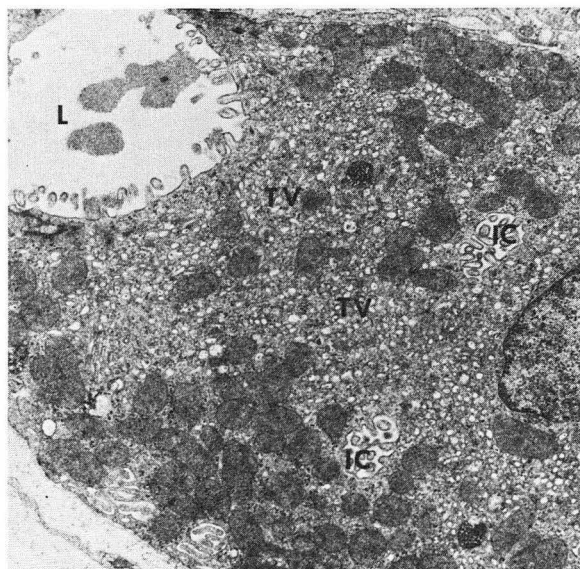


Figure 1. Electron micrograph of the apical portion of a nonsecreting oxyntic cell. Short microvilli project into gland lumen (L) and intracellular canaliculi (IC). Numerous smooth membrane profiles or tubulovesicles (TV) fill the cytoplasm.

membrane and that surface extensions are numerous and long (see Fig. 2).

3. *Late stage.* This is associated with maximal H^+ secretion. The cytoplasm is almost devoid of TV while microvilli remain elongated with many of the microfilaments aggregated in the core of the microvillus structure (see Fig. 3).

Recovery of oxyntic cells after removal of histamine can best be described in two phases.

1. *Early recovery.* This takes place 5-20 minutes after histamine removal and is accompanied by condensation of surface extensions, occlusion of canalicular space and appearance of pentalaminar membrane structures. The pentalaminar membranes have a thickness of 240 Å (single membrane 119 Å) and appear to represent closely apposed secretory membranes which have been internalized (see Fig. 4). During early stages of recovery the microfilaments within surface extensions are disoriented, which may be a factor in membrane condensation.
2. *Late recovery.* At this stage (30 minutes or more) most oxyntic cells have an overall "resting" morphology. TV are again

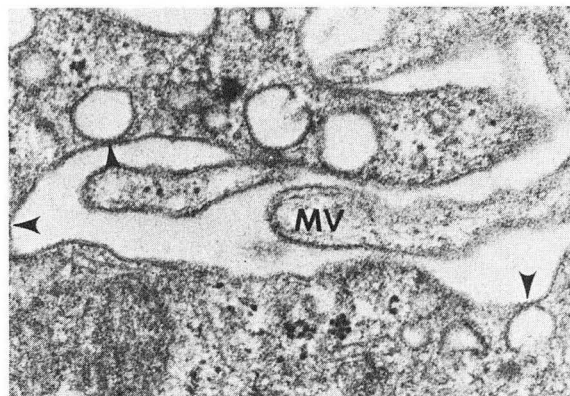


Figure 2. Electron micrograph of the secretory surface of an HCl -secreting oxyntic cell. Microvilli (MV) are long and slender and numerous profiles of tubulovesicles (arrows) lie adjacent to or fused with the plasma membrane. Fusion of the tubulovesicles with the surface greatly increases the surface area of the secreting cells.

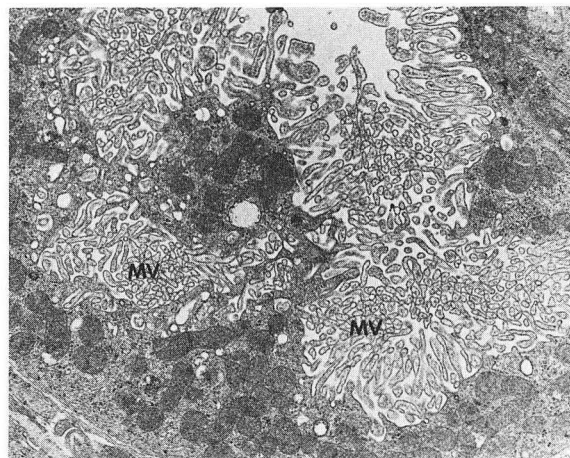


Figure 3. Electron micrograph of a portion of a maximally secreting oxyntic cell. The cytoplasm of the cell is almost devoid of tubulovesicles while the secretory surface is replete with numerous, long, slender microvilli (MV).

apparent within the cytoplasm and microvilli are short with normal microfilaments. Some pentalaminar structures still persist as well. Studies also revealed that oxyntic cells in the recovery stage can be restimulated with histamine. In this case, reformed TV contribute to the surface membrane but pentalaminar

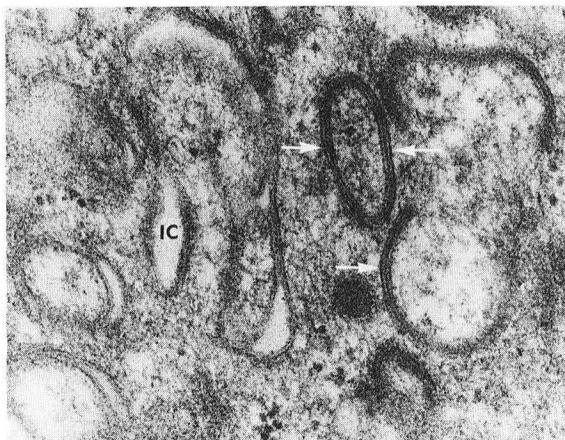


Figure 4. High-magnification micrograph of an oxyntic cell seven minutes after the removal of histamine and cessation of HCl secretion. The canalicular lumen (IC) is occluded by collapsed microvilli. Excess surface membrane appears to be internalized into the cell in the form of closely apposed membrane surfaces, which form pentalaminar profiles (arrows).

membrane structures were never seen to fuse with the plasma membrane.

Maximally stimulated (histamine) tissue can be inhibited with SCN^- . Within 20 minutes, tissue treated with SCN^- had baseline secretion; however, inhibited cells were morphologically similar to maximally secreting cells—that is, TV were depleted and microvilli were long and elaborate.

Morphological events suggest that during stimulation intracellular TV migrate to the secretory surface and fuse. This step may be controlled by microtubules and microfilaments. Membrane fusion is followed by formation of long microvilli. During stimulus withdrawal secretory membranes are returned to cells as endocytosed pentalaminar structures. These latter structures appear to be recycled within the cell to produce tubulovesicles.

Lipoprotein Studies

LIPROPROTEIN METHODOLOGY AND BIOMEDICAL APPLICATIONS INCLUDING EVALUATIONS OF POLLUTANT DAMAGE

F. T. Lindgren and R. M. Krauss

The full automation of a stand-alone micro-densitometry computer system for quantitative lipoprotein microelectrophoresis has now been achieved, and is being used in several research programs at Donner Laboratory. This method, developed by F. T. Lindgren and his colleagues, can perform lipoprotein analyses in a fraction of the time previously required. This is accomplished by using microelectrophoresis to separate each lipoprotein component in a serum sample, and then determining the concentrations of the lipoproteins with a scanning densitometer, which produces a graph that can be analyzed in a computer. All calculations and comparisons with normal lipoprotein distributions are done in seconds. A trained technician can perform 300 analyses per week with this computerized system.

Blood fats, or lipids, are combined with proteins to form molecules referred to as

lipoproteins. When enough of these molecules bind together and attach themselves along artery walls, the results are often fatal. With the new lipoprotein analysis we can determine an individual's lipoprotein pattern and detect abnormalities by comparing it with a set of "normal reference values" derived from a population of healthy subjects. Thus, lipoprotein disorders can be detected and many can be treated medically. Certain lipoproteins predispose individuals to cardiovascular disorders, while some lipoproteins in the presence of other biochemical factors seem to have a "preventative" effect. Our research program attempts, in part, to obtain further knowledge of the nature and control of cardiovascular disease. We are interested in what contributes to the biochemical structure (apoproteins, for example) of the nonatherogenic high-density lipoprotein class (HDL) as a function of con-

centrations and characteristics of the two atherogenic low-density classes—very low-density lipoproteins (VLDL) and low-density lipoproteins (LDL). We study in detail the composition and structure of subfractions of HDL as a function of VLDL and HDL levels.

In collaboration with Drs. Goldring and Burton of Washington University School of Medicine in St. Louis, a preliminary study has been carried out with 99 adolescent subjects divided into hypertensive and normotensive groups. Preliminary findings confirm higher levels of HDL in normal females compared with males. Furthermore, in white male hypertensive subjects the level of LDL was elevated, whereas in white female hypertensive subjects the VLDL was elevated and the HDL depressed. In contrast, no significant differences were observed in the corresponding black groups. This study is continuing, and with sufficient numbers we will verify and extend our preliminary findings.

We are helping to evaluate pollutant damage by using this facility for quantitative serum lipoprotein analysis in individual mice and rats exposed to ozone. In order to achieve accurate microanalysis of cholesterol and triglyceride, we are now standardizing our Gilford 3500 enzymatic autoanalyzer with the Center for Disease Control (CDC). In addition, evaluation by ultracentrifugal techniques reveals that exposure of rats to ozone (1 ppm for 24 hr) and NO_2 (20 ppm for 24 hr) increases plasma levels of HDL of high flotation rates. The absolute and relative content of the arginine-rich apoprotein is of interest because it is a major structural component of apparently atherogenic lipoproteins in hypercholesterolemic animals and humans. Decreased food intake of oxidant-exposed animals contributed to the observed apoprotein and lipoprotein changes but maximal effects were observed with the combination of ozone plus fasting.

In collaboration with Dr. Nichols *three* HDL subfractions (HDL_{2a} , HDL_{2b} , and HDL_3) in a normal population have been studied and significant interrelationships found within LDL subfractions of S_f 0-12. Appropriately, a density gradient ultracentrifugal method for fractionation of S_f 0-12 into at least six subfractions has been developed. Detailed physical chemical studies are beginning in collaboration with Drs. Forte and Nichols. Subfractions from both normals and various hyperlipoproteinemias will be studied.

In collaboration with Dr. Peter Wood of Stanford University, we have demonstrated a significant and specific elevation of HDL_{2a} and HDL_{2b} in runners as compared with sedentary subjects. Similar lipoprotein elevations were observed in comparing normal females with males, suggesting that the anti-atherogenic portion of the HDL spectrum may be HDL_{2a} and HDL_{2b} . Furthermore, the significant elevation of HDL_3 in women using oral contraceptives suggests that this HDL class is not anti-atherogenic.

Figure 1 shows lipoprotein Schlieren-difference plots. For each S_f° interval, the difference between the curves of two groups is plotted and the resulting "difference-plot" provides information concerning the differences in lipoprotein patterns between the two groups being compared. This difference-plot can also be compared with those from other groups to look for similarities of lipoprotein-pattern differences. The shaded areas below the baseline represent increased lipoprotein concentration in runners (a,b) or in men (c,d); the open areas above the baseline represent reduced lipoprotein concentration in the same groups. Note that there are three components in all curves, and that the "difference-plots" in all four groups are similar for LDL and HDL.

Other collaborative studies have demonstrated that both LDL and particularly HDL are significantly depressed in cystic fibrosis (CF) patients, but not in the parent carriers. We plan to continue and extend this study with full pattern recognition type of analysis of the serum proteins to potentially identify CF carriers.

Improvements in Schlieren analysis are planned using an x-y sonic digitizer. Evaluation with a loan instrument is underway. Also, ultracentrifugal techniques have been shared by training of scientists from the Minneapolis and Leningrad Lipid Research Clinics. Similarly, our computerized electrophoresis methodology has been shared with the Cleveland Clinic. Additional protein and apoprotein studies using polyacrylamide gel electrophoresis and SDs slab gel electrophoresis for protein characterization and quantification are planned. All these methodology improvements will need a flexible and portable data gathering instrument. The more complicated programs will be run on a larger instrument requiring an appropriate magnetic tape system for our PDP8e computer system.

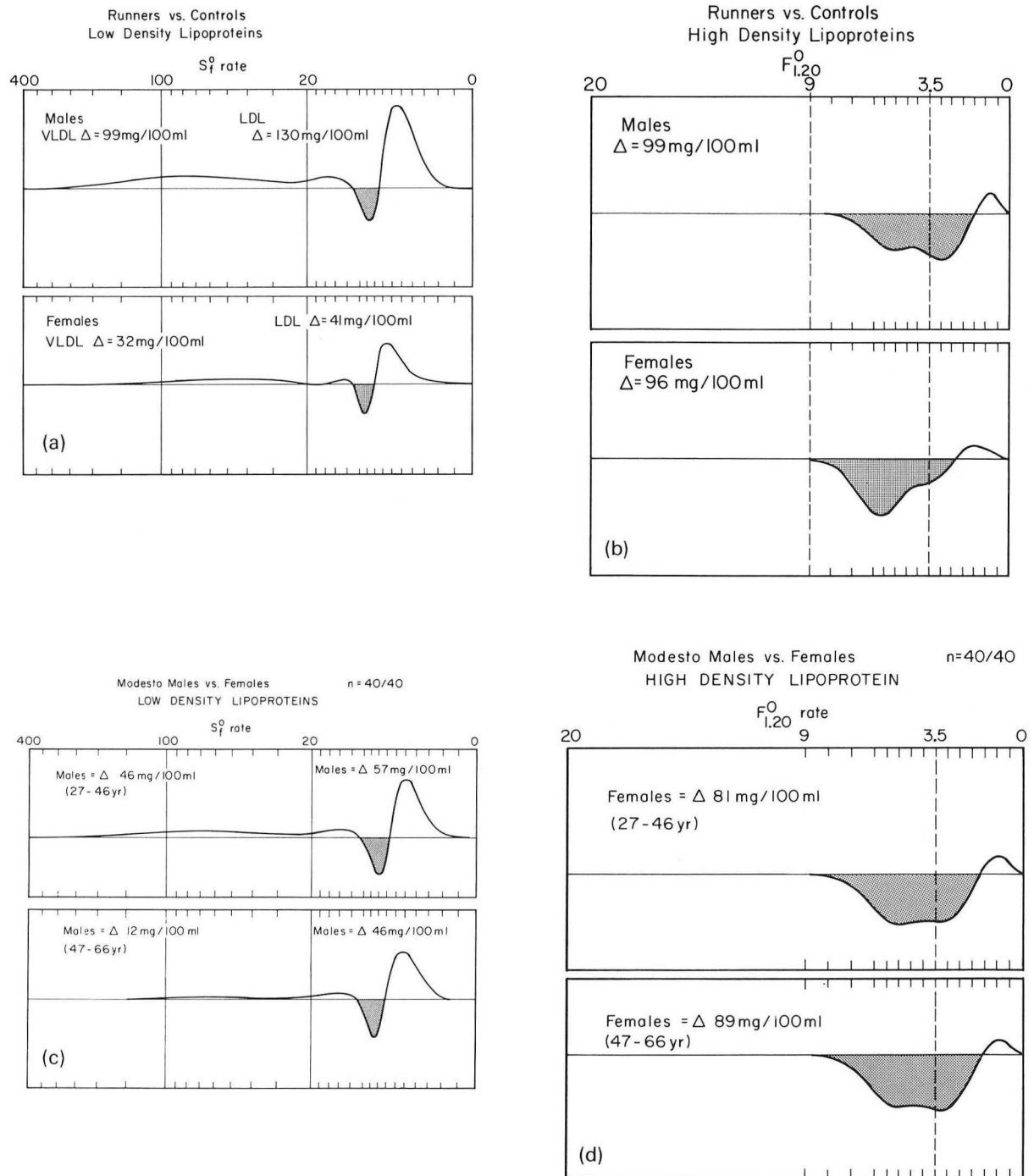


Figure 1. Low-density-lipoprotein (LDL) and high-density lipoprotein (HDL) difference-plots for four groups: (a) LDL difference plots of runners versus sedentary control subjects in men (7 runners and 15 controls) and premenopausal women (6 runners and 12 controls); (b) HDL difference-plots of same groups as in (a); (c) LDL difference-plots of normal males versus normal females in a younger group (ages 27-46) and an older group (ages 47-66) [$n = 40/40$]; (d) HDL difference-plots of same groups as in (c).

SERUM HIGH-DENSITY LIPOPROTEINS IN HEALTH AND DISEASE

A. V. Nichols

Epidemiologic studies on human populations have demonstrated an inverse statistical relationship between the incidence of coronary heart disease and serum concentrations of the total high-density lipoproteins (HDL). HDL consist of a distribution of particles of considerable diversity both in composition and size. On the average, females exhibit significantly higher serum concentrations of HDL than males, particularly of the larger type of HDL species. Because females encounter a considerably lower risk of coronary heart disease than males, it is possible that only certain subspecies within the HDL distribution may serve as indicators of decreased disease risk.

During 1977, we identified three major components within the HDL distribution by equilibrium density gradient ultracentrifuga-

tion. Subsequently, serum levels of these three components were determined in 160 normal subjects by analytic ultracentrifugation and computer analysis. Our results indicate that the major differences in serum total HDL levels observed among normal subjects, both males and females, arise predominantly from differences in levels of only two of the three major HDL components. This would suggest that the reported inverse relationship between serum HDL levels and the risk of a coronary heart disease is a function primarily of the serum levels of the two HDL components, which we have designated HDL_{2a} and HDL_{2b}. Based on this information, we are investigating the structural properties of these compounds in order to understand, on a molecular basis, their statistical associations with the risk of disease.

LIPOPROTEIN SYNTHESIS BY RAT HEPATOCYTE MONOLAYER CULTURES

T. M. Forte, J. B. Quint, and R. W. Nordhausen

The liver plays an important role in the synthesis and catabolism of plasma lipoproteins. Lipids transported by lipoproteins are essential as energy sources for cells and also for the production of vitamins and hormones. In some circumstances, elevation of certain blood lipids have been associated with increased risk to atherosclerosis.

In the past year we have been studying the nature of lipoproteins secreted by primary hepatocyte cultures and some of the parameters controlling synthesis of lipoproteins. In these studies we have isolated hepatocytes from rat livers by perfusion with the enzyme collagenase. The freshly isolated hepatocytes are spherical cells covered with numerous short surface microvilli (see Fig. 1). Dissociated cells are subsequently grown in monolayer culture for periods of up to five

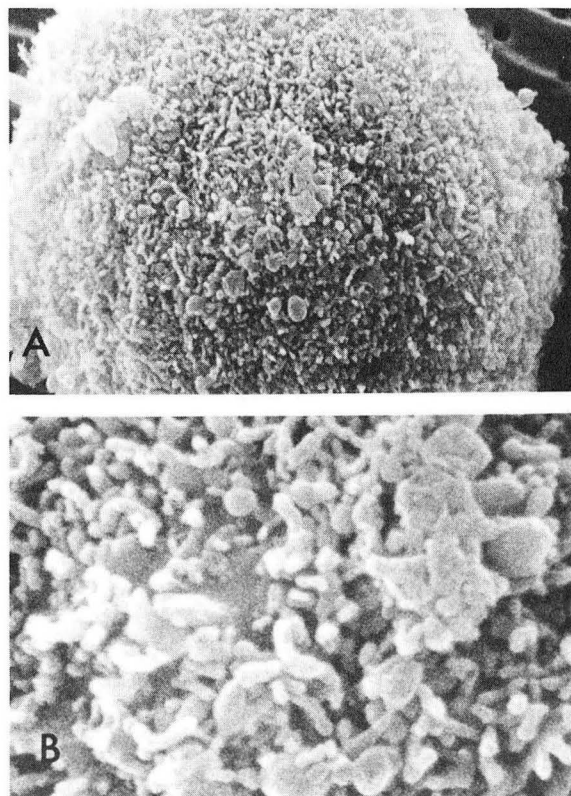


Figure 1. Scanning electron micrographs of dissociated hepatocytes prior to culturing. A, low magnification micrograph reveals that the isolated cells are spherical and covered with short microvilli. B, surface detail seen at higher magnification.

days. We have found that good monolayer formation depends on at least two factors: coating of the culture plates with collagen, and the presence of 10 to 20% fetal calf serum in the medium during the first 24 hours of culture.

Electron microscopy reveals that on the second day in culture, the rat hepatocytes form highly organized structures. The cells appear to become polarized and form regions similar to bile canaliculi in the intact liver (Fig. 2). Electron dense lipoprotein particles similar in size to plasma very low density lipoproteins (VLDL) are found in the intercellular spaces and can be isolated from the medium by ultracentrifugal techniques. The VLDL can be visualized within the Golgi complex of the hepatocytes (Fig. 3); from the Golgi the VLDL are transported within vesicles to the cell surface where they are released.

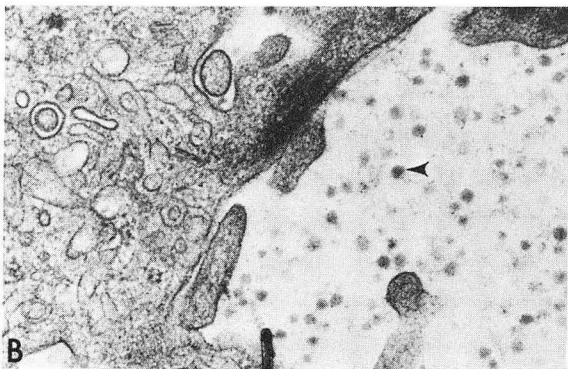
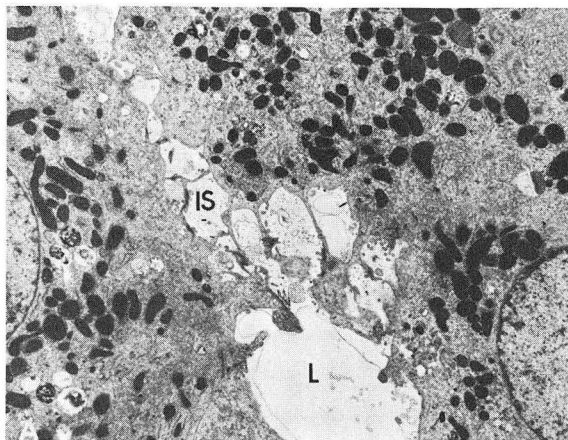


Figure 2. Transmission electron micrograph of hepatocytes after two days in culture. Top: several cells surround a lumen (L), which is similar to a bile canaliculus in morphology. Numerous very low density lipoproteins are present in the intercellular space (IS). Bottom: high magnification view of the intercellular space and its included very low density lipoproteins (arrows).

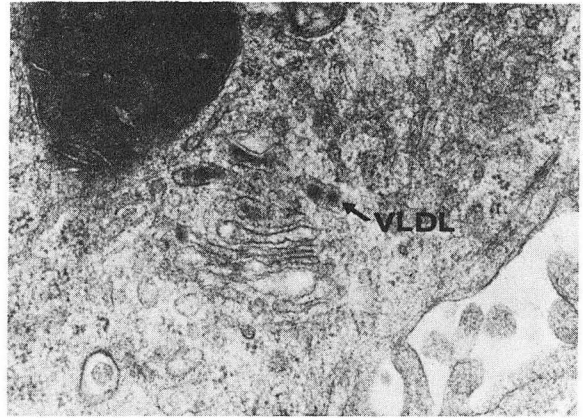


Figure 3. Part of a hepatocyte showing very low density lipoproteins (VLDL) within the cisternae of the Golgi complex.

VLDL newly synthesized by the hepatocytes are similar in composition to plasma VLDL. These particles contain approximately 10% protein and 90% lipid. The major lipid is triglyceride (75%), while phospholipid and cholesterol constitute 15% and 10% respectively of the lipid mass. The structure of the isolated VLDL can be seen in Figure 4; the particles are spherical and range from 300 to 900 Å in diameter.

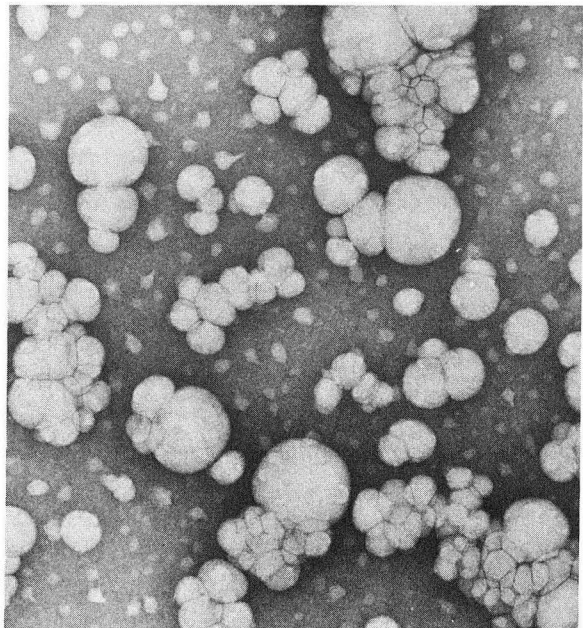


Figure 4. Negatively stained VLDL isolated from hepatocyte cultures after two days in culture. The majority of particles are between 450 and 750 Å diameter (range 300-900 Å).

The rat hepatocyte culture proved to be a very valuable tool for studying synthesis of high density lipoproteins (HDL). We have been able to demonstrate that HDL are the other major lipoproteins secreted by the cultured hepatocytes. The secreted HDL contain 50% protein and 50% lipid, with phospholipid accounting for 63% of the lipid; cholesterol, 32% of the lipid; and triglyceride, 5% of the lipid. The HDL are spherical, 100-Å-diameter particles (Fig. 5) and are thus not seen in thin sections of cells. Factors controlling the synthesis of HDL are indeed important to know, since it is now commonly believed that plasma HDL play an anti-atherogenic role. Future studies will be directed toward understanding the mechanism of HDL secretion by hepatocytes.

The hepatocyte monolayer system may become a useful research tool for studying the effects of various agents, including hormones, carcinogens, and environmental pollutants on lipoprotein metabolism.

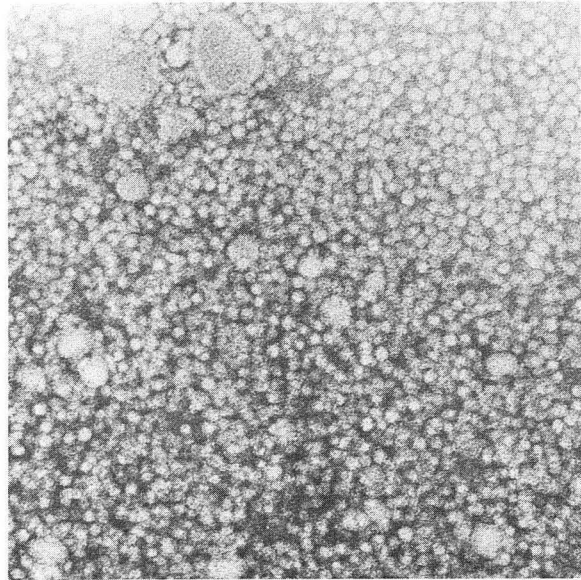


Figure 5. High-density lipoproteins isolated from hepatocyte cultures and visualized by negative staining. The particles are small spheres approximately 100 Å diameter.

Genetic Studies

MAMMALIAN CELL MUTAGENESIS

H. J. Burki

SYNCHRONOUS CELL STUDIES

We have been able to show that the induction of mutations by incorporation of bromodeoxyuridine (BUdR) into synchronous cells is a function of the time of incorporation during the DNA replication period. These data were very similar to previous data obtained with drug-induced synchrony. The results are important because they suggest that specific genes, associated with drug resistance in mammalian cells, can be located and damaged with agents that may be incorporated into DNA.¹ The experiments above are done in the dark. If the cells are exposed to fluorescent light during growth or synchronization, mutations can be induced throughout the DNA synthesis period and the G₁- and G₂-M periods. Fluorescent light alone will induce mutations. This was quite unexpected, and forces us to

reevaluate all old experiments that might have received some exposure to room fluorescent light.²

The simplest interpretation of our data with BUdR is that we are damaging specific DNA regions associated with drug resistance in the early replicating euchromatic DNA. This "hot position" hypothesis is challenged by some data of others, suggesting that there may be a "hot time" for mutagenesis during the first half of the DNA synthesis period. Data of others show a large increase in mutations throughout the cycle with a small peak of additional mutagenesis during early DNA synthesis. We have repeated synchronous mutagenesis experiments with moderate doses of uv (16 J/m² and alkylating agents such as ethyl nitrosourea (ENU) and so far have not seen marked time dependent response for mutagenesis.

FLUORESCENT LIGHT STUDIES

We have completed a number of experiments to determine the effects of white fluorescent light on induced reproductive death and mutagenesis in our cell system. We have verified that cool white fluorescent light is both toxic and mutagenic in asynchronous cells, both in optimum culture conditions and in balanced salt solution at ice temperatures. However, the most important part of this work was to show that gold fluorescent lights do *not* induce the effect. This suggests that laboratories engaged in mutagenesis work convert to gold fluorescent light.² In that paper (Ref. 2) we point out that the health hazard from fluorescent light is quite small compared with the normal exposure to sunlight received almost every day.

Of course, the effects of fluorescent lights are also seen in synchronous cells where the background is raised throughout the cell cycle, and new mutagenic peaks are seen in the DNA synthesis period when the cells are labeled with BUdR. We are doing active research in this area to determine the effects of fluorescent light exposure of the standard BUdR plus visible light procedures. It appears that using fluorescent light (a general mutagen) in combination with pulses of BUdR (a non-random mutagen) leads to additional mutagenic peaks in the DNA synthesis period which are not seen in the dark. This latter result may

DNA REPAIR MECHANISM

J. Hosoda

It has been established that DNA is replicated by means of a multi-enzyme complex, sometimes called the "replication apparatus" in which components are held together by relatively weak protein-protein interactions. The activity of each component within the complex must be regulated by its relative position or interactions with other components. (Some components have no measurable activity outside the apparatus.) The target of our research in the past few years has been to obtain some insight into the control mechanisms operating within the replication apparatus. Our attention has been focused on bacteriophage T4 gene 32 product (gp32).

Gp32 activity is known to be essential for

suggest that inducible repair processes are present.

We have begun to expose cells to sunlight, and have found that the sun is a potent mutagenic source.

CHROMOSOME STUDIES

We have done experiments to determine the "G"-band karyotype of the Chinese hamster ovary (CHO) cells used for our studies, and find that it is different from the normal Chinese hamster "G"-banded karyotype. There appears to be one normal banded chromosome of each type, and several abnormal banded chromosomes. There appears to be only one normal x chromosome. This suggests to us that we attempt to develop or use diploid material in the future for synchrony studies to insure that our results apply to cells with "normal" chromosomes.

REFERENCES

1. Burki, H. J. and Aebersold, P. V. BUdR induced mutagenesis in synchronous Chinese hamster cells: temporal induction of 6TG and OUA resistance during DNA replication. *Genetics* (in press).
2. Burki, H. J. and Lam, C. K. Comparison of the lethal and mutagenic effects of gold and white fluorescent lights on cultured mammalian cells. Submitted to *Mutation Research*.

a multitude of important cellular processes such as DNA replication, recombination, repair of uv or chemically damaged DNA, and protection of the chromosome from nucleases. There are indications that gp32 also controls other enzymes related to DNA replication and repair such as DNA-polymerase, DNA-ligase, and exonucleases, through direct protein-protein interactions.

Within the replication apparatus, the primary role of gp32 seems to be unwinding of the double-stranded (ds) DNA template ahead of the replication fork. This protein and its analogues are generally grouped as helix-destabilizing or DNA-unwinding proteins (HDP or UP). They greatly reduce the thermodynamic

cost of DNA helix melting within the cell by binding tightly, cooperatively and specifically, to single-stranded (ss) DNA. By itself, gp32 cannot melt (T4) dsDNA under experimental conditions similar to those within the cell. Instead, it facilitates renaturation of denatured DNA by melting the intrastrand helix, which prevents complementary pairing. This inability to melt the dsDNA may be vital in the prevention of uncontrolled melting of the T4 chromosome by gp32.

We have found that two regions (A and B) of gp32 protrude from the intact molecule making them easily removable by proteolysis. We named the proteolysis products gp32*I = gp32 - A, gp32*II = gp32 - B, and gp32*III = gp32 - (A + B). Our research efforts in 1977 were aimed at establishing relationships between structure and functions of gp32 through the comparative studies of its limited proteolysis products.

Highlighting the year was the crystallization of gp32*I, which is now being analyzed electronmicroscopically by W. Chiu. We have also established the following. (1) The A-region is highly acidic, approximately 70 amino acids long, and is located at the carboxy-terminal. (2) The B-region is basic, 13-16 amino acids long, and is located at the amino-terminal. (3) The amino acid sequence of the B-region is: Met-Phe-Lys-Arg-Lys-Ser-Thr-Ala-Glu-Leu-Ala-Ala-Gln-Met-Ala-Lys. (4) B is related to the tight binding to ss-DNA because those products which have lost B (gp32*II and gp32*III) do not bind as tightly as those which have B (gp32 and gp32*I). (5) The A-region is related to the regulatory function, which keeps gp32 as a renaturation protein outside the replication apparatus. Gp32*I (without A) becomes a far stronger DNA-unwinding protein and melts T4

DNA under conditions similar to those within the cell. (6) Circular dichroism studies with Dr. M. Maestre, showed that in both gp32 and gp32*I complexes, DNA-bases are held in a stacked position. The conformation of gp32 and gp32*I complexes are different from each other.

Based upon the above, we present a model in which DNA-melting activity of gp32 is confined to a certain position at the replication fork. When gp32 is placed at this position, interaction by other proteins in the complex changes the conformation of A-region so that gp32 becomes as active as gp32*I and melts the helix ahead of the replication fork. This model is presented in Figure 1.

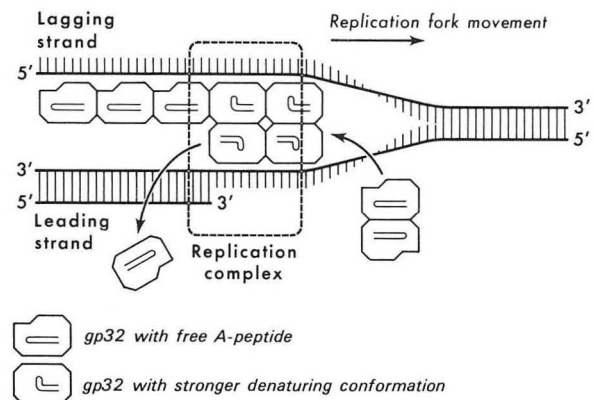


Figure 1. Model for role of gp32 in DNA replication. DNA-melting activity of gp32 is confined to a certain position at the replication fork. When gp32 is placed at this position, interaction by other proteins in the complex change the conformation of A-region so that gp32 becomes as active as gp32*I and melts the helix ahead of the replication fork.

GENETIC STUDY OF YEAST

R. K. Mortimer

INTRODUCTION

All our research falls under the general title of "genetics of yeast." The yeast *Saccharomyces cerevisiae* has replaced *Escherichia coli* as the microorganism of choice. Advanced yeast genetics and molecular biology studies are being carried out in more than 100 laboratories around the world (including five at Berkeley). This yeast is a eucaryote with a highly developed genetics and biochemistry which undoubtedly is the reason for the current popularity of yeast. Our basic understanding of cell division, meiosis, gene regulation, genetic recombination, mutagenesis, mitochondrial biogenesis, and cell ultrastructure in eucaryotes is being advanced to a great extent by studies on this organism. For example, more than 30 genes that control various steps of the yeast cell cycle have been identified and another set of mutants have been used to dissect the meiotic cycle. A group at Rochester has contributed to our basic understanding of mutagenesis, while the work of Fogel (U.C. Berkeley) and the author has provided one of the best sets of data with which to assess various recombination models. More than five yeast genes have been cloned in bacteria. Recently, several groups have effected transformation of yeast using cloned genes. Exciting developments in many other areas are being reported with increasing frequency.

Our research studies are divided into different areas, and a summary of our results in each of these follows.

GENETIC MAPPING

Using a variation of our previously described aneuploid mapping technique, we were able to locate four arginine structural and regulatory genes as well as three conditional lethals associated with RNA metabolism. Strains carrying up to five extra chromosomes ($n+5$) were found to be quite stable and were used in this analysis.

GENETIC RECOMBINATION

In collaboration with S. Fogel we completed the analysis of over 20,000 unselected meiotic tetrads. Over 200,000 segregations were scored

in this study. The main conclusions from our analysis of the data are:

1. The model proposed by Meselson and Radding is best able to account for all our results. The recombination event must involve formation of asymmetrical hybrid DNA more than 95% of the time.
2. The corrected frequency of outside marker exchange associated with conversion varies from 20% to greater than 50% depending on the site analyzed.
3. Polarity cannot be explained by assuming that all events at a locus start at a fixed point and proceed various distances into the gene. The associated exchanges, which should be on the opposite side of the site relative to the starting point, were found to be about equally divided between the proximal and distal intervals.
4. Gene conversion occurs at a frequency sufficient to explain all recombination. That is, gene conversion is a signal of the basic recombination event.

MUTAGENESIS

Progress on this project has been slower than anticipated. Part of this delay was due to the time needed to set up a safe chamber for working with mutagens and carcinogens. The reversion and recombination systems detailed in our earlier reports have been tested and found to be satisfactory for testing a variety of chemical mutagens. A diploid strain has been developed which should make it possible to select nondisjunctional events ($2n \rightarrow 2n-1$). This strain is now being checked to determine what percent of the selected events are due to nondisjunction.

X-RAY SENSITIVE MUTANTS

A new set of x-ray sensitive mutants was isolated. Of these mutants, 26 were found to complement all known x-ray sensitive mutants. Preliminary tests within this set of mutants shows little allelism. This suggests that these new mutants represent a number of new genes. Genetic analysis of these mutants is now in progress.

EFFECTS OF POLLUTANTS ON SOMATIC MAMMALIAN CELLS

D. A. Glaser

INTRODUCTION

The overall goal of this project is to detect and measure mutagenic, carcinogenic, and teratogenic effects of environmental pollutants and other agents by making quantitative observations on the growth of mammalian cells in culture. Automated techniques for carrying out large-scale experiments in cell biology developed in this laboratory are being used to make quantitative measurements of growth rate and morphology on each of 100,000 colonies of mammalian cells per experiment. The extensive instrumentation and computer facilities necessary for this work comprise our NIH-funded National Research Resource: "Facility for Automated Experiments in Cell Biology." Collaborations with a number of other laboratories engaged in studying the same biological problems allows correlation of our observations with those made using more conventional methodologies, as well as ensuring that our facilities are used for the widest range of work for which they are useful.

INSTRUMENTATION DEVELOPMENT

Environmental control for the clean room housing the Cyclops apparatus has been completed. This computer-controlled system regulates the temperature to within 0.1°C, and the humidity to within 2%. Since our incubators open directly into the clean room, this allows complete control of the environment of the cells throughout an experiment (Fig. 1).

A "cell sorter," modified to our design, has been purchased from the Becton Dickinson Corporation. This device detects the presence, size, and fluorescence characteristics of cells in a thin stream of fluid illuminated by a laser. In our application, the droplets formed from this stream, containing cells, are used to inoculate the agar surface after being directed electrostatically to precise positions. In conjunction with electronics of our own design, this device gives us the capability of selecting cells of specific size and selecting cells that bind certain amounts of fluorescent dyes specific for cellular components, e.g. DNA.



Figure 1. Cyclops inoculates single mammalian cells onto agar to seed 3,000 colonies per minute in a sterile walk-in warm room.

BIOLOGICAL RESEARCH

We have tested a large number of cell lines for their susceptibility to several carcinogens. Four were extremely sensitive to benzo(a)-pyrene (BP), dimethylbenz(a)anthracene (DMBA), and aflatoxin B1 toxicity. The two selected for further study were a mouse hepatoma line (Hepa-1), and a rat hepatoma line (H-4-II-E). Because they were the most sensitive to the agents, these cell lines grew well on agar with little colony size or morphology heterogeneity, and had high levels of mixed function oxidase (an enzyme necessary for the activation of many carcinogens). Other workers have reported instability in the level of carcinogen-activating activity in some animal cell lines, but we have established that the level of activity in these lines is stable. BP-resistant variants of both the H-4-II-E and the Hepa-1 line have been isolated, and mutation rates of 4×10^{-5} and 10^{-7} per cell per generation have been established. The mutation rate of the more stable line, Hepa-1, has been shown to

increase in a linear fashion with concentration of several known mutagens. The isolation of these unique mutants has biochemical interest, and it provides us with a very selective and precise tool for the further study for carcinogens and mutagens.

Studies of the effects of the hormone insulin on the growth of animal cell colonies have underlined the differences and advantages of our system compared with more conventional methods of monitoring cell growth. One strain has a very simple colony morphology: a flat sheet one or two cells thick, spreading out over the agar. Insulin does not change the colony morphology of this strain, but does stimulate the growth rate very noticeably, at a concentration of 50 ng/ml. However, this

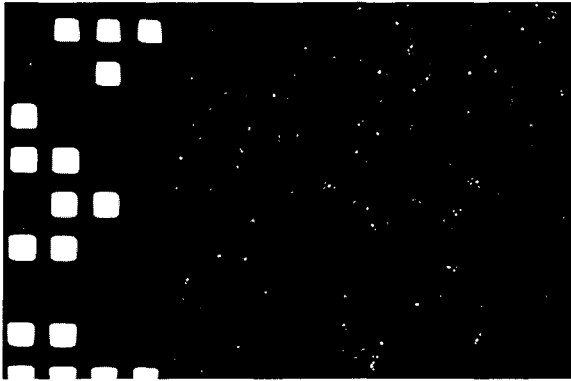


Figure 2. Chinese hamster ovary cells grown on agar containing 2% fetal calf serum and 5 ng/ml insulin form very small colonies.

stimulation occurs primarily after the phase of rapid exponential cell growth, when the cellular division rate is slowing due to effects of neighboring cells in the colony. Another strain forms colonies that pile up in the center at a characteristic stage of growth. Insulin was found to have a smaller effect on the growth rate of such colonies; however, it did change the shape of the colonies—at a concentration one-tenth of that needed to stimulate the growth of the other cell strains (Figs. 2 and 3). Other investigators, using conventional tissue culture techniques, have found little or no effect of insulin on these cells, even at doses 1,000 times larger than mentioned here.

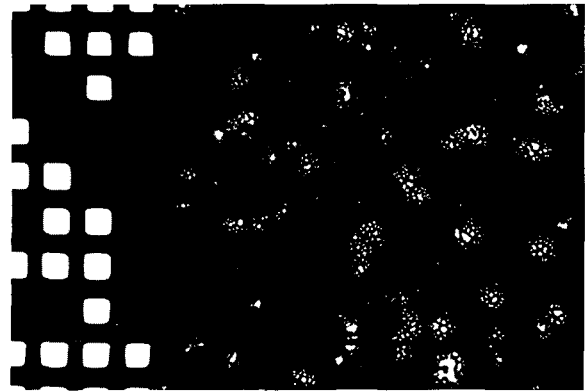


Figure 3. Chinese hamster ovary cells grown on agar, containing 2% fetal calf serum and 5,000 ng/ml insulin, migrate away from their parental colony and form clusters of tiny colonies all descended from a common parental cell.

Biophysical Studies

RESONANCE STUDIES IN PHOTOSYNTHESIS

A. J. Bearden

This research, in the field of molecular biophysics, examines experimentally the mechanisms of light excitation and energy transfer, photochemical energy transfer and storage, and subsequent electron-transfer and chemical-free energy production in both green-plant (chloroplast) and bacterial photosynthesis. Techniques used include high-sensitivity low-temperature (down to 4°K) electron paramagnetic resonance (EPR) spectroscopy, associated resonance techniques, rapid EPR passage methods, measurements of inhomogeneous line-broadening and spin relaxation, and lasers as fast high-intensity light sources. Investigations are being made on the following topics: (1) the effect of photochemical rates in chloroplasts of varying the size and coupling of antenna chlorophyll by chemical means; (2) the intensity dependence of photochemical processes in chloroplasts; (3) the further identification of the primary electron donors and acceptors in green-plant photosynthesis; (4) the effects of chemical pretreatment with inhibitors on the oxidation-reduction properties of components of the "dark" electron-transport chain in chloroplast photosynthesis; (5) the involvement of chlorophyll and carotenoid triplet states in photosynthesis; and (6) the molecular mechanism of oxygen evolution in chloroplasts.

A major effort during this period has been the development of a Low Noise Figure EPR Spectrometer by reconsidering the design of the reflection-cavity spectrometer in light of available microwave oscillators and detectors. Since the analysis of EPR spectrometers by George Feher in 1959, a considerable improve-

ment has been made in low-noise microwave oscillators (Gunn Effect devices, phase-locked loop oscillator systems, frequency synthesizers) and in high-efficiency, low-noise microwave detectors and frequency mixers. The impetus for the development of these components has been largely derived from the technology of radar and satellite communications. The new spectrometer performs a careful consideration of noise sources inherent in the EPR method and then implementation based on these theoretical studies. The net results so far indicate a "signal-to-noise" improvement over the standard 100 kHz field-modulation instrument of about 20dB; that is about the improvement theoretically possible with components operating at room temperature.

Having this instrument completed, except for minor changes to improve reliability, has permitted renewed studies on: the charge-separation process in green-plant photosynthesis in Photosystem I, the monitoring of molecular oxidation-reduction steps in the splitting of water to dioxygen in Photosystem II, and further microsecond kinetics monitored by EPR spectroscopy in the chloroplast electron-transport system. Measurements on Photosystem I photoreduction of bound iron-sulfur proteins using the green algae *Dunaliella parva* has shown that, in contrast to chloroplasts from higher plants, both Fe-S centers are photoreduced at low temperatures rather than Center A only. Studies on the relation of these experimental data to the state of membrane organization in this algae using EPR data and electron micrographs are currently under way.

APPENDICES

Appendix A: 1977 Publications

CONTRIBUTIONS TO JOURNALS, BOOKS, AND PROCEEDINGS

- Anderson, D.W., Nichols, A.V., Forte, T.M., and Lindgren, F.T.** Particle distribution of human serum high density lipoproteins. *Biochem. Biophys. Acta* 493, 55-68 (1977).
- Assman, G., Herbert, P.N., Fredrickson, D.S., and Forte, T.** Isolation and characterization of an abnormal high density lipoprotein in Tangier disease. *J. Clin. Invest.* 60, 242-252 (1977).
- Bearden, A. J., and Malkin, R.** Chloroplast photosynthesis: the reaction center of photosystem I, *in* Chlorophyll-proteins, reaction centers and photosynthetic membranes. (Brookhaven Symposia in Biology: No. 28, 247-266 (1976).
- Bentfeld-Barker, M.E., and Bainton, D.F.** Ultrastructure of rat megakaryocytes after prolonged thrombocytopenia. *J. Ultrastruct. Res.* 61, 201-214 (1977).
- Bentfeld, M.E., Nichols, B.A., and Bainton, D.F.** Ultrastructural localization of peroxidase in leukocytes of rat bone marrow. *Anat. Rec.* 187, 219-240 (1977).
- Benz, R.D., and Burki, H.J.,** Preparation and identification of partially fractionated Chinese hamster M3-1 chromosomes. *Exp. Cell Res.*, 112 143-153 (1978).
- The distribution of middle-repeated DNA sequences among Chinese hamster M3-1 chromosomes. *Exp. Cell Res.* 112, 155-165 (1978).
- Bjarngard, B.E., Chen, G.T., Piontek, P.W., et al.** Analysis of dose distributions in whole body superficial electron therapy. *Internat. J. Radiat. Oncol. Biol., Phys.*, 2, 319-324 1977.
- Braun, U., Shulgrin, A. T., Braun, G. and Sargent, T. III.** Synthesis and body distribution of several iodine-131 labeled centrally acting drugs. *J. Med. Chem.* 20, 1543-1546 (1977).
- Bruenger, F.W., Atherton, D.R., Stevens, W., and Durbin, P.W.** Early distribution of ²³⁸Pu in the liver of a cynomolgous monkey *in* Research in radiobiology, annual report radiobiology laboratory. University of Utah, COO-119-252, 191-195 (1977).
- Budinger, T.F.** Instrumentation trends in nuclear medicine. *Seminars in Nuclear Medicine* 7, 285-297 (1977).
- Budinger, T.F., Cahoon, J.L., Derenzo, S.E., Gullberg, G.T., Moyer, B.R., and Yano, Y.** Three dimensional imaging of the myocardium with radionuclides. *Radiology* 12, 433-439 (1977).
- Budinger, T.F., Derenzo, S.E., Greenberg, W.L., Gullberg, G.T., and Huesman, R.H.** Quantitative potentials of dynamic emission computed tomography. *J. Nucl. Med.* 19, 309-315 (1978).
- Emission computer assisted tomography with single-photon and positron annihilation photon emitters. *J. Computer Assisted Tomography* 1(1), 131-145 (1977).
- Budinger, T.F., and Glaeser, R.M.** Measurement of focus and spherical aberration of an electron microscope objective lens. *Ultramicroscopy* 2, 31-41 (1976).
- Budinger, T.F., and Gullberg, G.T.** Transverse section reconstruction of gamma-ray emitting radionuclides in patients, *in* Ter-Pogossian, M., ed., Reconstruction tomography in diagnostic radiology and nuclear medicine. Baltimore: University Park Press, 315-342 (1977).
- Budinger T.F., and Rollo, F.D.** Physics and instrumentation. *Progress in Cardiovascular Diseases* 20, 19-53 (1977).
- Budinger, T.F., Tobias, C.A., Huesman, R.H., Upham, F.T., Wieskamp, T.F., and Hoffman, R.A.** Apollo-Soyuz light-flash observations, *in* Holmquist, R. and Strickland, A.C., eds.,

- COSPAR life sciences and space research. Elmsford, Pergamon Press, 141-146 (1977).
- Burki, H.J., Koch, C., and Wolff, S.** Molecular suicide studies of ^{125}I and ^3H disintegration in the DNA of Chinese hamster cells. *Current Topics in Radiat. Res.* 12, 408-425 (1977).
- Burki, H. J., and Moustacchi, E.** Tritium-induced lethal and genetic changes in *Saccharomyces cerevisiae*. *Radiat. Res.* 71, 635-640 (1977).
- Byers, V.S., LeCam, L., Levin, A.S., Stone, W.H., and Hackett, A.J.** Identification of human populations with a high incidence of cellular immunity against breast carcinoma. *Cancer Immunol. Immunother.* 2, 163-172 (1977).
- Castro, J.R., and Quivey, J.M.** Clinical experience and expectations with helium and heavy ion irradiation in Proceedings of the international conference on particles and radiation therapy, Lawrence Berkely Laboratory, Berkeley, California (September 1976). *Internat. J. Radiat. Oncol., Biol., Phys., Part II*, 3, 127-132 (1977).
- Chapman, J.D., Blakely, E.A., Smith, K.C., and Urtasun, R.C.** Radiobiological characterization of the inactivating events produced in mammalian cells by helium and heavy ions. *Internat. J. Radiat. Oncol., Biol., Phys.* 2(2) 97-102 (1977).
- Chiu, W., and Glaeser, R.M.** Factors affecting high resolution fixed-beam transmission electron microscopy. *Ultramicroscopy* 2, 207-217 (1977).
- Chiu, W. and Grano, D.** Molecular structure of the outermost cell wall component of *Spirillum serpens*, in 35th ann. proc. Electron Microscopy Soc. Amer. Boston, Mass., 342-343 (1977).
- Clemons, G.K.** Development and preliminary application of a homologous radioimmunoassay for bullfrog growth hormone. *Gen. Comp. Endocrinol.* 30, 357-363 (1976).
- Clemons, G.K. and Nicoll, C.S.** Development and preliminary application of a homologous radioimmunoassay for bullfrog prolactin. *Gen. Comp. Endocrinol.* 32, 531-535 (1977).
- Effects of antisera to bullfrog prolactin and growth hormone on metamorphosis of *Rana catesbeiana* tadpoles. *Gen. Comp. Endocrinol.* 31, 495-497 (1977).
- Connell, C.J. and Connell, G.M.** The interstitial tissue of the testis in Johnson, A.D., and Gomes, W.R., eds., *The testis*. New York, Academic Press, IV, 333-369 (1977).
- Curtis, S.B.** Calculated LET distributions of heavy ion beams. *Int. J. Radiat. Oncol., Biol., Phys.* 3, 87-91 (1977).
- Derenzo, S.E.** Positron ring cameras for emission-computed tomography. *IEEE Trans. Nucl. Sci.*, v. NS-24, 881-885 (April 1977).
- Approximations for hand calculators using small integer coefficients. *Mathematics of Computation* 31, 214-222 (1977).
- Derenzo, S.E., Banchemo, P.G., Cahoon, J.L., Huesman, R.H., Vuletic, T., and Budinger, T.F.** Design and construction of the Donner 280-crystal positron ring for dynamic transverse section emission imaging. *IEEE Proc., conference on decision and control*, New Orleans, Dec. 7-9, 1, 341-349 (1977).
- Derenzo, S.E., and Budinger, T.F.** Resolution limit for positron-imaging devices. *J. Nucl. Med.* 18, 491-492 (1977).
- Derenzo S.E., Budinger, T.F., Cahoon, J.L., Huesman, R.H., and Jackson, H.G.** High resolution computed tomography of positron emitters. *IEEE Trans. Nucl. Sci.* vol. NS-24 544-558 (1977).
- Derenzo, S.E., Zaklad, H. and Budinger, T.F.** Analytical study of a high-resolution positron ring detector system for transaxial reconstruction tomography, in Ter-Pogossian, M.M., ed. *Reconstruction tomography in diagnostic radiology and nuclear medicine*, Baltimore, University Park Press, 343-358 (1977).
- Ebbe, S., Phalen, E., and Ryan, M.K.** The production of megakaryocytic macrocytosis by systemic factors in Sl/Sl^d mice. *Proc. Exp. Biol. Med.* 155, 243 (1977).
- Ebbe, S., Phalen, E., D'Amore, P., and Howard, D.** Megakaryocytic responses to thrombocytopenia and thrombocytosis in Sl/Sl^d mice. *Exp. Hemat.* 6, 201 (1978).
- Forte, T.M., Machen, T.E., and Forte, J.G.** Ultrastructural changes in oxyntic cells associated with secretory function: a membrane recycling hypothesis. *Gastroenterology* 73, 941 (1977).

- Gaffey, C.T. and Montoya, V.J.** Attempts to block transmission of epileptic discharges in cats with heavy ion irradiation. *Radiat. Res.* 50, 625-626 (1977).
- Glaeser, R., Bauer, T., and Grano, D.** Three-dimensional reconstruction using stereo pairs from serial thick sections. Proceedings of the Electron Microscopy Society of America (August 1977).
- Glaeser, R.M., and Taylor, K.A.** Frozen hydrated biological specimens for electron microscopy and structure analysis. 6th European Congress on Electron Microscopy, Jerusalem, Israel, 69-72 (1976).
- . Radiation damage relative to transmission electron microscopy. *J. Microsc.* 112, 127 (1978).
- Greve, J., Maestre, M.F., Moise, H., and Hosoda, J.** Circular dichroism studies of the interaction between T4 gene 32 protein and polynucleotides. *Biochemistry* 17, 887-893 (1978).
- . Circular dichroism studies of the interaction of a limited hydrolysate of T4 gene 32 protein with T4 DNA and poly[d(A-T)]-poly[d(A-T)]. *Biochemistry*, 17, 893-898 (1978).
- Hackett, A.J., Smith, H.S., Springer, E.L., Owens, R.B., Nelson-Rees, W.A., Riggs, J.L., and Gardner, M.** Two syngeneic cell lines from human breast tissue: one aneuploid mammary epithelial (Hs578T) and one diploid myoepithelial (Hs578Bst). *J. Natl. Cancer Inst.* 58, 1795-1806 (1977).
- Hackett, A.J. and Springer, E.L.** Scanning and transmission electron microscopy of human metastatic mammary carcinoma, in *The third international symposium on detection and prevention of cancer*. New York, Academic Press, v. 1 (1977).
- Hayes, T.L.** The frozen biological specimen in fly ash investigations, in Bailey, G., ed., 35th annual proc. Electron Microsc. Soc. Amer. Boston, p. 584-587 (1977).
- Henke, R.P., Benton, E.V., and Tobias, C.A.** Calibration of high-energy heavy-particle beams with plastic nuclear track detectors. *Nuclear Track Detection* 1(2), 139-143 (1977).
- Huesman, R.H.** The effects of a finite number of projection angles and finite lateral sampling of projections on the propagation of statistical errors in transverse section reconstruction. *Phys. in Med. and Biol.* 22, 511-521 (1977).
- Jap, B.K. and Glaeser, R. M.** The scattering of high-energy electrons: I. Feynman path-integral formulation. *Acta Crystallographica* A34, 94-102 (1978).
- Jones, H.** Dose-effect relationships in carcinogenesis and the matter of threshold of carcinogenesis. *Environmental Health Perspectives* (February 1978).
- Koch, C. and Burki, H.J.** Enhancement of x-ray induced potentially lethal damage by low temperature storage of mammalian cells. *Brit. J. Radiol.* 50, 290-293 (1977).
- Konrad, M.W., Storrie, B., and Glaser, D.A.** Clonal variation in colony morphology and growth of Chinese hamster ovary cells cultures on agar. *Cell* 10, 305-312 (1977).
- Krauss, R.M., Lindgren, F. T., Silvers, A., Jutagir, R., and Bradley, D.D.** Changes in high density lipoproteins in women on oral contraceptive drugs. *Clinica Chimica Acta* 80, 465-470 (1977).
- Landaw, S.A., Tenforde, T.S., and Schooley, J. C.** Decreased surface charge and accelerated senescence of red blood cells following neuraminidase treatment. *J. Lab. Clin. Med.* 89, 581-591 (1977).
- Lawrence, J.H., Tobias, C.A., Chong, C., Lyman, J., Born, J.L., Linfoot, J.A., and Manougian, E.** Heavy particle irradiation of the pituitary, in Allen, M.B., Jr., and Mahesh, V.B. eds., *The pituitary*. New York, Academic Press, pp. 443-451 (1977).
- Leith, J.T., Smith, P., Ross-Riveros, P., and Wheeler, K.T.** Cellular response of a rat brain tumour to a therapeutic neon ion beam. *Int. J. Radiat. Biol.* 32, 401-407 (1977).
- Levy, R.I., Grizzle, J., Nichols, A.V., Sheffield, T., Tyroler, H.A., Williams, O.D., Klimov, A.N., Gerasimova, E.N., Glasunov, I.S., and Deev, A.D.** Collaborative US-USSR study on the prevalence of dyslipoproteinemias and ischemic heart disease in American and Soviet populations. *Am. J. Cardiol.*, 40, 260-268 (1977).
- Lindgren, F.T., Silvers, A., Jutagir, R., Layshot, L. and Bradley, D.D.** A comparison of simplified

- methods for lipoprotein quantification using the analytic ultracentrifuge as a standard. *Lipids* 12, 278-282 (1977).
- McNulty, P.J., Farrell, G.E., Filz, R.C., Schimmerling, W., and Vosburg, K.G.** Threshold pion production and multiplicity in heavy-ion collisions. *Phys. Rev. Lett.* 38, 1519-1522 (1977).
- Maestre, M. F., Greve, J., and Hosoda, J.** Optical studies on T4 gene 32 protein DNA interaction, in Pullman, B., and Goldblum, N., eds., *Excited states in organic chemistry and biochemistry*. Dordrecht, The Netherlands, D. Reidel, pp. 99-111 (1977).
- Magee, J.L.** Electron energy loss processes at subelectronic excitation energies in liquids. *Can. J. Chem.* 55, 1847-1859 (1977).
- Magee, J.L., and Helman, W.P.** Energy loss of electrons in random motion. *J. Chem. Phys.* 66, 310-318 (1977).
- Malkin, R., and Bearden, A.** Electron paramagnetic resonance studies of plastocyanin in the photosynthetic electron transport chain, in *Proceedings of the fourth international congress on photosynthesis*, Reading, England, September, 1977. Essex, England, William Clowes, Ltd.
- Mall, J., Hoffer, P., Murray, W., Rodrigo, J., Anger, H.O., and Samual, A.** Heterotopic bone, a potential source of error in evaluating hip prosthesis by radionuclide techniques. *J. Nucl. Med.* 18, 604 (1977).
- Martins, B.I., Raju, M.R., Hayes, T.L., and Tobias, C.A.** Survival of cultured mammalian cells exposed to ultrasound. *Rad. and Environ. Biophys.* 14, 243-250 (1977).
- Mel, H.C., ed.** Aharon Katchalsky memorial symposium, in Lawrence, J.H., Gofman, J.W., and Hayes, T.L., eds., *Advances in biological and medical physics*. New York, Academic Press, v. 16, (1978).
- Mel, H.C., Prenant, M. and Mohandas, N.** Reticulocyte motility and form: studies on maturation and classification. *Blood* 49, 1001-1009 (1977).
- Ngo, F.Q.H., Han, A., and Elkind, M.M.** On the repair of sublethal damage in V79 cells resulting from irradiation with fast neutrons or fast neutrons combined with x-rays. *Int. J. Radiat. Biol.* 32, 507-511 (1977).
- Ngo, F.Q.H., Han, A., Utsumi, H., and Elkind, M.M.** Comparative radiobiology of fast neutrons: Relevance to radiotherapy and basic studies. *Int. J. Radiat. Oncol., Biol., Phys.* 2, suppl. 2, 187-193 (1977).
- Nichols, A.V.** Interconversion of plasma lipoproteins, in Peeters, H., ed., *The lipoprotein molecule* (NATO ASI). New York, Plenum Publ. Corp. (1977).
- Ogrydziak, D.M. and Mortimer, R.K.** Genetics of extracellular protease production in *Saccharomyces lipolytica*. *Genetics* 87, 621-632 (1977).
- Pawley, J.B., and Fisher, G.L.** Visualization of fly ash particles in pulmonary macrophages using color x-ray mapping in *Proc. 16th Hanford biology symposium. ERDA Symposium Series*, Oak Ridge, pp. 374-381 (1977).
- Rapid elemental characterization of coal combustion by-products using simultaneous three color x-ray mapping and digital scan-stop. *J. Microsc.* 110, 87 (1977).
- Pawley, J.B., and Hayes, T.L.** A freeze fracture preparation chamber attached to the SEM, in 35th annual proceedings of the Electron Microscopy Society of America. Boston, Mass., p. 588-589 (1977).
- Pawley, J.B., and Norton, J.T.** A chamber attached to the SEM for fracturing and coating frozen biological samples, in *Proc. 1st international meeting on low temperature biological microscopy*, Cambridge, England. *J. Microsc.* 112, 169-182 (1978).
- Pawley, J., Statham, P., and Menzel, T.** Using beam blanking and digital scan-stop in the microanalysis of particles, in Johari, O., ed., *Proc. 10th ann. scanning electron microscopy symposium*. Chicago, Inst. of Tech. Res. 1, 297-306 (1977).
- Prashad, N., and Hosoda, J.** Role of gene 46 and 47 in bacteriophage T4 reproduction. II. Formation of gaps on parental DNA of polynucleotide ligase defective mutants. *J. Mol. Biol.* 70, 617 (1972).
- Raybourn, M.S., and Keller, E.L.** Colliculoreticular organization in primate oculomotor system. *J. Neurophysiol.* 40(4), 861-878 (1977).
- Ritter, M.A., Cleaver, J.E., and Tobias, C.A.** High-LET radiations induce a large proportion of

- non-rejoining DNA breaks. *Nature* 266, 653-655 (1977).
- Rowland, R.E., and Durbin, P.W.** The plutonium injection cases: an update to 1977. Proc. World Health Organization conf., Geneva, Sept. 12-16, 1977.
- Saenger, P., Levine, L.S., Wiedemann, E., Schwartz, E., Korth-Schutz, S., Pareira, J., Heinig, B., and New, M.I.** Somatomedin and growth hormone in psycho-social dwarfism. *Paediatr. Paedol. Suppl.* 5, 1 (1977).
- Sargent, T., III, Braun, G., Braun, U., Budinger, T.F., and Shulgin, A.T.** Brain and retina uptake of a radioiodine labeled psychotomimetic in dog and monkey. *Commun. Psychopharmacol.* 2(1) (1978).
- Sargent, T. III, Budinger, T.F., Braun, G., Shulgin, A., and Braun, U.** An iodinated catecholamine congener for brain imaging and metabolic studies. *J. Nucl. Med.* 19, 71-76 (1978).
- Sartorius, O.W., Morris, P.L., Benedict, D.L., and Smith, H.S.** Contrast ductography for recognition and localization of benign and malignant breast lesions: an improved technique, in Logan, W.W., ed., *Breast carcinoma: the radiologist's expanded role.* New York, John Wiley (1977).
- Sartorius, O.W., Smith, H.S., Morris, P., Benedict, D., and Friesen, L.** Cytological evaluation of breast fluid in the detection of breast disease. *J. Natl. Cancer Inst.* 59, 1073-1080 (1977).
- Schimmerling, W., Curtis, S.B., and Vosburgh, K.G.** Velocity spectrometry of 3.5 GeV nitrogen ions. *Radiat. Res.* 72, 1-17 (1977).
- Schimmerling, W., Alonso, J., Morgado, R., Tobias, C., Grunder, H., Upham, F.T., Winsor, A., Armer, R., Yang, T.C.H., and Gunn, J.T.** The Bevalac minibeam facility. *IEEE Trans. Nucl. Sci.* NS-24, 1049-1051 (1977).
- Schooley, J.C.** *In vivo* immunologic studies of erythropoietin using anti-erythropoietin immune serum, in Fisher, J.W., ed., *Kidney hormones II*, London, Academic Press, 151-163 (1977).
- Smith, H.S., Owens, R.B., Nelson-Rees, W.A., Springer, E.L., Hackett, A.J., Williams, R., and Dollbaum, C.M.** Epithelial cell cultures from human carcinomas. The third international symposium on detection and prevention of cancer. London, Academic Press, v. 2 (1977).
- Smith, H.S., Riggs, J.L., and Springer, E.L.** Expression of antigenic crossreactivity to RD114 p30 protein in human fibrosarcoma cell line. *Proc. Nat. Acad. Sci.* 74, 744-748 (1977).
- Smith, P.P., and Leith, J.T.** Effects of topically applied olive oil on the response of hamster skin to single or multiple doses of 230 kV x-rays. *Int. J. Radiat. Biol.* 31, 467-475 (1977).
- Springer, E.L., and Roth, I.L.** Micrographs included in Holt, S.C., ed., *Electron microscopy in human medicine.* Philadelphia, McGraw-Hill (1977).
- , Micrographs included in Bandoni, R.J., ed., *Plants: an evolutionary survey.* Belmont, Wadsworth Publishing Co. (1977).
- Svensson, G.G., Bjarngard, B.E., Chen, G.T.Y., Marck, A., and Weichselbaum, R.R.** Superficial doses in treatment of breast with tangential fields using 4 MV x-ray. *Int. J. Rad. Onc., Biol., Phys.*, 2, 705-710 (1977).
- Tobias, C.A., Benton, E.V., Capp, M.P., Chatterjee, A., Cruty, M.R., and Henke, R.P.** Particle radiography and autoactivation. *Int. J. Rad. Oncol., Biol. Phys.* 3, 35-44 (1977).
- Tobias, C.A., and Yang, T.C.H.** Biophysics of gravity, in *Yearbook of science and technology.* New York, McGraw-Hill, 246-251 (1977).
- Vaughan, W.J., and Calvin, M.** Electrophoretic analysis of brain proteins from young adult and aged mice. *Gerontology* 23, 110-126 (1977).
- Vaughan, W.J., Lindgren, F.T., Whalen, J.B., and Abraham, S.** Serum lipoprotein concentrations in cystic fibrosis. *Science* 199, 783-786 (1978).
- Wiedemann, E., Saito, T., Linfoot, J.A., and Li, C.H.** Radioimmunoassay of human β -lipotropin in unextracted plasma. *J. Clin. Endocrin. and Metab.* 45, 1108-1111 (1977).
- Wong, R.A., Banchemo, P.G., Jensen, L.C., Pan, S.S., Adamson, G.L., and Lindgren, F.T.** Automated microdensitometry and quantification of lipoproteins by agarose gel electrophoresis. *J. Lab. Clin. Med.* 89, 1341-1348 (1977).

Wrenn, M.E., LoSasso, T., and Durbin, P.W. A metabolic model for uranium metabolism in man. Progress Report, Institute of Environmental Medicine, New York University, COO-3382-16, XI-1-17 (1977).

Yang, T.C.H., Blakely, E.A., Chatterjee, A., Welch, G., and Tobias, C.A. Response of cultured mammalian cells to accelerated krypton particles in Holmquist, R., and Strickland, A.C., eds., COSPAR life sciences and space research. Oxford and New York, Pergamon Press XV 169-174 (1977).

Yang, T.C.H., Risius, J., Madfes, I.A., Tobias, C.A., Lyman, J.T., and Howard, J. Enhancement of viral transformation of cells *in vitro* by heavy-ion radiation. *Radiat. Res.* 70, 650 (1977).

Yano, Y., and Budinger, T.F. Cyclotron-produced Zn-62: its possible use in prostate and pancreas scanning as a Zn-62 amino acid chelate. *J. Nucl. Med.* 18, 815-822 (1977).

Yano, Y., Chu, P., Budinger, T.F., Grant, P.H., Ogard, A.E., Barnes, J.W., O'Brien, H.A., Jr., and Hoop, B. Jr. Rubidium-82 generators for imaging studies. *J. Nucl. Med.* 18, 46-50 (1977).

LBL REPORTS ISSUED

Anderson, D.W. Separation and characterization of subclasses of human serum high density lipoproteins and their determination in a California population sample. Ph.D. Thesis, LBL-5627 (May 1977), 105 p.

Bauer, T. The electron microscopy of hydrocarbon production in parthenium argentatum (Guayule). Thesis, LBL-5688 (Nov. 1977), 182 p.

Bennett, L.F. Application of generalized inverses in the solution of underdetermined systems of equation. LBL-5681 (Aug. 1978), 24 p.

Biology and Medicine Division. Biological and medical research with accelerated heavy ions at the Bevalac 1974-1977. LBL-5610 (April 1977), 227 p.

Davis, D. Analyses of iron content in individual human red blood cells by electron microprobe and scanning electron microscope. LBL-5636 (Aug. 1977), 55 p.

Deans, S.R. The radon transform for higher even dimension. LBL-5696 (Dec. 1977), 4 p.

—. The radon transform: some remarks and formulas for two dimension. LBL-5691 (Nov. 1977), 20 p.

Derenzo, S.E. Positron ring cameras for emission-computed tomography. Presented at the Nuclear Medicine Scientist Short Course, New Orleans, La., Oct. 23, 1976. LBL-5612 (Dec. 1976), 5 p.

Derenzo, S.E., Banchemo, P.G., Cahoon, J.L., Huesman, R.H., Vuletic, T., and Budinger, T.F. Design and construction of the Donner 280-crystal positron ring for dynamic transverse section emission imaging. LBL-5679 (Sept. 1977) 9 p. (Presented at the IEEE Conference on Decision and Control, New Orleans, La. December 7-9, 1977).

Derenzo, S.E., Zaklad, H., and Budinger, T.F. Positron emission camera for transverse section tomography. LBL-2848 (Dec. 1975), 89 p.

Dole, S.R. The pulmonary adenoma of the mouse: a simple model of its growth based on scanning electron microscopy. LBL-5624 (May 1977), 125 p.

Gullberg, G.T. The reconstruction of fan-beam data by filtering the back-projection. LBL-5693 (Dec. 1977), 51 p.

Huesman, R.H., Gullberg, G.T., Greenberg, W.L., and Budinger, T.F. Users manual—Donner algorithms for reconstruction tomography. LBL Pub-214 (1977), 285 p.

Johnson, J.E., Jr. A view on techniques of preparation of cell and tissue culture specimens for electron microscopy. LBL-5638 (May 1977), 15 p.

Llacer, J., Chatterjee, A., Gauger, G.E., Tobias, C.A., and Goulding, F.S. Theory and design parameters for a positron-emitter beam-imaging device for biomedical research.

- LBL-5631 (May 1977), 56 p. Submitted to Phys. Med. Biol.
- Lim, T.H.** The kinetics of the trace-element chromium (III) in the human body. Ph.D. thesis, LBL-5615 (March 1977), 106 p.
- MacGregor, R.D., II.** Molecular sieving action of the cell membrane during gradual osmotic hemolysis. Ph.D. thesis, LBL-5634 (May 1977), 326 p.
- Roth, E.P.** Electronically compensated power supply for electrolytically labeled ^{99m}-technetium radiopharmaceuticals. LBL-5690 (Nov. 21, 1977), 12 p.
- Tenforde, T.S., Curtis, S.B., Woodruff, H.K., Parks, D.L., Daniels, S.J., Crabtree, K.E., Schilling, W.A., and DeGuzman, R.J.** Preliminary studies on factors controlling the rate of regrowth of heavily x-irradiated rat rhabdomyosarcoma tumors. LBL-7406 (Dec. 1977), 23 p.
- Yano, Y.** Effect of transport in distribution of radioions and radiolabeled metabolites. LBL-7407 (Dec. 22, 1977), 26 p.
- Yano, Y., and Roth, E.P.** An alumina column Rb-82 generator. LBL-7422 (Oct. 1977), 10 p.
- Yee, J.P., and Mel, H.C.** Cell-membrane and rheological mechanisms in dynamic osmotic hemolysis and repair of erythrocytes and ghosts. LBL-5651 (July 1977), 20 p.

Appendix B: Biology and Medicine Division Staff

DIVISION HEAD

Edward L. Alpen

DIVISION ADMINISTRATIVE STAFF

Janice C. DeMoor
Laurie E. Graves
Allan W. Long
Robert W. Springsteen
Baird Whaley
Herbert Wiener

DIVISION SCIENTIFIC STAFF

E. John Ainsworth
Hal O. Anger

Mary E. Barker
John B. Bassel
Thomas E. Bauer
Alan J. Bearden
Eugene V. Benton
Eleanor A. Blakely
James L. Born
Thomas F. Budinger
H. John Burki

Joseph R. Castro
Aloke Chatterjee
George T. Y. Chen
Wah Chiu
William T. Chu
Gisela K. Clemons
Gerald M. Connell
Stanley B. Curtis
Hunter O. Cutting
Jefferson W. Davis
Stephen E. Derenzo
Jonathan S. Dixon
Kenneth H. Downing
Patricia W. Durbin

Shirley N. Ebbe

Jacob I. Fabrikant
Trudy M. Forte

Cornelius T. Gaffey
Joseph F. Garcia
Robert M. Glaeser
Donald A. Glaser

Joseph D. Goldstein
Regine Goth-Goldstein
Martin H. Graham
David A. Grano
Alexander Grendon
Grant T. Gullberg

Adeline J. Hackett
Thomas L. Hayes
Lester Hollander
William R. Holley
Junko Hosoda
Jerry Howard
Ronald H. Huesman

Lin C. Jensen
Nylan M. Jeung
*Hardin B. Jones

John W. Kast
Lola S. Kelly
Esther H. Knudson
Ronald M. Krauss

John H. Lawrence
Frank T. Lindgren
John A. Linfoot
John T. Lyman

Marcos F. Maestre
John L. Magee
Howard C. Mel
Robert K. Mortimer

Frank Q. Ngo
Alex V. Nichols

Suzanne S. T. Pan
James B. Pawley
Theodore L. Phillips
Donald A. Pointer

Julia B. Quint
Jeanne M. Quivey

Rose M. Ray
Michael S. Raybourn
Ruth J. Roots
Donald J. Rosenthal

*Dr. Hardin B. Jones died Feb. 18, 1978.

Thornton W. Sargent
 Walter Schimmerling
 John C. Schooley
 Mason M-S. Shen
 Helen P. Shu
 Alexander T. Shulgin
 Jerome R. Singer
 Helene S. Smith
 Lisa Snow
 E. Louise Springer
 Henry H. Stauffer

Tom S. Tenforde
 Cornelius A. Tobias

William J. Vaughan

Graeme P. Welch
 Margaret R. White
 Eckehart Wiedemann
 Priscilla D. Wong

Tracy C. Yang
 Yukio Yano

DIVISION SUPPORT STAFF

Frederick E. Abrams
 Gerald L. Adamson
 Gabriel A. Adebiji
 Hilda M. Alexander
 Cathryne C. Allan
 Sheila F. Anderson
 Arlette S. Atwater

Patricia J. Blanche
 Carol S. Bohlen
 S. Kay Bristol
 Gerald L. Brooks

John L. Cahoon
 Dorothy A. Carpenter
 Betsy C. Carr
 Emanuela N. Catena
 Polly Y. Chang
 Huey-Ling C. Chu
 M. Jeanette Cornell
 Karen E. Crabtree
 Laurie M. Craise
 Freddie L. Crenshaw, Jr.

Susan J. Daniels
 Randy J. DeGuzman
 Clardell L. Deuberry
 Martha L. Dixon
 Greta S. Duke

Diana E. Fajardo
 Sherry L. Fitzsimmons

Michael B. Fizer
 Fern V. Forsberg
 Myrtle L. Foster
 Roscoe Frazier
 Charlie M. Fuller

Patricia A. Garbutt
 Christine Giotas
 Queen E. Gipson
 Bahram Goliaei
 Elaine L. Gong
 Victoria E. Gorum
 Joan M. Graham
 Mary R. Graham
 William L. Greenberg

Virginia C. Havens
 Lilian E. Hawkins
 Steven B. Hayward
 Dorothy B. Hedquist
 Gretchen Hermes
 Minghsiu Ho
 James R. Holmes
 Gregory R. Hook
 Mildred K. Hughes
 James A. Hunter
 Stephen L. Hurst

Barbara W. Jansen
 Muriel B. Johnston

Sandra V. Karpenko
 Heroka Kasai
 William L. Kennedy
 Jonathan A. Kerner
 Barbara R. Komatsu
 William Koppes
 Natalia Kusubov

Clifford E. Lai
 Lennetta G. Lai
 Francine P. Lauderdale
 Deborah A. Leach
 Josephine A. Lundberg

Mara A. McDonald
 Tommy J. McKey
 Velma B. McNeal
 Ian S. Madfes
 Lynn J. Mahlmann
 Tamara B. Mihailovski
 Marie B. Mizelle
 Herbert W. Moise III
 Carol J. Mortensen
 Brian R. Moyer
 Linda J. Mundy

Jeanette S. Nakagawa

Robert W. Nordhausen

Virginia I. Obie

Theresa C. Peters

Elizabeth A. Phalen

Mary C. Pirruccello

Patricia P. Powers-Risius

John C. Risius

Pepi Ross-Riveros

Eugene P. Roth

Gwendolyn J. Ryan

Wolfgang A. Schilling

Thea B. Scott-Garner

Ruth T. Showalter

Carla J. Simmons

Karen C. Smith

Ester F. Solis

Dorothy S. Sprague

Marlena T. Stallings

Lore S. Stein

Nancy J. Steinhaus

Stephen S. Sylvester

Frances B. Taylor

Vicki J. Truex

Grace V. Walpole

Jon I. White

Robert D. Wills

Wennie H. Wu

Ann S. Yabusaki

COMMITTEES

Division Advisory Committee

Edward L. Alpen

James L. Born

Thomas F. Budinger

Robert M. Glaeser

John C. Schooley

Cornelius A. Tobias

Eleanor A. Blakely

Alex V. Nichols

Herbert Wiener*

Baird Whaley*

Interim Division Staff Committee

John T. Lyman, chairman

Thomas L. Hayes

Frank T. Lindgren

Alan J. Bearden

Trudy M. Forte

Equipment Committee

Joseph F. Garcia, chairman

H. John Burki

Aloke Chatterjee

Cornelius T. Gaffey

Jonathan S. Dixon

Herbert Wiener*

Salary Committee

Edward L. Alpen

James L. Born

Thomas F. Budinger

Robert M. Glaeser

John C. Schooley

Cornelius A. Tobias

Baird Whaley*

Donner Library Committee

Robert M. Glaeser, chairman

Edward L. Bennett

Thomas F. Budinger

Gerald M. Connell

Thomas L. Hayes

Frank T. Lindgren

Dorothy E. Denney*

Roy J. Nielsen*

Human Use Committee

James L. Born, chairman

Thomas F. Budinger

Shirley N. Ebbe

William E. Siri

Henry H. Stauffer

Janice C. DeMoor*

Baird Whaley*

Radioactive Drug Research Committee

James L. Born, chairman

Edward L. Alpen

Aloke Chatterjee

John C. Schooley

Henry H. Stauffer

Joseph D. Goldstein (consultant)

Janice C. DeMoor*

Baird Whaley*

*Ex-officio, nonvoting member

This report was done with support from the Department of Energy. Any conclusions or opinions expressed in this report represent solely those of the author(s) and not necessarily those of The Regents of the University of California, the Lawrence Berkeley Laboratory or the Department of Energy.

Reference to a company or product name does not imply approval or recommendation of the product by the University of California or the U.S. Department of Energy to the exclusion of others that may be suitable.

LBL-7448